Functional Characterizations of Plant Uracil Phosphoribosyltransferase and Phytaspase for their Potential in Cancer Therapy

A Thesis

Submitted in Partial Fulfillment of the

Requirements for the award of the degree of

Doctor of Philosophy

by

N SHARMILA

Roll no. 11610618

Department of Biosciences and Bioengineering

Indian Institute of Technology Guwahati

Guwahati 781039, Assam, India

December 2016

Functional Characterizations of Plant Uracil Phosphoribosyltransferase and Phytaspase for their Potential in Cancer Therapy

A Thesis

Submitted in Partial Fulfillment of the

Requirements for the award of the degree of

Doctor of Philosophy

by

N SHARMILA

Roll no. 11610618

Department of Biosciences and Bioengineering

Indian Institute of Technology Guwahati

Guwahati 781039, Assam, India

December 2016

Dedicated to

God and my Family

DECLARATION

I, hereby, declare that the matter embodied in this thesis titled "**Functional Characterizations of Plant Uracil Phosphoribosyltransferase and Phytaspase for their Potential in Cancer Therapy**" is the result of investigations carried out by me under the supervision of Prof. Siddhartha Sankar Ghosh and Prof. Lingaraj Sahoo, Department of Biosciences and Bioengineering, Indian Institute of Technology Guwahati, India for the award of the degree of Doctor of Philosophy. This work has not been submitted elsewhere for any degree, diploma, associateship or membership etc. of any institute or university to the best of my knowledge and belief.

December 2016

N Sharmila

Roll no. - 11610618

INDIAN INSTITUTE OF TECHNOLOGY GUWAHATI

DEPARTMENT OF BIOSCIENCES AND BIOENGINEERING

CERTIFICATE

This is to certify that the thesis titled "**Functional Characterizations of Plant Uracil Phosphoribosyltransferase and Phytaspase for their Potential in Cancer Therapy**" being submitted to the Indian Institute of Technology Guwahati by **N Sharmila** (Roll No. **11610618)** for the award of the degree of Doctor of Philosophy in Department of Biosciences and Bioengineering, is a bonafide record of research work carried out by her. The contents of this thesis have not been submitted to any other University or Institute for the award of any degree or diploma.

Prof. Siddhartha Sankar Ghosh
Thesis Supervisor

Prof. Lingaraj Sahoo
Thesis Co-Supervisor

Acknowledgements

First of all, I thank you God for being always there with me. Without you, I would have not found such a wonderful people in my life. Yes Lord, you made everything much easier and beautiful than I could ever imagine.

I express my deep sense of gratitude to my supervisor Prof. Siddhartha Sankar Ghosh for his continuous guidance and unflagging encouragement. Thank you very much Sir, for allowing me to conduct the thesis work with abundant freedom. It was his endless support which strengthened and motivated me in every difficult situation in research to keep pressing forward.

I am also grateful to my co-supervisor Prof. Lingaraj Sahoo for his ready help during the time of need. I thank my doctoral committee members- Prof. K. Pakshirajan, Dr. Debasish Das and Dr. V. Vaibhav Goud and also Dr. Biplab Bose for their suggestion and comments which perked me up to tackle the problems involved in the work. I am thankful to Department of Biosciences and Bioengineering, Centre for Nanotechnology, and Central Instrumentation Facility, IIT Guwahati, for supporting me throughout my thesis work. I am also thankful to the Centre for International Co-operation in Science (CICS) and Department of Biotechnology (DBT), India for providing me financial assistances for participating in an international conference in Oxford, United Kingdom.

I take this opportunity to express my gratefulness to my senior Dr. Pallab Sanpui and collaborator who is also my labmate- Deepanjalee, for their valuable time and stretched helping hands. I also owe my gratitude towards my seniors- Dr. V. Kohila, Dr. Chockalingam, Dr. Subhamoy Banerjee, Dr. Nidhi Chaubey Dr. Amaresh Kumar Sahoo and Dr. Amit Jaiswal for their kind guidance in my thesis work. Special thanks to my labmates and friends- Dr. Archita, Asif, Upashi, Neha, Bandhan, Anil, Vanitha, Srirupa, Anita, Gargi, Rajib and Gavya, for their support at the time of need in my thesis work. I am also extremely thankful to Vimal for being good friend and colleague. I extend my

thanks to my friends Nivedita, Deepika, Basu, Somaiah, Mohan and others for their help in times of need.

I cherish my wonderful memories with my IITG family- Satu Anna, Kiran, Sheeba, Mercy, Malathi, Priya Akka, Priya, Darilang, Uncle Hoakip, Aunty Hoakip, Christy Akka, Them, Swaroopa, Aurie di, Churchill, Kavish, Wanrisa, Ashok, Kalyan, Pradeep, Forbi, Newlife and many other lovely faces who made this beautiful home for me away from home. It is all your prayers which kept me safe and sound throughout my research journey.

I dedicate once again my research and also all my acheivement to my loving family, without them I would have not come so far. Dad and mom, you both mean a lot to me. It is your endless love, affection and guidance which helped me to face every difficult situation with strong spirit during these years of research journey. My lovely siblings- Prabha and Priya-my first friends, your love and constant encouragement is a positive force which always pushed me forward in my life. I am also grateful to my jijjus- Ramesh jijju and Arun jijju. Beloved Paul, when I need, you are always there throughout every step of my life as my bestie and strongest support. I can't thank you all enough, even if I do, it will only demean the love and care you have for me.

CONTENTS

ABBREVIATIONS

AAV	- Adenoassociated viruses
Ac-DMQD-pNA	- Acetyl-Asp-Met-Gln-Asp-p-Nitroaniline
Ac-VAD-CHO	- Acetyl-Tyr-Val-Ala-Asp-Aldehyde
Ac-VETD-AMC	- Acetyl-Val-Glu-Thr-Asp-7-Amino-4-methylcoumarin
AMC	- Amino-4-methylcoumarin
ATP	- Adenosine triphosphate
AZT	- Azidothymidine
Bik	- Bcl 2-interacting killer
BLAST	- Basic Local Alignment Search Tool
CCK	- Cholecystokinin
CD	- Cytosine deaminase
CD	- Circular dichroism
CD19	- Cluster of Differentiation 19
CHAPS	- 3-[(3-Cholamidopropyl) dimethylammonio]-1-Propanesulfonate
CHCA	- α-Cyano-4-hydroxycinnamic acid
CPP	- Cell penetrating peptides
DLS	- Dynamic light scattering
DMEM	- Dulbecco's Modified Eagle's Medium
DNA	- Deoxyribo nucleic acid
dTMP	- deoxy Thymidine monophosphate
DTT	- Dithiothreitol
FACS	- Fluorescence-activated cell sorting
FBS	- Fetal bovine serum
5-FC	- 5-Fluorocytosine
5-FD	- 5-Fluorouridine
FESEM	- Field Emission Scanning Electron Microscopy
FITC	- Fluorescein isothiocyanate

5-FU	- 5-Fluorouracil
5-FUMP	- 5-Fluorouridine monophosphate
GBM	- Glioblastoma multiforme
GCV	- Ganciclovir
GDEPT	- Gene directed enzyme prodrug therapy
GFP	- Green fluorescent protein
GST	- Glutathione S-transferase
HCN	- Hydrogen cyanide
HDFs	- Human dermal fibroblasts
HEPES	- 4-(2-Hydroxyethyl)-1-piperazineethanesulfonic acid
HRP	- Horseradish peroxidase
HSV-TK	- Herpes Simplex Virus-Thymidine Kinase
IAA	- Indole 3 Acetic Acid
IBs	- Inclusion bodies
CID	- Chemical inducer of dimerization
IPTG	- Isopropyl β-D-1-thiogalactopyranoside
LB	- Luria Bertani
LGP	- Latex glycoprotein
MALDI-TOF/TOF	- Matrix-assisted laser desorption/ionization-time of flight/time of flight
mIL-12	- murine Interleukin-12
Mn doped ZnS QDs-Chitosan NPs	- Manganese doped Zinc Sulfide Quantum Dots-Chitosan Nanoparticles
MSCs	- Mesenchymal stem cells
MTT	- 3-(4,5-Dimethylthiazol-2-yl)-2,5- diphenyltetrazolium bromide
NCBI	- National Center for Biotechnology Information
QD	- Quantum Dot
PBS	- Phosphate buffered saline
PBST	- Phosphate buffered saline Tween-20
PCD	- Programmed cell death

PCR	- Polymerase chain reaction
PDB	- Protein Data Bank
PEG	- Polyethylene glycol
PI	- Propidium iodide
PRPP	- Phosphoribosyl-1-pyrophosphate
PVDF	- Polyvinylidene fluoride
QY	- Quantum yield
RIP	- Ribosome-inactivating protein
RNA	- Ribo nucleic acid
RT-PCR	- Reverse transcriptase polymerase chain reaction
SAP	- Saporin
SAVES	- Structure Analysis and Verification Server
SDS-PAGE	- Sodium dodecyl sulfate-polyacrylamide gel electrophoresis
TCA	- Trichloroacetic acid
TEM	- Transmission Electron Microscopy
TMV	- Tobacco mosaic virus
TNF	- Tumor necrosis factor
TNFR	-Tumor necrosis factor receptor
ToTK1	- Tomato thymidine kinase 1
TPP	- Tripolyphosphate
TRAIL	- TNF-α related apoptosis inducing ligand
UK	- Uridine kinase
UMP	- Uridine 5-monophosphate
UPRT	- Uracil phosphoribosyltransferase
UV	- Ultra violet
ZnO	- Zinc Oxide

ABSTRACT

In burgeoning field of cancer research, plant bioactive compounds and plant therapeutic proteins have been found very effective on persisting drug resistant cancer. Although many plant derived compounds are either in market or under clinical trials, there is still need of in-depth analysis on the plant functional proteins. Uracil phosphoribosyltransferase (UPRT) and phytaspase caspase-like protease are two such functional plant proteins, which are reported to have their functional counterparts in bacterial (bUPRT) and mammalian (caspase) system, respectively. In turn, these counterparts have been already very well exploited for their major role in the cancer treatment. Bacterial UPRT, pyrimidine salvage pathway enzyme converts the prodrug 5-FU into toxic metabolite 5-FUMP inside the cancer cells leading to apoptosis. Whereas, caspases are intracellular mammalian cysteine dependent proteases, which are mainly involved in the execution of apoptosis.

However, thorough characterization of recombinant AtUPRT and phytaspase, and their potential in complementing their functional counterparts in cancer treatment have been conducted in detail in this current thesis. More specifically, this thesis addresses the raising question of how far these two proteins mimic their counterparts in contributing themselves in the cancer therapy either by gene or by protein therapeutics. In **Chapter 1**, the emerging importance of cancer gene and protein therapy has been discussed. It also brings the deeper value of preliminarily investigated or yet to be explored plant suicide genes encoding therapeutic protein's application in cancer therapy into the limelight. More specifically, it deals exclusively with the significance of *Arabidopsis thaliana* uracil phosphoribosyltransferase (AtUPRT) and *Nicotiana tabacum* phytaspase. The chapter deciphers the possibilities of utilizing the potential of phytaspase in cancer therapy. The last section of this chapter encompasses on the future significance of devising these recombinant proteins into the mammalian system either exogenously or by expression and finally, through their mode of action sensitizing the cancer cells towards

chemotherapeutic drugs. At the end, development of quantum dots embedded polymeric nanocarriers for delivering therapeutic agents have been illustrated.

Chapter 2 began with the *in silico* investigation on *A. thialana* UPRT (AtUPRT), where AtUPRT was shown to have lower binding energy with its substrate 5-FU, as compared to *E. coli* UPRT. Cloning of AtUPRT into the mammalian expression vector has been delineated. Further, the therapeutic implication of AtUPRT expressed in HeLa cells by sensitizing the cells towards prodrug 5-FU was established by cell viability assay, cell cycle analysis and cell apoptosis analysis through flow cytometric analysis. The low survival efficiency of the AtUPRT expressing HeLa cells post 5-FU treatment was finally determined by quantitative clonogenic assay.

In **Chapter 3,** cloning (in bacterial and mammalian expression vector), expression and characterization of *Nicotiana tabacum* pre-prophytaspase and mature phytaspase in *E. coli* have been reported. This chapter is also stressed on the difficulties involved in purifying the bacterially expressed pre-prophytaspase and mature phytaspase. Recombinant mature phytaspase after cleaving GST tag retained its functionality towards caspase-8 substrate and its kinetic parameters were analyzed by enzymatic assay. Also theranostic potential of recombinant mature phytaspase (after removal of GST) bound to Mn doped ZnS QDs-Chitosan NPs (nanocomposites) have been elucidated. The quantum dots were useful for tracking and bio-imaging studies. The effect of phytaspase-nanocomposites on HeLa cells in the presence of apoptosis inducing drug, cisplatin was analyzed using cell viability assay. Also the prominent chemo-sensitizing effect of transfected mature phytaspase in A549 (adenocarcinoma human alveolar basal epithelial) cells towards drug is reported in this chapter.

The final **Chapter 4** on conclusions and future prospects, highlights the emerging importance of this study as well as and the important pack of information obtained in the current thesis. In brief, for the first time, AtUPRT have been cloned in mammalian expression vector and expressed in HeLa cells. The sensitizing effect of its expression in cancer cells towards 5-FU was studied through various techniques. The other part of the section focused on phytaspase-caspase like protease. *N. tabacum* phytaspase was cloned and expressed in bacterial system. Its thorough sequence and structural characterization

was carried out. Retaliation of functionality of recombinant phytaspase assessed by caspase activity assay illustrates its implication in cancer therapy. Thereafter, therapeutic efficacy of the recombinant phytaspase was established in the presence of cisplatin by its exogenous supply to the cancer cells upon loading onto quantum dots embedded polymeric nanocarriers. Similarly, phytaspase was also cloned in mammalian expression vector and transiently expressed to evaluate its anti-cancer potential on A549 cells in the presence of doxorubicin. The optimized protocols in this current work may serve as easier way to obtain these recombinant proteins avoiding the cumbersome process of isolating proteins from their native plant source. This detailed characterization information on these plant genes really serve as a platform for deeper investigation and holds their immense importance in the future of cancer therapy.

CHAPTER 1

Introduction and Literature Review

CHAPTER 1

Introduction and Literature Review

In context to the substantial percentage of mortality worldwide in several diseases due to persistence of drug resistance and many other reasons, plant natural products or its derivatives are found to be very useful, where some plant products have either been clinically approved or under clinical trials [1]. Cancer is one such deadly disease, which is a leading cause to the high rate of mortality in the world [2].There have been various available treatments for cancer, such as surgery, chemotherapy and radiation therapy [3]. Though both chemotherapy and radio-therapy are effective of combating cancer cells, these methods also indistinguishably kill normal cells and the chances of cancer relapsing is high in several cases after treatment. Nevertheless, current evolution in recombinant DNA technology, without a doubt, have played an important role in bringing a twist by making it possible to introduce cancer gene therapy and protein therapy, which elucidate major promising solutions over conventional cancer treatment.

1.1 Gene therapy

Gene therapy is one of the most promising therapeutic strategies, which promise to completely eliminate the cancer cells without harming the normal cells. In gene therapy, gene is used to rectify or supplant the disease controlling mechanism of cell, which has lost its function [4, 5]. At the current count, totally 2356 clinical trials of gene therapy have been carried out in the world wide. These constitute 22 different types of genes with different functions. Out of these 2356 genes, 169 (7.2%) genes are suicide genes (http://www.abedia.com/wiley/).

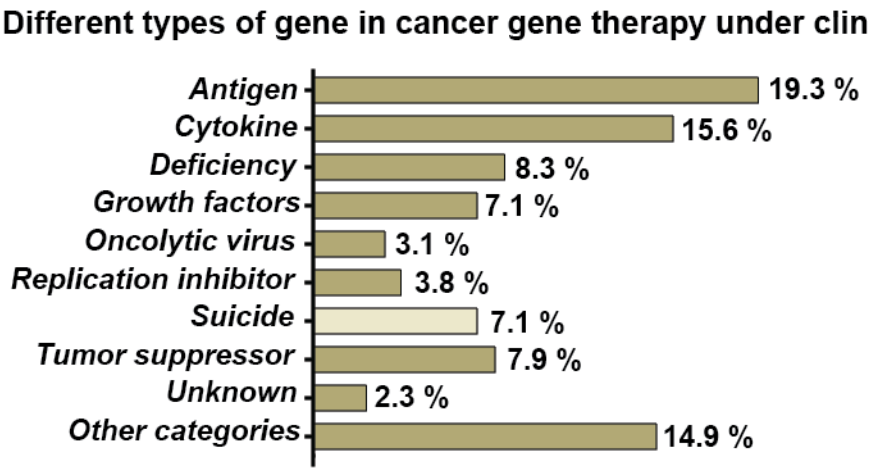

Figure 1.1: Conceptualized and redrawn from "Gene Therapy Cinical Trials Worldwide"- provided by the Journal of Gene Medicine (www.abedia.com/wiley /genes.php). The bars represent percentage of different types of clinical trial genes involved in cancer gene therapy.

1.1.1 Suicide gene therapy

Suicide gene therapy for cancer relies on a gene, which once expressed, catalyzes the conversion of the administered prodrug into the toxic metabolites making the cells to undergo apoptosis or programmed cell death (PCD) [6]. These foreign genes are called suicide genes. This therapy is also called as gene directed enzyme prodrug therapy (GDEPT). The most extensively investigated suicide gene therapy systems, which advanced to the clinical trials are- cytosine deaminase (CD)-5-Fluorocytosine (5-FC) [7, 8] and Uracil phosphoribosyltransferase (UPRT)-5-Fluorouracil (5-FU) [9-11] and Herpes Simplex Virus-Thymidine Kinase (HSV-TK)-ganciclovir (GCV) therapy system [6, 12, 13].

CD-5-FC and UPRT-5-FU therapy system

CD and UPRT are the pyrimidine salvage pathway enzymes catalyzing the deamination of cytosine into uracil and converts uracil to uridine monophosphate (UMP), respectively. Till to date, CD has been only reported to be found in prokaryotes and fungi [14], whereas UPRT has been widely studied in bacterial system and recently in yeasts. The UPRT homolog is reported in human, which lacks UPRTase activity *in vitro* because of

the missing uracil binding region [15]. This fundamental fact of absence of CD and inactive UPRT homolog in human are exploited by many scientists to devise the bacterial counterpart of these enzymes in suicide gene therapy. The fused CD-UPRT gene system when incorporated into the cancer cells, the cells are provided with chemotherapeutic nucleoside analog for cytosine and uracil such as, 5-FC and 5-FU. CD deaminates the less toxic 5-FC to the toxic 5-FU [7, 8], in turn UPRT converts 5-FU into highly toxic metabolite 5-FUMP. 5-FUMP inhibits the thymidylate synthetase, thereby creating scarcity of dTMP (deoxy thymidine monophosphate) in the cancer cells leading to cell death [16]. CD and UPRT are effective in killing cells individually, but their effect is augmented when employed together [17-20].

HSV-TK-GCV therapy system

The HSV-TK metabolizes GCV, a nucleoside analogue of guanosine and also an antiviral drug, into a GCV-monophosphate, which is further converted into a cytotoxic GCV-triphosphate form by cellular mechanism involving kinases. GCV-triphosphate acts as a competitive inhibitor of deoxyguanosine triphosphate, incorporates into the replicating cellular DNA inhibiting DNA replication. Eventually the cells undergo cell death [21]. However, this system is not devoid of limitation, as it is relatively slow [22] and imposes very high immunogenicity causing rejection of transduced cells by host immune system [23, 24].

1.1.2 Gene therapy aiming cellular apoptotic machinery

Apoptosis is the process of programmed cell death, where the cells execute itself to undergo cell death. The underlying failure of apoptosis mechanism of cells is the root cause of occurring cancer [25]. Apoptosis deficient nature of cancer cells could be due to numerous reasons. Therefore, attempts to compensate this deficiency, the genes encoding main players involved in apoptosis are introduced into the cancer cells to compensate the activity of their endogenous counterparts [26]. Mostly, gene therapy includes the molecular targets, which are involved in the extrinsic apoptotic pathway. In this pathway, tumor necrosis family (TNF) protein family (Fas ligands) binds to transmembrane death receptors and TNF receptor (TNFR) superfamily present on the cell membrane leading to

its trimerization. A cascade of reactions activates the initiator caspase 8, which in turn activates other downstream caspases (caspases-3, -6 and -7). These downstream caspases perform the cleavage of intracellular target cellular structural and functional protein substrates forcing the cells to undergo cell death [26]. Caspase are the cysteine dependent protease, which can be broadly divided into two initiator (caspase-2, -8, -9,-10 and -12) and effector (caspase -3, -6 and -7) caspases. The initiator caspases when activated by the external stimuli are processed and activate the effector procaspases. As caspases, TNF-α, Bik (Bcl 2-interacting killer) and TRAIL (TNF-α related apoptosis inducing ligand) are critically involved in apoptosis; clinical trials have been undertaken targeting these factors in cancer therapy. Targeting apoptotic machinery also renders antiproliferative effects on cancer cells [26-30].

Restoration of Caspases: Molecular targets in gene therapy

Since, caspases are the prime executioners of apoptosis, scientists have demonstrated that restoring the expression and activity of caspases in many cancer cells have chemosensitized the cells via apoptotic induction leading to cell death. Most of the cancer cells show lack of expression of caspases, which could be due to the genetic defects, such as deletion (in caspases 8 and 10) and mutation (in caspase 3,5,6 and 7) [31]. The solution to compensate this expression loss is to either deliver the caspase genes or to induce the endogenous expression of caspases. Phase I clinical trials have been successfully undergoing on iCasp9/CID system-fusion of human caspase 9 and modified FK-binding protein. When this system is exposed to synthetic dimerization drug, caspase 9 gets activated leading to cell death [26, 29, 32]. It is also seen the overexpression of caspase 9 have resulted in the rapid progression of cell death in HeLa cells [33]. Regaining of caspase 8 activities have resulted in diminishing the resistance that cancer cells possessed towards death receptor ligands [34]. Chimeric caspase1 and caspase 3 domain incorporated into the cancer cells and induced through death switch approach caused apoptosis in the targeted cancer cells [32]. Additionally, there are several reports stating the overexpression of procaspase 3,7,8 and 9 and engineered autocatalytic caspase 3 led to apoptotic induction in the cancer cells [35].

1.1.3 Delivery systems to deliver the suicide genes into the cells

The accurate delivery of the therapeutic agents (genes/proteins/drugs) is an intermediate step to exploit the potential of the agents in exhibiting their therapeutic importance. Delivery vehicles are the carriers carrying therapeutic agents such as, genes, proteins and drugs inside the cells [36-38]. The transfer of the suicide genes inside can be made more efficient by perfectly designed vectors. There are several vectors till to date have been used to develop more efficient strategies to make suicide gene therapy to be a better alternative over cancer therapies. These delivery systems can be broadly divided into- viral vectors and non-viral vectors [39, 40]. Due to the nature of escaping immunosurveillance and delivering the genomes into the infected cells, viruses are the excellent for being used as the vector for the delivery of foreign deoxyribo nucleic acid (DNA). The viruses used for the gene delivery are adenoassociated viruses (AAV), adenoviruses, herpes simplex virus, retroviruses, lentiviruses and vaccinia virus. The viral vectors are designed by the removal of viral genes, which are pathogenic to the cells, by replacing them with the therapeutic genes to be delivered. Though the viral vectors are highly efficient systems, safety has become a major issue. To overcome this, non-viral vectors have become the second popular method of gene delivery [41]. These vectors are further broadly divided into three types: naked DNA, physical method like electroporation and chemical methods such as cationic liposomes and cationic polymers. The third type includes nanovectors due to their structure and sizes, non-viral biological agents (bacteria, bacteriophages, erythrocytes and exosomes) and some mammalian cells like mesenchymal stem cells (MSCs) [42].

Liposomes-Non-viral vector

Due to the limitation of lower uptake and severe toxicity of naked DNA and physical methods respectively, chemical methods have been widely investigated [43]. The electrostatic interaction between the positively charge liposomes and the negatively charged DNA, makes it a suitable vector for the delivery of gene into the cells [41]. Additionally, the advantages of being cost effective, broad range transfection and low

immunogenic response makes it further more suitable as gene delivery system [40]. To date, 4.2% of the clinical trial gene therapies are done using liposomes (http://www.wiley.com/legacy/wileychi/genmed/clinical).

1.2 Protein therapy

In addition to gene therapy, cancer cells can also be targeted by cytotoxic proteins. Protein therapy is one such significant breakthrough therapeutic modality, which could be a platform for designing a rationale combination therapy using proteins and then performing targeted delivery into the diseased cells [44]. Isolating proteins from the native sources is a cumbersome process that includes disadvantages of more time, high cost of production, limited availability of animal models and laborious. These limitations can be overcome by recombinant protein production in heterologous system such as, bacterial system [45, 46], which adds the advantages of low cost of production, easy availability of bacterial culture, less time consuming. Recombinant proteins can be supplied exogenously to the cancer, to recapture cell's apoptosis undergoing ability, leading to cell growth inhibition and cell death [47].

1.2.1 Protein therapy in targeting cellular apoptosis

Similar to apoptotic machinery genes, some of the cellular apoptotic recombinant proteins such as rTNFα [48] and rTRAIL [27, 49] have been pursued in clinical phase trials. Recombinant protein therapy still faces challenges due to the higher toxicity and the difficulties in delivering functionally active protein. In spite of these restrictions, the results obtained in incorporating recombinant caspases targeting deficient apoptosis in cancer cells is a feasible approach. Many experiments have been done by several groups employing intracellular delivery vehicle to deliver recombinant caspases *in vitro* and *in vivo* condition. It was observed that delivery of the recombinant caspases (caspase-3,-6 and -8) [50-53] intratumorly resulted in effective induction of apoptosis. The whole concept of recombinant protein therapy increases the effect of the therapy by employing recombinant proteins having endogenous counterparts over the other therapeutic agents, which is always advantageous- such as low immunogenicity and high specificity.

1.2.2 Delivery system to deliver the therapeutic proteins into the cells

The medical application of protein therapy is limited, due to the difficulties in delivering the functionally active protein into the cells and bioavailability of the protein because of their high molecular weight, which extremely makes them difficult to cross the tissue barriers [54]. Surmounting these limitations, researchers have come up with many promising delivery systems, such as biodegradable polymeric nanocarriers, polymeric microspheres, quantum dots and covalent attachment of polymers such as PEG (eg. PEGylation or PEGnology) [54-57]. Recently proteins have also been delivered using cell penetrating peptides (CPP) [58, 59].

Polymeric nanocarriers

The self assembling small molecules aggregating through intermolecular forces are termed as nanocarriers. Generally nanoparticles (NPs) are nanocarriers that include liposomes, polyplexes, NPs made up of proteins and peptide assemblies. Complexes based on quantum dots, silica, gold nanoshells, etc also possess the characteristics of nanocarriers. Nanocarriers assist protein delivery by providing various advantages- protecting protein from inactivation/degradation by encapsulation, helping to track the intracellular localization of protein and also providing platforms for the surface conjugation of protein [54]. Nanocarriers have high surface area to volume ratio, which helps in wide distribution of protein increasing their shelf life and stability [54, 56, 58]. Nanocarriers made of biodegradable polymeric materials have superseded the other systems in delivering the drug molecules, as they reduce the risk of immune response and are biocompatible [54, 60]. Polymeric nanocarriers can be made up of synthetic homopolymer (eg. polylactide and poly(lactide-co-glycolide), natural polymer (eg., chitosan and alginate), copolymers (eg., polylactide-poly(ethylene glycol (PEG)) and poly(ε-caprolactone)-poly(ethylene glycol)) and colloid stabilizers (dextran and pluronic F68) [54, 61-64].

Quantum dots (QDs)

Quantum dots, a nanometer sized semiconductor particles consisting of unique optical and electronic properties. Along with the successful delivery of therapeutic agents such

as proteins and drugs, QDs being highly photostable and bright fluorescent probe also aid in tracking localization, movement, interaction and also release within the cells [58, 60, 65]. It was reported that protein-QDs conjugate was exceptionally internalized by the HeLa cells with the help of cationic nanogel [66]. Successful delivery of cardiac troponin C to the cardiac myocytes using conjugation with CPP tagged QdotITK™ Carboxyl QDs has been already reported [58].

Quantum dots-Nanoparticles (QDs-NPs) conjugate promising delivery vehicle for proteins

Though QDs are proved to be an efficient delivery probe, still it is less striking choice for proteins due to its less accessible surface for protein conjugation and its unstable optical properties against chemical reaction [60]. Addition to the usage of CPP [58, 66, 67], it is reported that the conjugation of QDs with NPs has become unavoidable approach to deliver therapeutic proteins [60, 68]. Delivering the protein or drug molecule using QDs-NPs conjugates serves a dual purpose of increases the efficiency/controlled delivery and tracking of protein/drug molecules. Preparation of only QDs followed by surface modification of QDs with biocompatible polymeric NPs is an easy approach to prepare QDs-NPs conjugates [60]. But loading of protein drug into QD-NPs conjugates is possible by either linking protein to QD surface then encapsulating with polymeric NPs or charging the protein to the biocompatible polymeric nanoparticle that already contains core/shell QDs [68]. Complexing QDs especially with carbohydrate polymeric NPs (eg, chitosan) increases their water solubility and biocompatibility. QDs coated with chitosan were successfully delivered into the yeast cells [60]. For instance, Yaun *et al*, have used blue emitting ZnO complexed with chitosan NPs for targeting the delivery of anticancer drug to tumor [69]. It was also reported by Mathew *et al*, Mn-doped ZnS QDs complexed with folic acid conjugated carboxymethyl chitosan loaded with 5-FU was successfully targeted to breast cancer cells MCF-7 *in vitro* [70].

1.3 Plants in cancer treatment

Plants have always been referred as medicinal factory in contributing treatment to various diseases including cancer. In fact, plant bioactive compounds have superseded many

other synthetic compounds in the contemporary field of research. Vincristine [71] and vinblastine [72] from periwinkle plant and paclitaxel (Taxol) from bark of pacific yew tree are the examples of development of plant based chemotherapeutic drugs for cancer treatment. Additionally, plants also show to have efficient genes/proteins playing an immense role in cancer therapeutic strategies.

1.3.1 Plant genes used in cancer gene therapy

Linamarase

Linamarase, enzyme is found in plant species like cassava. They are majorly located in the cell wall. Linamarase takes part in plant cyanogenesis, the process of liberating respiratory poison- hydrogen cyanide (HCN).

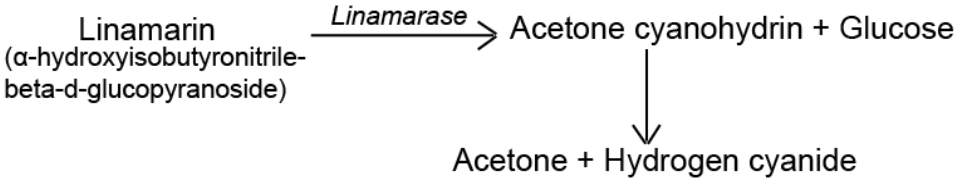

This process accounts for plant defense against many herbivores. HCN interferes in the production of ATP. This action is further enhanced due to the free diffusion of HCN across cellular membranes. Based on the therapeutic potential of linamarase, scientists have developed new strategies for cancer gene therapy by employing linamarase. Retro/adenoviral vectors carrying linamarase have shown marked increase in the cell death in the presence of linamarin substrate. The effective action of linamarase is increased due to diffusion of HCN to the neighboring cells resulting in strong bystander effect [73, 74].

Saporin

Saporin (SAP) from *Saporin officinalis*, is a ribosome-inactivating protein (RIP). SAP irreversibly inactivates ribosomal RNA by depurination, resulting in permanent protein synthesis inhibition, ultimately, causing cell apoptosis. The mode of action of SAP has widely opened the door for devising SAP in cancer gene therapy. This plant toxin has been used as recombinant chimera conjugated with monoclonal antibody for their easy

internalization in the targeted cells. For example, SAP conjugated to anti-CD19, anti-CD22 and anti-CD38 antibodies were found to be useful in treating B-cell lymphoma in animal models. Additionally, the amount of SAP protein required to show its efficacy is in picomolar range, which also compensates the less expression of SAP due to the inhibitory effect of SAP on its own translation [75, 76].

Tomato Thymidine Kinase 1

HSV-TK-GCV system has been widely studied for its potential as GDEPT. The disappointment with the system still remains due to low enzymatic activity and the lipophobicity of the drugs as previously mentioned. Recently group of scientists have come up with the new hope of exploiting the potential of tomato thymidine kinase enzyme (ToTK1) with the nucleoside analog-AZT (Azidothymidine). ToTK1 phosphorylates AZT to AZT monophosphate and AZT diphosphate. Thorough investigation has shown that ToTK1-AZT system is successfully an equivalent alternative to HSV-TK-GCV system in treating malignant gliomas. It is reported that human glioblastoma cells showed many fold increase in sensitivity to AZT when transduced with ToTK1. Exposure of ToTK1 transduced nude rats having glioblastoma multiforme (GBM) to AZT has also shown visibly large decrease in tumor growth [77, 78].

Horse radish peroxidase

Plant enzyme horseradish peroxidase (HRP) and plant hormone indole 3-acetic acid (IAA) are also shown to be the novel system for GDEPT. Under normoxic and hypoxic tumor conditions, HRP-IAA system has potential cytotoxicity and also exhibit bystander effect. However, the mechanism of action for HRP-IAA system is still in need to be discovered. A few studies indicated that the HRP/IAA treated cells showed apoptotic characteristics. This system along with murine interleukin-12 (mIL-12) has resulted in significant tumor growth inhibition in cancer cells [6, 79-81].

1.3.2 Plant proteins- anticancer agent in cancer therapy

Similar to plant genes, plant bioactive proteins have also showcased their benefits in cancer therapy [82]. Proteins extract from *Gynura procumbens* containing peroxidase, thaumatin-like proteins and miraculin was found to inhibit the growth of MDA-MB-231 breast cancer cell line [83]. Lectins, plant proteins have showed to have significant anticancer effect on cancer cells *in vitro* as well as *in vivo* [84]. Ricin, RIP from castor bean seed has been examined in Phase I clinical trials for its anticancer properties [85-88]. However, to overcome the challenges of ricin chain-B non-specificity [85, 89], immunotoxin studies were carried out using chain-A which showed very high toxicity towards cancer cells [90, 91]. A deeper exploration is a basic prerequisite for the successful exploitation of cytotoxic effect of these plant proteins.

1.3.3 Plant UPRT and plant phytaspase- two promising therapeutic agents in cancer therapy

Though the above mentioned plant genes and plant proteins could be an effective alternative to currently employed cancer treatments, but the priority focus is on those plant proteins, which seem to have their counterparts in animal system. The whole concept of expressing the plant counterparts of animal apoptotic factors and bacterial therapeutic suicide gene was strengthened by the fact of similarities between plant and animal PCD such as cell shrinkage, cyt c release and DNA fragmentation [92, 93]. Beside the PCD commonalities, expression of animal pro-apoptotic genes (bax) have shown to increased tobacco plants resistance to pathogens [94]. Whereas expression of anti-apoptotic genes such as human Bcl-xl, Bcl-2, baculovirus Op-IAP and *C. elegan* CED-9 in the transgenic plants have increased their tolerance against various stress such as salinity, disease resistance, heat, UV-B, drought, cold and oxidative stress [95-97]. These valued reports further strengthen the fact that the factors involved in animal and plant PCD also share functional similarities. Through ages of discovery, a wealth of studies have shown that plants have some functional analogs of mammalian caspases and bacterial uracil phosphoribosyltransferase (bUPRT) to respond to the various stressed conditions such as, biotic and abiotic stress [98] and molecular pathway [99, 100], respectively. The striking fact is that, these analogs, such as plant caspase-like protein or

plant UPRT (pUPRT) have only attained preliminary investigation for their potential in replacing their counterparts such as caspases and bUPRT. Caspases are the key factor in carrying out apoptosis. As previously mentioned under section 1.1.2, it has been observed that overexpression of caspase in the cancer cells sensitizes the cells to undergo drug induced apoptosis [101], whereas, UPRT enzyme has been fully exploited for forcing the cells to commit suicide (mentioned in section 1.1.1).

Uracil phosphoribosyltransferase: The plant UPRT

One of the reasons for the investigation on plant UPRT to be still confined to its primitive stage is that till now only *Arabidopsis thaliana* and *Oryza sativa* are reported to have functionally active UPRT [99, 100, 102]. But this few counts of pUPRT is surpassed by the finding that expressing *Arabidopsis thaliana* UPRT in UPRT mutant *E.coli* led to the growth inhibition when treated with 5-FU and 5-fluorouridine (5-FD) [99, 100]. It eventually becomes necessary to shed light on this observation as it projects the possibilities of therapeutically important pUPRT as a better suicide gene candidate.

Phytaspase: The Plant serine Caspase like protease

Phytaspase is serine dependent protease, which came very recently insight in 2010. Like caspase, phytaspase also degrade their intracellular target proteins by aspartate-specific hydrolysis [103, 104]. As of recent update, addition to cleaving multiple caspase synthetic substrates, phytaspase also have shown to cleave human peptide hormones– gastrin and cholecystokinin (CCK), which makes it therapeutically important [105]. According to the current data, phytaspase expression is reported in *Nicotiana tabacum, Oryza sativa* and *Solanum lycopersicum* and it is also discerned that it actively participate in programmed cell death during abiotic stress (Tobacco mosaic virus (TMV) infection) or biotic stress (High salinity or oxidative stress). Though, functionally phytaspase show similarity to caspase, they share no similarity in their structure [98, 103].

This potential and concise overview of future success on plant caspase like protein-phytaspase and pUPRT as suicide genes have driven the interest to seek the knowledge of how far these two genes when expressed in heterologous systems are able to mimic their

counterparts and induce apoptosis in cancer cells by exogenous supply or by directly expressing in cancer cells?

1.4 Objectives of the present work

1.4.1 A. thaliana UPRT (AtUPRT)

- Cloning of AtUPRT from synthesized full length cDNA by PCR amplification
- Functionally characterize the chemosensitizing effect of AtUPRT expression in cancer cells towards the cancer cells
- Study the molecular events involved behind the antiproliferative effects of AtUPRT

1.4.2 N. tabacum phytaspase

- Cloning of *N. tabaccum* phytaspase from synthesized full length cDNA by PCR amplification
- Expression and affinity chromatography based purification of recombinant phytaspase
- Structural and functional characterization of recombinant phytaspase
- Encapsulation and delivery of recombinant phytaspase using biocompatible nanocarriers
- Molecular mechanism studies involving cell growth inhibition

1.5 Salient features of this work

1.5.1 *Salient features of the work on AtUPRT*

- Cultivation of *Arabidopsis thaliana* in green house
- AtUPRT gene amplification and subcloning into mammalian expression vector pEGFP-N1
- Establishment of AtUPRT stably expressing HeLa cells (HeLa-UPP cells)
- Comparative *in silico* studies on structure and binding affinity between AtUPRT and *E.coli* UPRT with their substrates uracil and 5-FU
- Chemosensitization of HeLa-UPP cells towards 5-FU

1.5.2 *Salient features of the work on N. tabacum phytaspase*

- Cultivation of *N. tabaccum* in green house
- Cloning, expression and purification of glutathione S-transferase (GST) tagged precursor and active enzyme- pre-prophytaspase and mature phytaspase
- Sequence characterization of GST-pre-prophytaspase and GST-mature phytaspase
- Structural characterization and caspase-like activity of recombinant GST- mature phytaspase and mature phytaspase
- Reduced cell viability of HeLa cells on exogenous supply of phytaspase bound to Mn doped ZnS quantum dots-Chitosan nanoparticles (Mn doped ZnS QDs-Chitosan NPs) in the presence of cisplatin
- Chemosensitization of mature phytaspase expressing A549 cells (A549-Phytaspase cells) towards doxorubicin

CHAPTER 2

A new uracil phosphoribosyltransferase (UPRT) from *A. thaliana* for sensitization of HeLa cells towards 5-fluorouracil

[The major part of this work is published as- Sharmila Narayanan, Pallab Sanpui, Lingaraj Sahoo and Siddhartha Sankar Ghosh **(2016).** Unravelling the potential of a new uracil phosphoribosyltransferase (UPRT) from *Arabidopsis thaliana* in sensitizing HeLa cells towards 5-fluorouracil, ***International Journal of Biological Macromolecules.*** 91, 310-316]

CHAPTER 2

A New Uracil phosphoribosyltransferase (UPRT) from *A. thaliana* for Sensitization of HeLa Cells Towards 5-Fluorouracil

2.1 Introduction

Uracil phosphoribosyltransferase (UPRT) is an important enzyme in the bacterial pyrimidine salvage pathway as it catalyzes the formation of uridine 5-monophosphate (UMP) from uracil and phosphoribosyl-1-pyrophosphate (PRPP) [99, 106]. Although plant and human UPRT homologs have been reported; human one lacks UPRTase activity *in vitro* because of the missing uracil binding region [15]. Instead, human has uridine kinase (UK), which recycles uridine in pyrimidine salvage pathway. The absence of functional UPRT in human has been cleverly exploited in 'suicide gene therapy' where bacterial UPRT is employed as a candidate gene for efficient conversion of the prodrug, 5-fluorouracil (5-FU) into more toxic metabolites [6]. On the other hand, emerging reports indicate the existence of functionally active plant UPRTs in *Arabidopsis thaliana [99, 100]* and *Oryza sativa* [102]; and elucidation of their full potential as candidate 'suicide genes' is still an active area of research. The genome sequencing of *A. thaliana* revealed six homologous genes predicted to encode UPRTs—one is a single nuclear gene (NM 115250.2) responsible for a putative UPRT (herein denoted as AtUPRT), while the other five (NM 123452.4, At3g27190, At1g55810, At4g26510 and At3g27440) are predicted to encode for dual domain (AtUK/UPRTs) having uridine kinase at N-terminal and UPRT at C-terminal region [99, 100]. Among these six homologs, till now, only AtUPRT (891 bp) and AtUK/UPRT1 (1.46 kbp) (NM 123452.4) genes have been characterized for their functionality. Interestingly, the AtUPRT and AtUK/UPRT1 mutant *A. thaliana* do not show any growth retardation upon 5-FU treatment while the growth of wild type *A. thaliana* is significantly inhibited in presence of the prodrug. The

sequence alignment of UPRT domain of AtUK/UPRT1 with *E. coli* UPRT (GenBank accession number-P25532) shows that the binding motifs for PRPP and uracil are well conserved. Moreover, the AtUPRT and AtUK/UPRT1 have been successfully demonstrated to functionally complement the UPRT activity in UPRT mutant *E. coli* resulting in growth inhibition when treated with 5-FU [99, 100]. From 'gene therapy' viewpoint, plant genes seem to be better choice over the bacterial ones as they share similar degree of complexity with their counterparts in animal kingdom. In other words, plant UPRTs could be more effective candidates in gene therapy than bacterial ones. Although the genes have shown functional activity in native plant and even in bacterial system, the question still remains unanswered whether these *A. thaliana* UPRTs would retain their activity in the mammalian cells. In order to address the issue in this chapter, the AtUPRT gene was cloned and stably expressed in human cervical cancer (HeLa) cells. The effect of prodrug 5-FU on the proliferation of AtUPRT expressing HeLa cells was investigated by cell viability assay while induction of apoptosis in those cells was studied by flow cytometric analysis. Moreover, the alteration in cell cycle of transfected HeLa cells and possible role of cell cycle related gene cyclin D1 and p21 in response to 5-FU was also investigated. Finally, the survival fraction of AtUPRT-transfected HeLa cells in presence of 5-FU was calculated and compared with their non-transfected and vector-transfected counterparts.

2.2 Outline of the research work

1) AtUPRT gene was amplified from the full length cDNA synthesized from mRNA isolated from *A. thaliana*.

2) AtUPRT gene was cloned and subcloned into pGEM-T Easy vector and pEGFP-N1 mammalian expression vector respectively.

3) Transfection of AtUPRT into HeLa cells established stable HeLa-UPP cell lines expressing AtUPRT.

4) Effect of AtUPRT expression in HeLa cells upon 5-FU treatment was investigated.

5) Survival efficiency of 5-FU treated HeLa-UPP cells was determined.

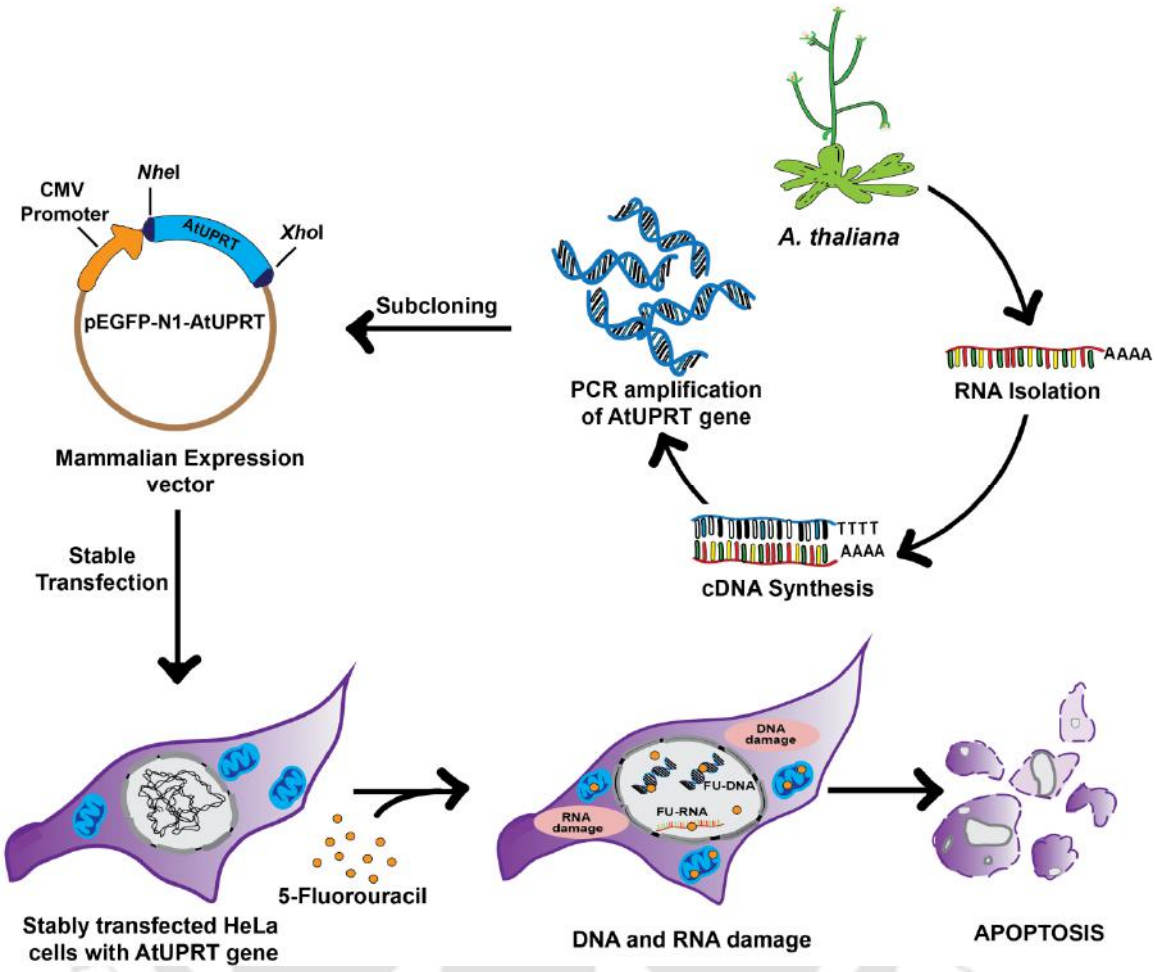

Figure 2.1: Schematic representation briefly demonstrating the outline of the research work carried out on AtUPRT gene expression in HeLa cells and its effect on the cells upon 5-FU treatment.

2.3 Experimental section

2.3.1 Materials

pGEM-T Easy cloning vector (Promega), pEGFP-N1 mammalian expression vector (Clontech), Dulbecco's Modified Eagle's Medium (DMEM) cell culture media, Fetal bovine serum (FBS), penicillin/streptomycin antibiotic, G418 antibiotic, 3-(4,5-Dimethylthiazol-2-yl)-2,5-diphenyltetrazolium bromide (MTT), JC-1, 5-FU, methylene blue and GenElute Mammalian Total RNA Miniprep kit were purchased from Sigma

Aldrich, Luria-bertani (LB) broth (Hi media), DNA polymerase I and ligation kit (CloneJET PCR cloning Kit, ThermoScientific), restriction enzymes (NEB), Lipofectamine 3000 Transfection kit (Invitrogen), High capacity cDNA Reverse transcription kit (Applied Biosystem) and Annexin-V FITC Apoptosis Detection kit I (BD Biosciences).

2.3.2 Instruments

Epi-fluorescence microscope (Nikon Eclipse Ti), FacsCalibur flow cytometer (BD Biosciences), Real Time PCR cycler (Rotor-Gene Q) and Multimode microplate reader (Infinite 200 PRO, TECAN)

2.3.3 Bacterial strain

The bacterial cloning strain used for cloning purpose was *E. coli* DH5α.

2.3.4 Cell lines

Human cervical cancer (HeLa) cells, human breast adenocarcinoma (MCF-7) cells and human adenocarcinomic alveolar basal epithelial (A549) cells were procured from National Centre for Cell Science (NCCS), Pune and maintained in DMEM supplemented with 10% FBS and penicillin (50U/ml)-streptomycin (50 mg/ml).

2.3.5 Primers used for amplification of AtUPRT gene

Sl.no	Primer Name	Type	Length	Sequence (5'-3')
1	UPP-F	pGEM-T Easy-Forward	21	CTCGTCGAAAATGGCGTGCTC
2	UPP-R	pGEM-T Easy-Reverse	28	GTATCACTTCACCCAATGTGTTTCTGTC
3	UPPNheI-F	pEGFP-N1-Forward	23	TATAGGCTAGCAATGGCGTGCTC
4	UPPXhoI-R	pEGFP-N1-Reverse	24	GCTCGAGTCACTTCACCCAATGTG

Table 2.1: Primers used for amplification of AtUPRT for cloning into pGEM-T Easy and PEGFP-N1 vectors.

2.3.6 PCR conditions used for amplifying AtUPRT gene for cloning into pGEM-T Easy and pEGFP-N1

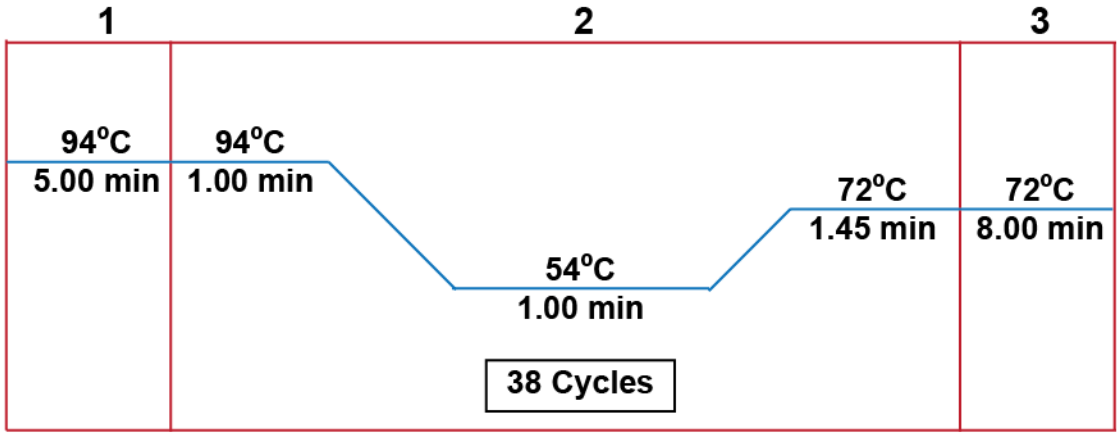

Figure 2.2: PCR conditions required for amplification of AtUPRT gene. Steps involved in PCR, 1-Denaturation, 2-Annealing and 3-Extension.

2.3.7 *Sequence alignment, homology modeling and molecular docking*

To estimate the similarities, the AtUPRT protein sequence was aligned with *E. coli* UPRT by ClustalW (http://www.ebi.ac.uk/Tools/msa/clustalw2/). Based on the further similarity search using Protein BLAST (http://blast.ncbi.nlm.nih.gov/Blast.cgi?PAGE =Proteins), three UPRT templates were chosen from Protein Data Bank (PDB) such as *Burkholderia pseudomallei* UPRT (PDB: 3DMP), *E. coli* UPRT (PDB: 2EHJ) and *Toxoplasma gondii* UPRT (PDB: 1BD4). These templates were used for generating 3D model of AtUPRT using EasyModeller along with the supporting softwares, Modeller 9.14 and Python 2.7. The generated model quality was verified by Structure Analysis and Verification server (SAVES) (nihserver.mbi.ucla.edu/SAVES). For the comparative docking studies, molecular docking of AtUPRT and *E. coli* UPRT was carried out using AutoDock 4.0 with uracil and 5-FU substrates for calculating the binding energies. For homology modeling and docking studies, PyMOL (www.pymol.org) visualization tool was utilized.

2.3.8 Full length cDNA synthesis and cloning of AtUPRT gene into pGEM-T Easy vector

Under optimum conditions of 70-80% humidity at 25^0C with the cycle of 16 h day and 8 h night, *A. thaliana* plant was cultivated in green house. From the well grown *A. thaliana* plant leaves, total RNA was isolated using the protocol employed by [107]. *A. thaliana* mRNA was used as a template for the synthesis of full length cDNA by RevertAid H-minus Reverse Transcriptase Kit (Fermentas) using Oligo(dT)18 primers. This full length cDNA was in turn used as a template for the amplification of AtUPRT gene by polymerase chain reaction (PCR) with the above mentioned (Section 2.3.6) conditions using gene specific primers such as UPP-F and UPP-R (Mentioned in section 2.3.5). Subsequently, the amplified AtUPRT gene was cloned into pGEM-T Easy cloning vector. The clones were confirmed by DNA sequencing (Xcelris, India).

2.3.9 Subcloning into mammalian expression vector pEGFP-N1

pGEM-T Easy-AtUPRT construct was used as the template for amplifying AtUPRT gene by PCR with overhangs having restrictions sites for restriction enzymes *Nhe*I and *Xho*I using the forward and reverse primers mentioned in section 2.3.5, respectively. To study the sole effect of AtUPRT, the reverse primer was designed to incorporate the stop codon resulting in AtUPRT gene expression without the expression of GFP-tag. Subsequently, AtUPRT gene was subcloned into pEGFP-N1 vector.

2.3.10 Construction of pEGFP-N1(-GFP) control plasmid

For appropriate control experiments, pEGFP-N1(-GFP) plasmid was also constructed by removing GFP sequence by restriction digestion using restriction enzymes, *Nhe*I and *Not*I. This was followed by blunt end formation by DNA Polymerase I and ligation.

2.3.11 Transient expression of AtUPRT in HeLa, MCF-7 and A549 and their viability following 5-FU treatment

All the three cell lines (10×10^3 cells/well) were seeded in each well of 96 well plate and kept overnight in 5% CO_2 incubator at 37^0C for the complete adherence of the cells. Plasmid constructs such as pEGFP-N1(-GFP) and pEGFP-N1-AtUPRT, each 100 ng

were transfected into the seeded cells in serum free DMEM media using Lipofectamine 3000 Transfection kit by employing manufacturer's procedure. The cells were incubated in the same transfection media for 6 h for complete transfection. After 6 h of transfection, media was replaced with DMEM media supplemented with 10% FBS for 24 h. The media was again replaced with media containing different concentrations of 5-FU. The transfected HeLa, MCF-7 and A549 were termed as HeLa-UPP, MCF-7-UPP and A549-UPP respectively. The cell viability, following treatment with 5-FU (1-5 µM for HeLa-UPP and 2-6 µM for MCF-7-UPP and A549-UPP) for 72 h, was determined by MTT assay. The whole experiment was carried out in triplicates. Also, the expression of AtUPRT at mRNA level in MCF-7-UPP was confirmed by reverse transcriptase PCR (RTPCR). For the AtUPRT expression confirmation at mRNA level in MCF-7-UPP, after 6 h transfection followed by fresh media (DMEM with 10% FBS) replacement for 24 h, the cells were harvested for mRNA isolation and subsequently the detailed procedure was followed as it has been mentioned in following section (2.3.12). The cell viability (%) using MTT assay was calculate by the equation,

$$\text{Cell Viability (\%)} = \frac{(Abs_{570} - Abs_{690}) \text{ of treated cells}}{(Abs_{570} - Abs_{690}) \text{ of control cells}} \times 100$$

2.3.12 Establishment of stably AtUPRT-expressing HeLa cells (HeLa-UPP)

For transfection, HeLa cells were seeded in the 60 mm culture dish such that around~70% confluency was reached after 24 h. Then, cells were transfected with pEGFP-N1-AtUPRT and pEGFP-N1(-GFP) separately using Lipofectamine 3000 Transfection kit as per manufacturer's protocol. For the selection of stably transfected cells, the media was replaced with DMEM containing G418 antibiotic (800 µg/ml) after 24 h. The cells were under continuous selection pressure with the gradual decrease in the concentration of G418 added from 800 µg/ml to 400 µg/ml. For confirming the HeLa cells stably expressing AtUPRT, non-transfected, pEGFP-N1(-GFP) and pEGFP-N1-AtUPRT transfected cells were seeded to attain 90% confluency. Total RNA was isolated from the cells using GenElute Mammalian Total RNA Miniprep Kit according to the manufacturer's protocol. Complete cDNA was synthesized from 2 µg of total RNA using

High Capacity cDNA Reverse Transcription Kit. Using the cDNA template, AtUPRT gene was amplified by PCR amplification with the conditions mentioned in section 2.3.6 using the forward primer 5'-TATAGGCTAGCAATGGCGTGCT C-3' and reverse primer 5'-GCTCGAGTCACTTCACCCAATGTG-3'.

2.3.13 Cell viability assessment to study the effects of 5-FU treatment

HeLa, HeLa-pEGFP-N1(-GFP) and HeLa-UPP cells were seeded (5000 cells/well) in 96-well plates and grown overnight. Next day, culture media was replaced with fresh media containing different concentrations of 5-FU (1–9 µM) and incubated for another 72 h. Post-treatment, cell viability was assessed by MTT assay using the equation as mentioned in section 2.3.11. All the experiments were performed in triplicates.

2.3.14 Methylene blue staining for analysis of morphological changes

To analyze morphological changes due to 5-FU (4 µM) treatment (24 h,48 h and 72 h), treated cells were fixed with chilled 70% ethanol, stained with 0.2% (w/v) methylene blue and observed under bright field microscope. A lower concentration of 5-FU (4 µM) was chosen in order to observe the morphological changes in the treated cells over a prolonged period of time (up to 72 h). All the experiments were performed in triplicates.

2.3.15 Annexin V-fluorescein isothiocyanate (FITC)/propidium iodide (PI) staining for detecting apoptosis

The extent of apoptosis in 5-FU treated HeLa-UPP cells was measured by using Annexin V-FITC Apoptosis Detection Kit I according to the manufacturer's protocol. HeLa-pEGFP-N1(-GFP) and HeLa-UPP cells (seeded at 8×10^4 cells/well in 6-well plate) were treated with 10 µM (~2 × IC50) 5-FU for 72 h. The experiment was performed at 10 µM of 5-FU based on preliminary experiments that demonstrated well-distinguished apoptosis in HeLa-UPP cells at this concentration. The treated cells were stained with Annexin V-FITC and PI (15 min in dark) for assessment in a FACS Calibur flow cytometer using CellQuest Pro software.

2.3.16 JC-1 staining to assess mitochondrial membrane potential in apoptotic cells

HeLa, HeLa-pEGFP-N1(-GFP) and HeLa-UPP were seeded (10×10^4 cells/well) in 6 well plate and treated with 4 µM 5-FU for 72 h. Similar to evaluating morphological changes, 4 µM of 5-FU was chosen to observe the mitochondrial integrity in treated cells over a prolonged period of time (72 h). After the treatment, the cells were washed twice with 1X phosphate buffered saline (PBS) and incubated with 5 µM JC-1 in 1 ml DMEM media at 37^0C in dark for 10 min. The JC-1 stained cells were immediately visualized under Epi-fluorescence microscope for green and red fluorescence [108].

2.3.17 Analysis of cell cycle in HeLa-UPP in response to 5-FU

For cell cycle analysis, HeLa-pEGFP-N1(-GFP) and HeLa-UPP cells, seeded in 6-well plate (9×10^4 cells/well), were serum starved for 48 h and then treated for 24 h with 10 µM 5-FU. The cells were harvested, washed, fixed, permeabilized and stained with PI according to previous methods [109] before analysing in a FacsCalibur flow cytometer. It may be mentioned here that HeLa-UPP cells were treated with higher concentration i.e. 10 µM (~2 × IC50) of 5-FU due to shorter incubation time (24 h) employed for cell cycle and following gene expression analyses.

2.3.18 Cell cycle related gene expression analyses in HeLa-UPP in response to 5-FU

For gene expression analysis, the cells were treated with 5-FU in similar way as mentioned in section 2.3.17. Cells were harvested and total RNA was isolated for cDNA synthesis as mentioned above. Real time PCR amplification of the cDNA was performed using Rotor-Gene SYBR Green PCR kit and the gene expression measured with Rotor-Gene Q Software 2.3.1.49.

2.3.19 Clonogenic assay

500 cells of untreated and treated (4 µM 5-FU for 72 h) HeLa,HeLa-pEGFP-N1 (-GFP) and HeLa-UPP were seeded in 4 ml fresh media in 6 well plate and incubated for 12 days with media replacement in every 3 days. After 12 days, formed colonies were fixed with chilled 70% ethanol, stained with crystal violet (4% w/v) for 2 min and then counted.

The plating efficiency and survival fraction were calculated as [110, 111]:

Plating efficiency (%) = (Number of colonies counted/Number of cells plated) × 100

Survival fraction = Plating efficiency of treated cells/ Plating efficiency of control cells

2.4 Results and discussion

2.4.1 Homology modeling and molecular docking

The result of sequence alignment of AtUPRT with *E. coli* UPRT protein showed 40.7% matching score. The uracil and PRPP binding motifs were found to be well conserved (Figure 2.3). The three-dimensional structure of AtUPRT (Figure 2.4) was generated by homology modeling and the best model was selected based on dope score. The modeled structure was verified using ERRAT, PROCHECK and PROVE programs through SAVES for *in silico* docking studies. Molecular docking revealed that uracil and 5-FU were able to bind to the predicted uracil-binding motif of AtUPRT, with the calculated binding energies of −4.41 kcal/mol and −4.36 kcal/mol, respectively (Figure. 2.5a,b). These values were found to be lower than those of *E. coli* UPRT for uracil (−3.8 kcal/mol) and 5-FU (−3.74 kcal/mol) (Figure. 2.5c,d), indicating the potential of AtUPRT as a better candidate for binding 5-FU as compared to *E. coli* UPRT. Hence, further experiments were carried out to verify the effect of AtUPRT expression in cancer cells *in vitro*, especially in terms of their response toward prodrug 5-FU treatment.

```
A. thaliana UPRT MACSIGNAFRCSSDTLRFAPRQQCSSRLNPNPSSFLSFNSSPILAQNLGASSSSLSRRTI
E. coli UPRT     ----------------------------------------MAK-------------
                                                         :*:

A. thaliana UPRT RARTKMAASEASINGSNRMLVFVPPHPLIKHWISVLRNEQTPCPVFRNAIAELGRLLMYE
E. coli UPRT     -------------------IVEVKHPLVKHKLGLMREQDISTKRFRELASEVGSLLTYE
                                   :.   ***:** :.::*::: .   **:  :*:* ** **

A. thaliana UPRT ASREWLPTVVGEIMSPMGPASVEFIDPREPIAVVPILRAGLALAEHASSVLPANKIYHLG
E. coli UPRT     ATAD-LETEKVTIEGWNGPVEIDQIKGKK-ITVVPILRAGLGMMDGVLENVPSARISVVG
                 *: : * *    * .  **..:: *. :: *:*********.: : . . :*: :*  :*
                                                PRPP binding site
A. thaliana UPRT VSRDEKTLLPSVYLNKLPDEFPKNSRVFLVDPVLATGGTINAAMDLLKERGLSVQQIKVI
E. coli UPRT     MYRNEETLEPVPYFQKLVSNIDER-MALIVDPMLATGGSVIATIDLLKKAGCSS--IKVL
                 : *:*:** *  *::** .:: :.  .::***:*****::*::****: * *   ***:
                                                Uracil binding site
A. thaliana UPRT CAIAAPPALSKLNEKFPGLHVYAGIIDPEVNEKGYIIPGLGDAGDRSFGTE-HWVK
E. coli UPRT     VLVAAPEGIAALEKAHPDVELYTASIDQGLNEHGYIIPGLGDAGDKIFGTK-----
                   :*** .:: *:: .*.:.:*:. **  :**:************: ***:
```

Figure 2.3: Sequence alignment of AtUPRT gene with *E. coli* UPRT gene.

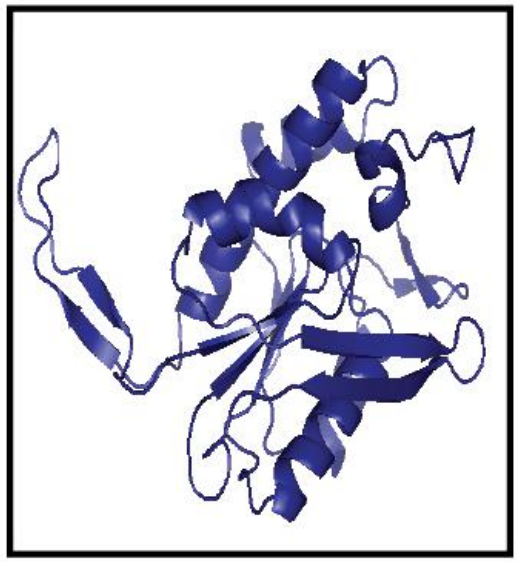

Figure 2.4: Homology modeling of AtUPRT using Easy Modeller.

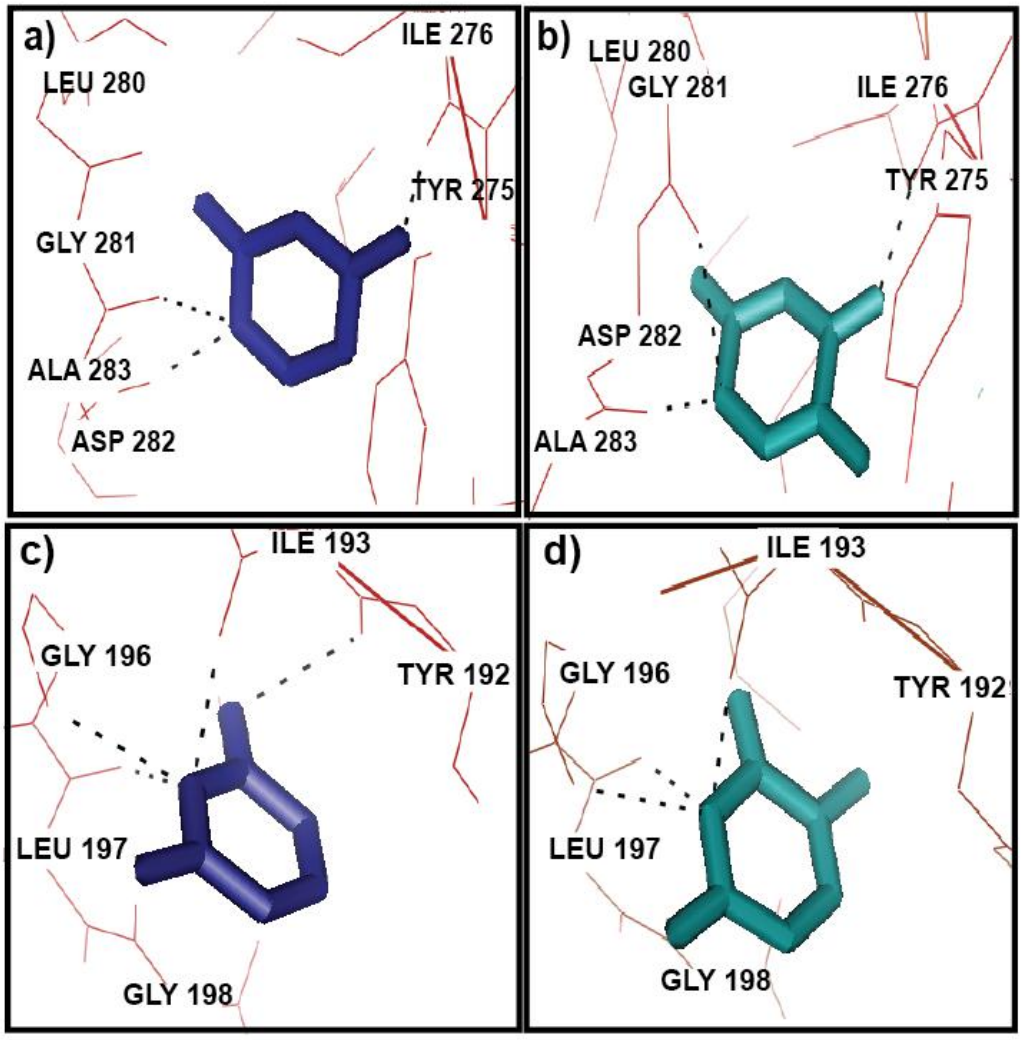

Figure 2.5: Molecular docking of AtUPRT (**a** & **b**) and *E. coli* UPRT (**c** & **d**) with uracil (blue) and 5-flurouracil (cyan) using AutoDock 4.0.

2.4.2 Full length cDNA synthesis, PCR amplification and cloning of AtUPRT gene into pGEM-T Easy vector

Full length cDNA was synthesized from the isolated total RNA which was followed by PCR amplification of AtUPRT gene (891 bp) (Figure 2.6a). Amplified AtUPRT gene was cloned into pGEM-T Easy cloning vector and subsequently confirmed by restriction digestion using *Eco*RI enzyme (Figure. 2.6b). The amplified AtUPRT gene was confirmed by sequence analysis (Figure 2.7).

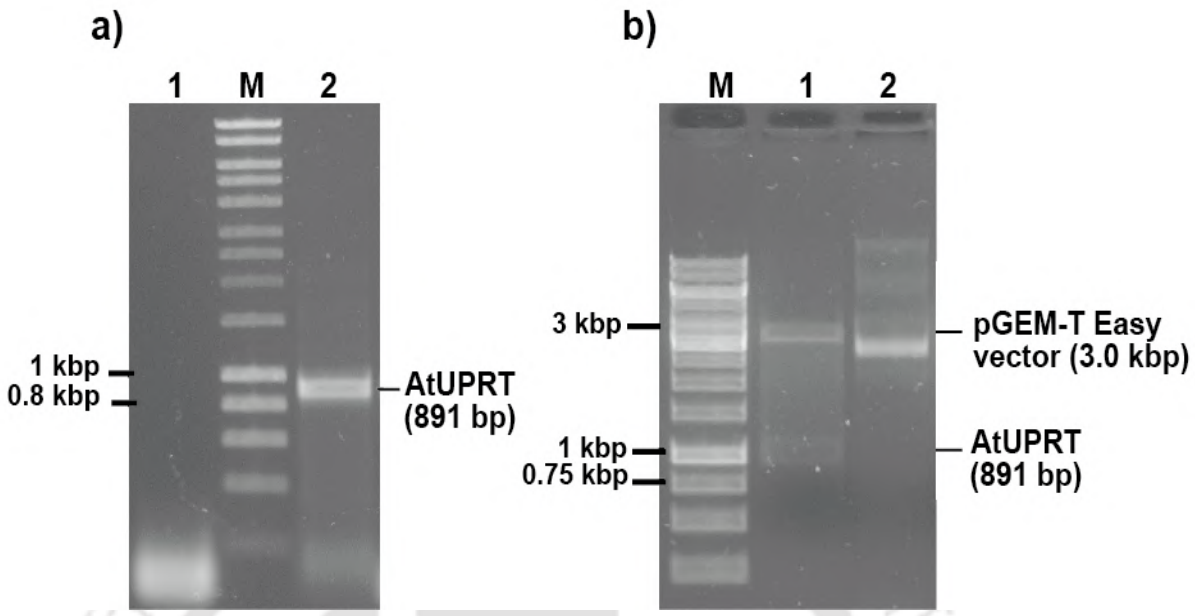

Figure 2.6: a. PCR amplification of AtUPRT gene (891 bp) from cDNA of *A. thaliana*. *Lane* 1- Negative control, *Lane* M- DNA marker (10 kbp- 200 bp) and *Lane* 2- PCR amplified AtUPRT gene. **b.** Cloning of AtUPRT gene into pGEM-T Easy vector. *Lane* M- DNA marker (10 kbp- 250 bp), *lane* 1- Digested pGEM-T Easy vector (3 kbp) containing AtUPRT insert (891 bp) by *Not*I restriction enzyme and *lane* 2- Uncut pGEM-T Easy vector containing AtUPRT insert.

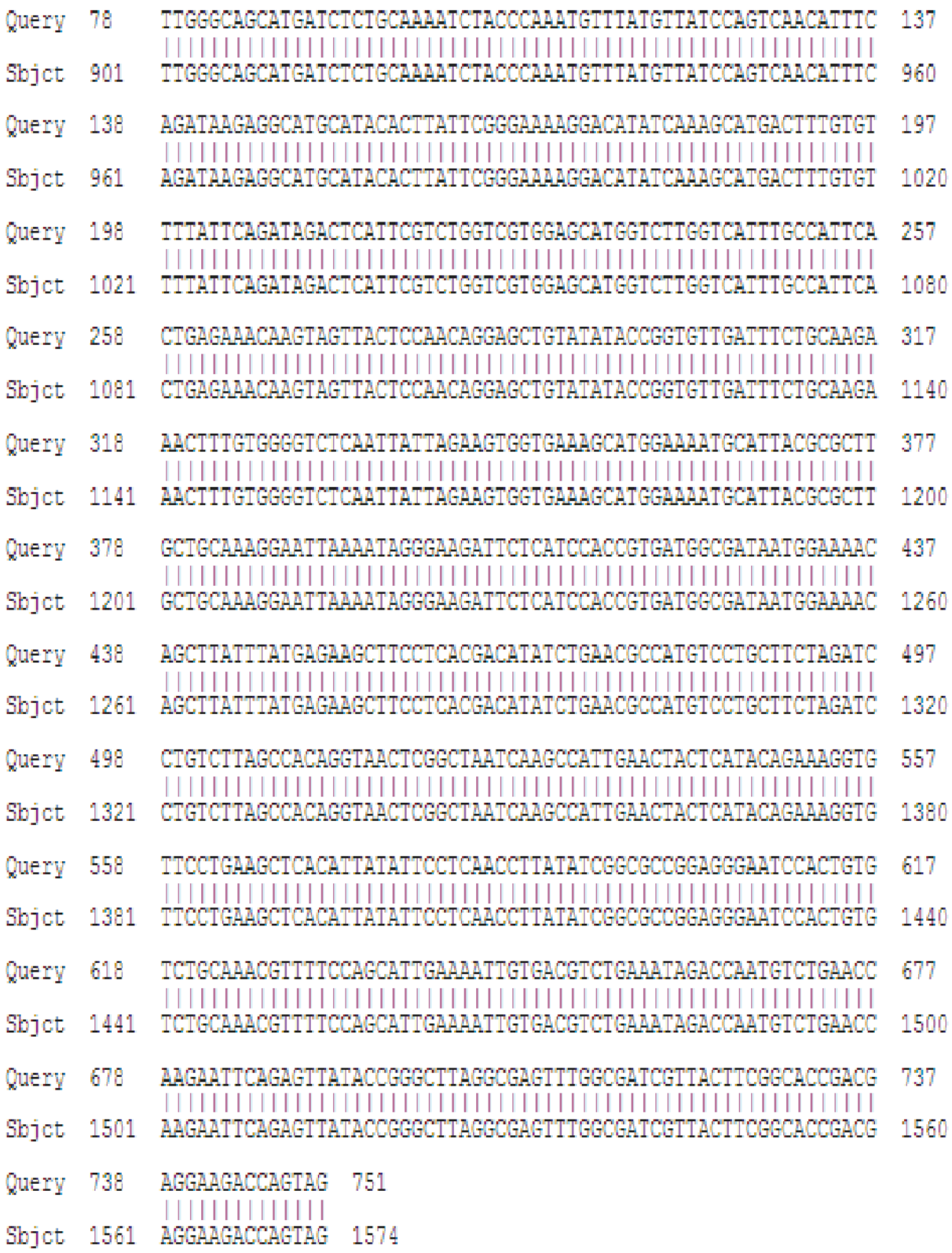

Figure 2.7: DNA sequence analysis of AtUPRT gene cloned into pGEM-T Easy vector.

2.4.3 Subcloning of AtUPRT gene into mammalian pEGFP-N1 expression vector and construction of pEGFP-N1(-GFP) vector control

Finally, AtUPRT gene was subcloned into the pEGFP-N1 (4.7 kbp) mammalian expression vector and the recombinant clone were confirmed by the release of 891 bp fragment upon double digestion with *Nhe*I and *Xho*I enzymes (Figure 2.8a).The constructed plasmid pEGFP-N1(-GFP) was also confirmed by the single restriction digestion of pEGFP-N1(-GFP) and pEGFP-N1 vector using *Nde*I. Based on the smaller size of pEGFP-N1(-GFP) (3.9 kbp) with respect to pEGFP-N1 (4.7 kbp), it was confirmed that there was a successful removal of GFP sequence from pEGFP-N1 vector (Figure 2.8b).

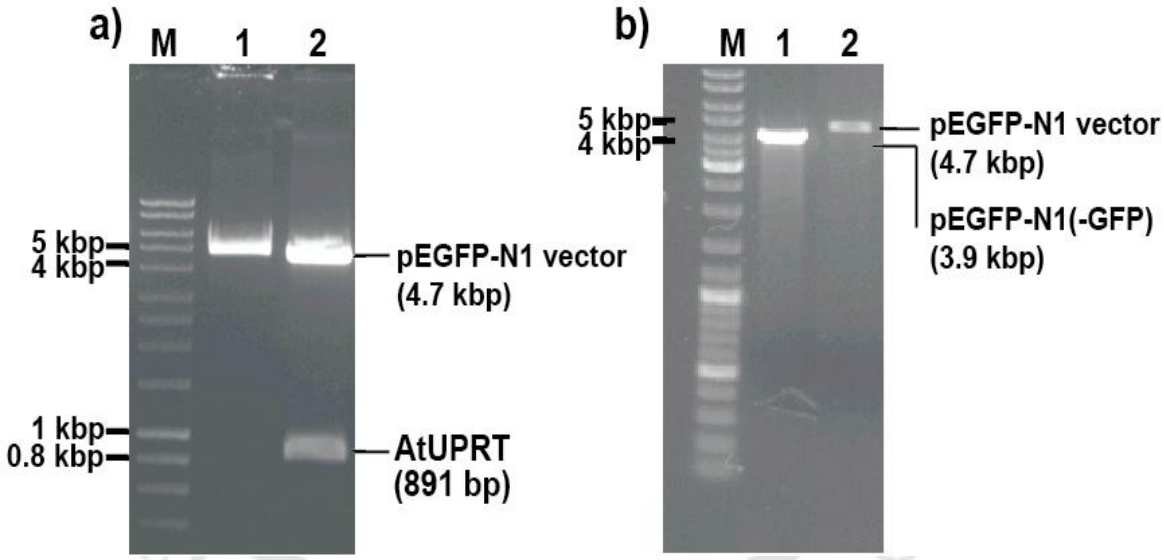

Figure 2.8: a. Subcloning of AtUPRT gene into pEGFP-N1 mammalian expression vector. *Lane* M- DNA marker (10 kbp-200 bp), *lane* 1- Uncut pEGFP-N1 vector (4.7 kbp) containing AtUPRT gene (891 bp) and *lane* 2- Digested pEGFP-N1 vector (4.7 kbp) releasing AtUPRT gene (891 bp). **b.** Construction of pEGFP-N1(-GFP) control plasmid. *Lane* M- DNA marker (10 kbp-200 bp), *lane* 2 & 3- Digested pEGFP-N1(-GFP) (3.9 kbp) and pEGFP-N1 (4.7 kbp) with *Nde*I restriction enzyme respectively.

2.4.4 Transient expression of AtUPRT in HeLa, MCF-7 and A549 and their viability following 5-FU treatment

The transient expression of AtUPRT was confirmed in MCF-7 cell line (Figure 2.9). The cell viability assessment of AtUPRT transiently expressing HeLa, MCF-7 and A549 cells showed that only HeLa cells showed a responsive decrease in cell viability along with the increase in the 5-FU dose within a lower concentration range (1- 5 µM) (Figure 2.10). Hence based on the result of the cell viability assays, HeLa cells were chosen for the further studies on stable expression of AtUPRT and its effect on cancer cells upon 5-FU treatment.

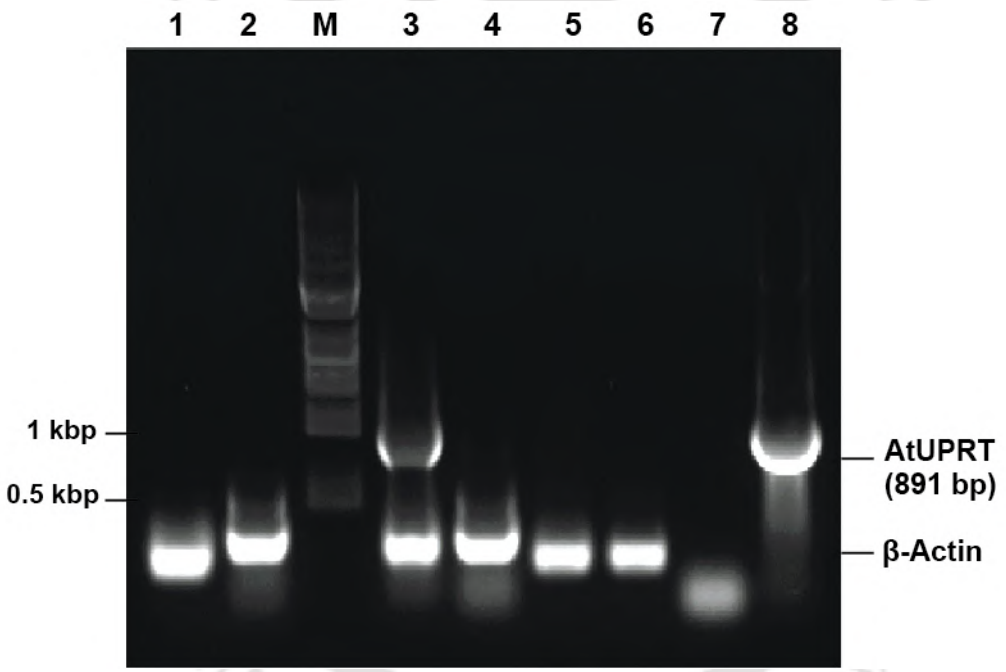

Figure 2.9: Confirmation of AtUPRT mRNA expression in MCF-7-UPP by RT-PCR. *Lane* M - DNA marker (10 kbp-0.5 kbp), *lane* 1, 5, 6 - β-Actin control of untransfected MCF-7, MCF-7-UPP and MCF-7-pEGFP-N1(-GFP),respectively, *lane* 3 - Amplification of AtUPRT gene (891 bp) on cDNA synthesized from MCF-7-UPP, *lane* 2, 4 -Absence of AtUPRT gene amplification in untransfected MCF-7 and MCF-7-pEGFP-N1(-GFP),respectively, *lane* 7- Negative control and *lane* 8- Positive control.

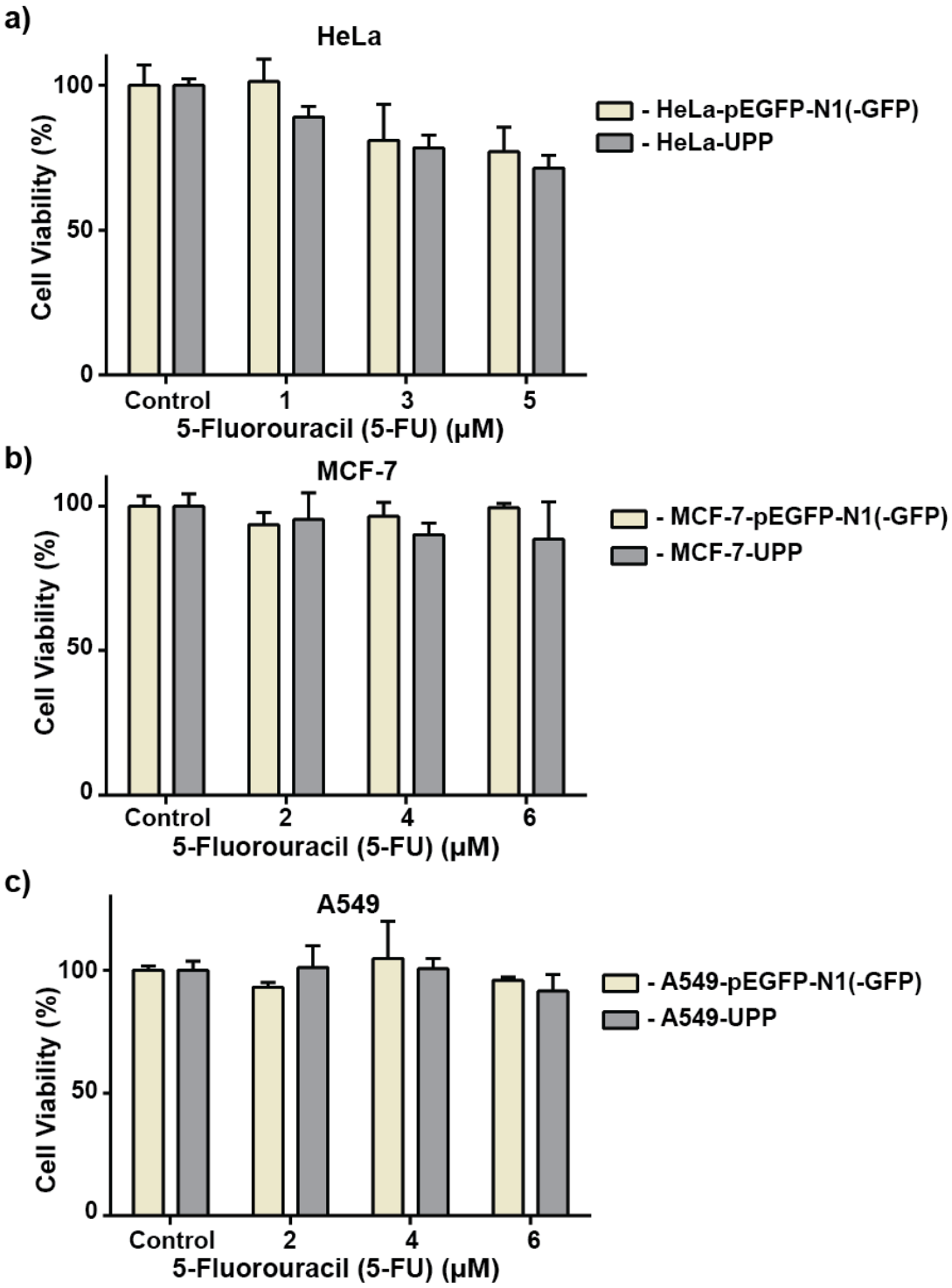

Figure 2.10: Cell viability assessment of 5-FU treated HeLa-UPP, MCF-7-UPP and A549-UPP cells which are transiently transfected with AtUPRT gene. HeLa-pEGFP-N1(-GFP), MCF-7-pEGFP-N1(-GFP) and A549-pEGFP-N1(-GFP) were transfected with control pEGFP-N1(-GFP) plasmid.

2.4.5 Establishment of stably AtUPRT-expressing HeLa cells (HeLa-UPP)

The HeLa cells were transfected with pEGFP-N1-AtUPRT and the stable cells were selected and designated as HeLa-UPP cells. The mRNA expression of AtUPRT in HeLa-UPP was confirmed by amplifying the gene from cDNA templates synthesized from the total RNA isolated from the transfected cells (Figure 2.11). However, the expression of AtUPRT at protein level could not be verified in the present study due to non-availability of commercial antibodies. Notably, HeLa cells were also transfected with only vector (pEGFP-N1(-GFP)), denoted as HeLa-pEGFP-N1(-GFP), for appropriate control experiments.

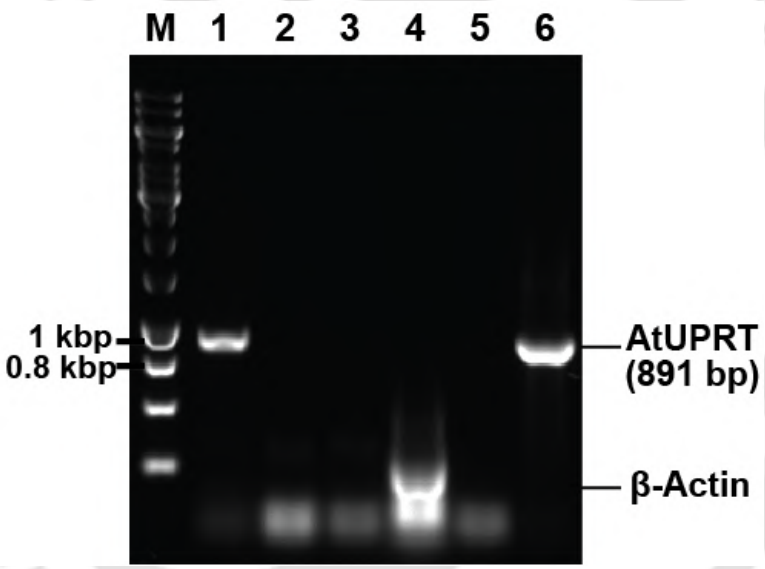

Figure 2.11: Reverse transcriptase PCR (RT- PCR) confirmation of HeLa cells stably expressing AtUPRT gene. *Lane* M- DNA marker (10 kbp–250 bp), *lane* 1- AtUPRT gene (891 bp) amplified on cDNA templates synthesized from RNA isolated from HeLa-UPP, *lane* 2 & 3- Absence of AtUPRT gene amplification in non-transfected HeLa and HeLa-pEGFP-N1(-GFP), respectively, *lane* 4- β-Actin control (254 bp), *lane* 5- Negative control and *lane* 6- Positive control.

2.4.6 MTT assay for cell viability analysis

Interestingly, the viability (%) of HeLa-UPP cells, when treated with 5-FU for 72 h, was observed to decrease significantly as compared to those of HeLa and HeLa-pEGFP-N1(-

GFP) cells (Figure 2.12). The IC50 of 5-FU for HeLa, HeLa-pEGFP-N1(-GFP)and HeLa-UPP cells were calculated to be 6.1 µM, 7 µM and 5.2 µM, respectively. These results indicated the possibility of exploiting AtUPRT in potential suicide gene therapy of cancer cells.

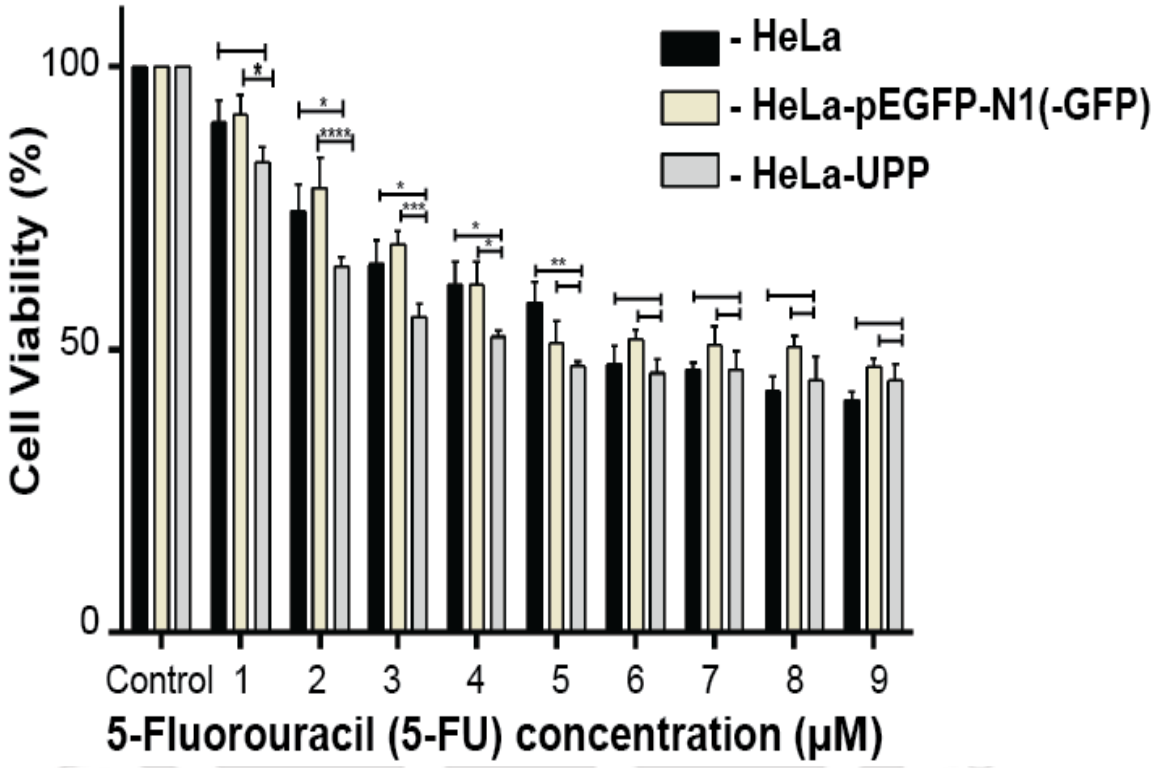

Figure 2.12: Cell viability in non-transfected HeLa, HeLa-pEGFP-N1(-GFP) and HeLa-UPP cells following 5-FU (1–9 µM) treatment for 72 h. The statistical significance was estimated by ANOVA using GraphPad Prism 6 software, where *p < 0.05, **p < 0.01, ***p < 0.001 and ****p < 0.0001.

2.4.7 Methylene blue staining for morphological changes analysis

The change in morphology of HeLa cells as a result of 5-FU treatment, if any, was examined by methylene blue staining (Figure 2.13). When compared with non-transfected HeLa cells, there were no apparent morphological changes observed in non-treated HeLa-UPP cells due to the expression of AtUPRT only. Moreover, non-transfected HeLa and HeLa-pEGFPN1(-GFP) cells remained morphologically unaltered during the 5-FU treatment (Figure 2.13a). However, even at early hours (24 h) of

treatment with 5-FU, the morphology of HeLa-UPP cells changed from regular shape to rounded one (Figure 2.13b). The results of the viability assay along with morphological analysis clearly indicated that the HeLa cells became more susceptible to prodrug (5-FU) treatment after transfection with AtUPRT.

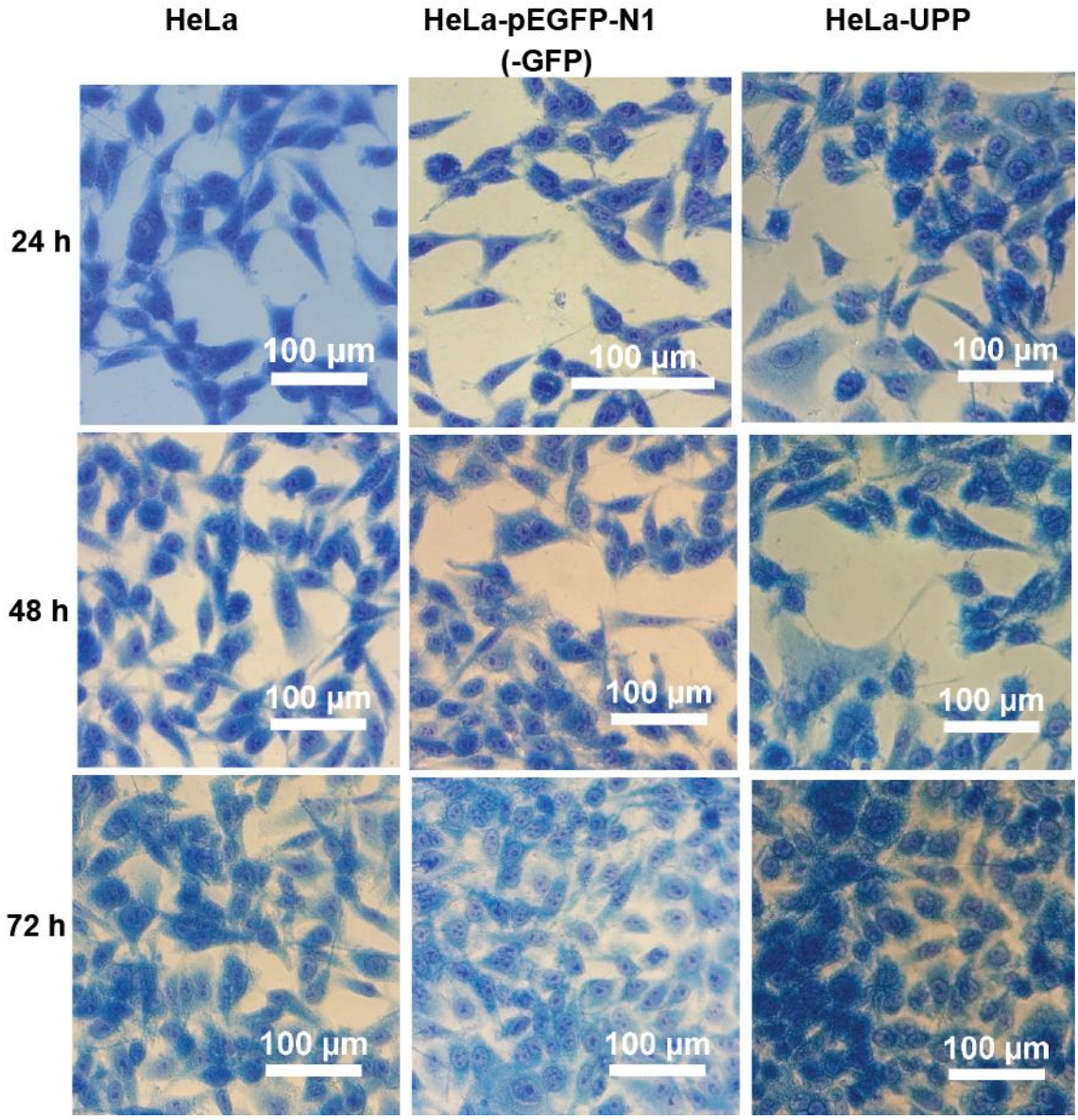

Figure 2.13a: Methylene blue staining to study the morphological changes in non-treated HeLa, HeLa-pEGFP-N1(-GFP) and HeLa-UPP at 24 h, 48 h and 72 h.

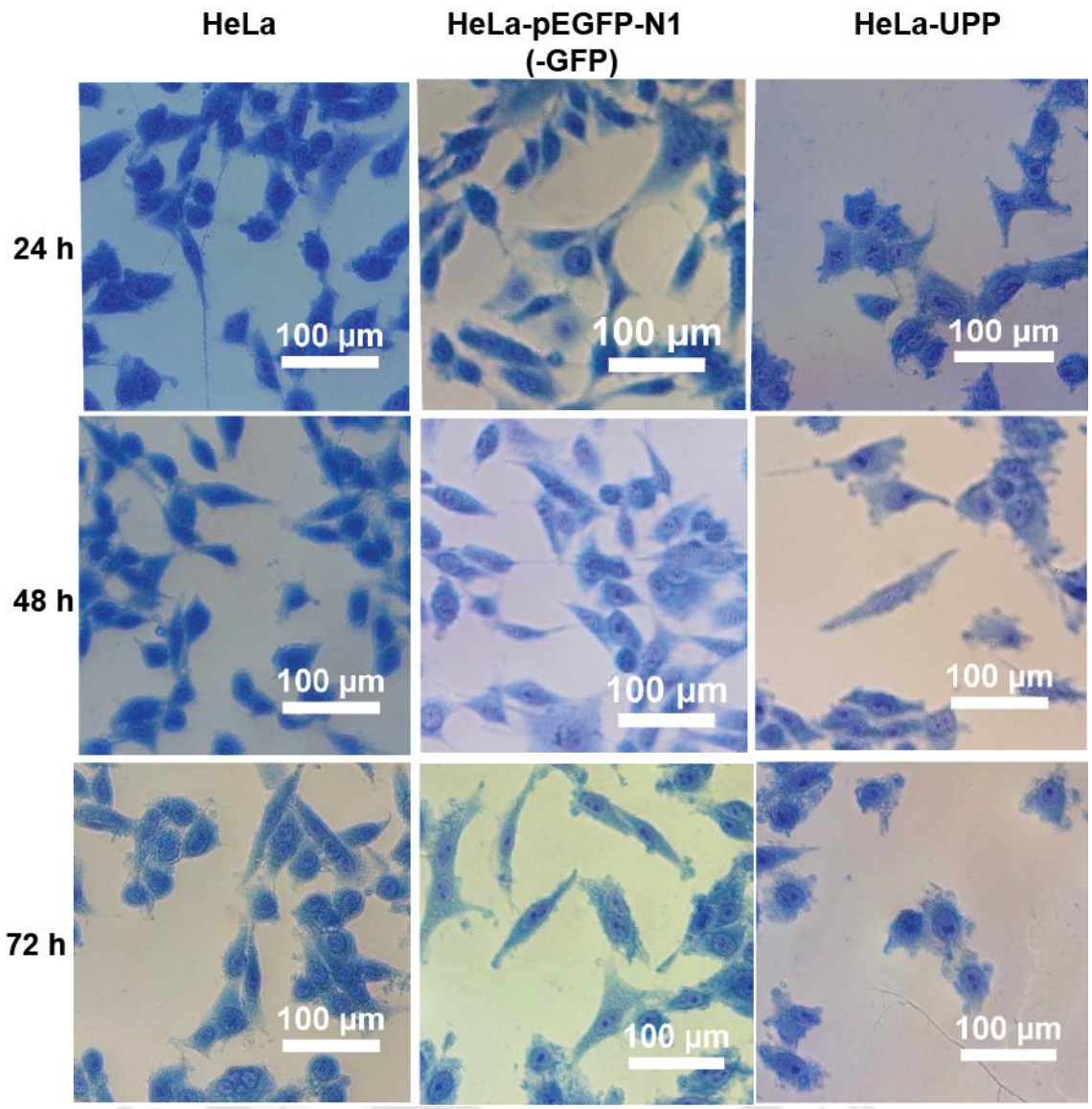

Figure 2.13b: Methylene blue staining to study the morphological changes in HeLa, HeLa-pEGFP-N1(-GFP) and HeLa-UPP upon 5-FU (4 µM) treatment at 24 h, 48 h and 72 h.

2.4.8 Annexin V-fluorescein isothiocyanate (FITC)/propidium iodide (PI) staining for detecting apoptosis using flow cytometer analysis

As 5-FU is reported to induce apoptosis in a number of cancer cells [112], the mode of cell death in 5-FU treated HeLa-UPP cells in the present study was investigated by flow cytometric analysis of Annexin V-FITC/PI stained cells. Figure 2.14 shows that 5-FU

induced apoptosis in both HeLa-pEGFP-N1(-GFP) (~17%) and HeLa-UPP (~27%) cells. However, the degree of apoptosis was more pronounced in case of HeLa-UPP cells.

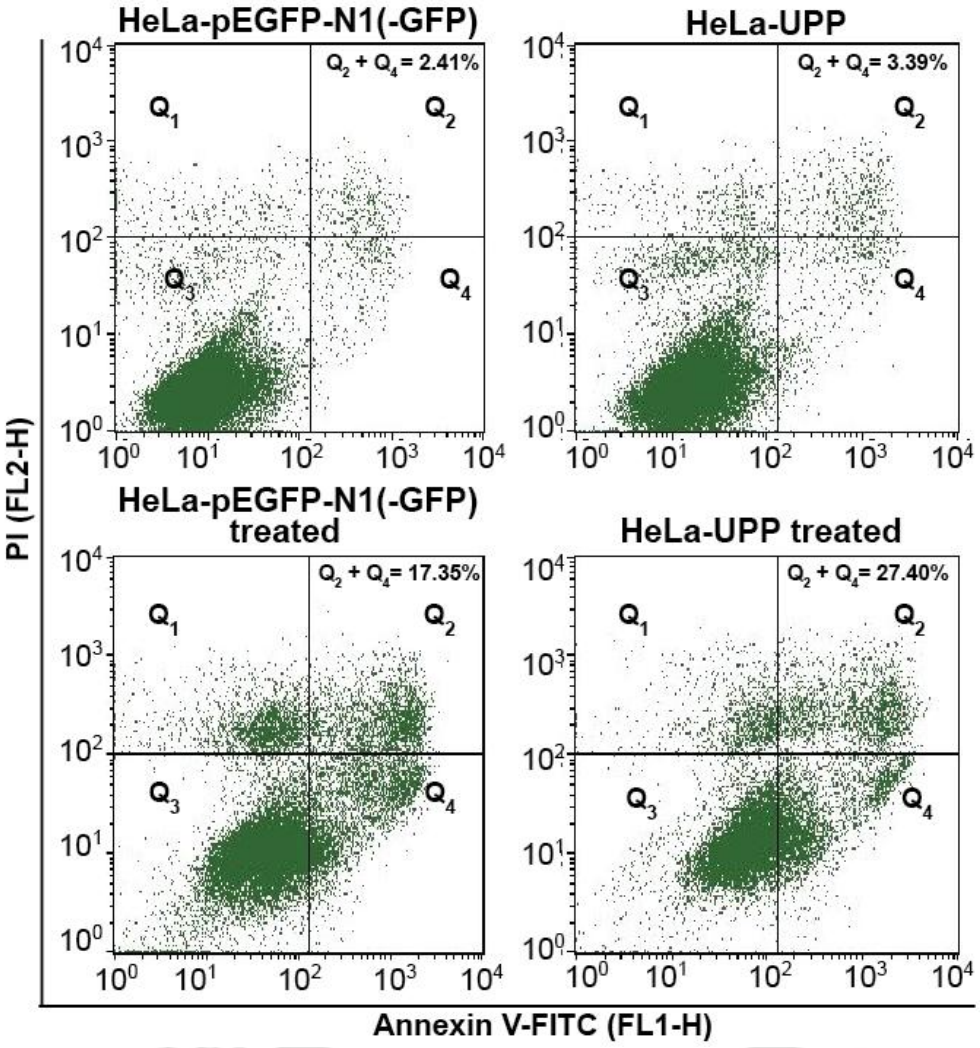

Figure 2.14: Flow cytometric assessment of apoptosis by Annexin V-FITC/PI staining in HeLa-pEGFP-N1(-GFP) and HeLa-UPP cells following 10 µM 5-FU treatment showed 17.35% and 27.4% apoptotic cells, respectively.

2.4.9 JC-1 staining to assess mitochondrial membrane potential (Δψm) in apoptotic cells

As the mitochondrial membrane gets affected during the apoptosis, we further examined the integrity of mitochondrial trans-membrane potential in 5-FU treated HeLa cells by JC-1 staining (Figure 2.15). Untreated healthy control cells with high Δψm displayed red

fluorescence due to JC-1 aggregates inside the mitochondria. However, compared to 5-FU treated HeLa and HeLa-pEGFP-N1(-GFP) cells, a majority of the treated HeLa-UPP cells were observed to emit green fluorescence because of the diffusion of the JC-1 monomer due to the damage in mitochondrial membrane potential.

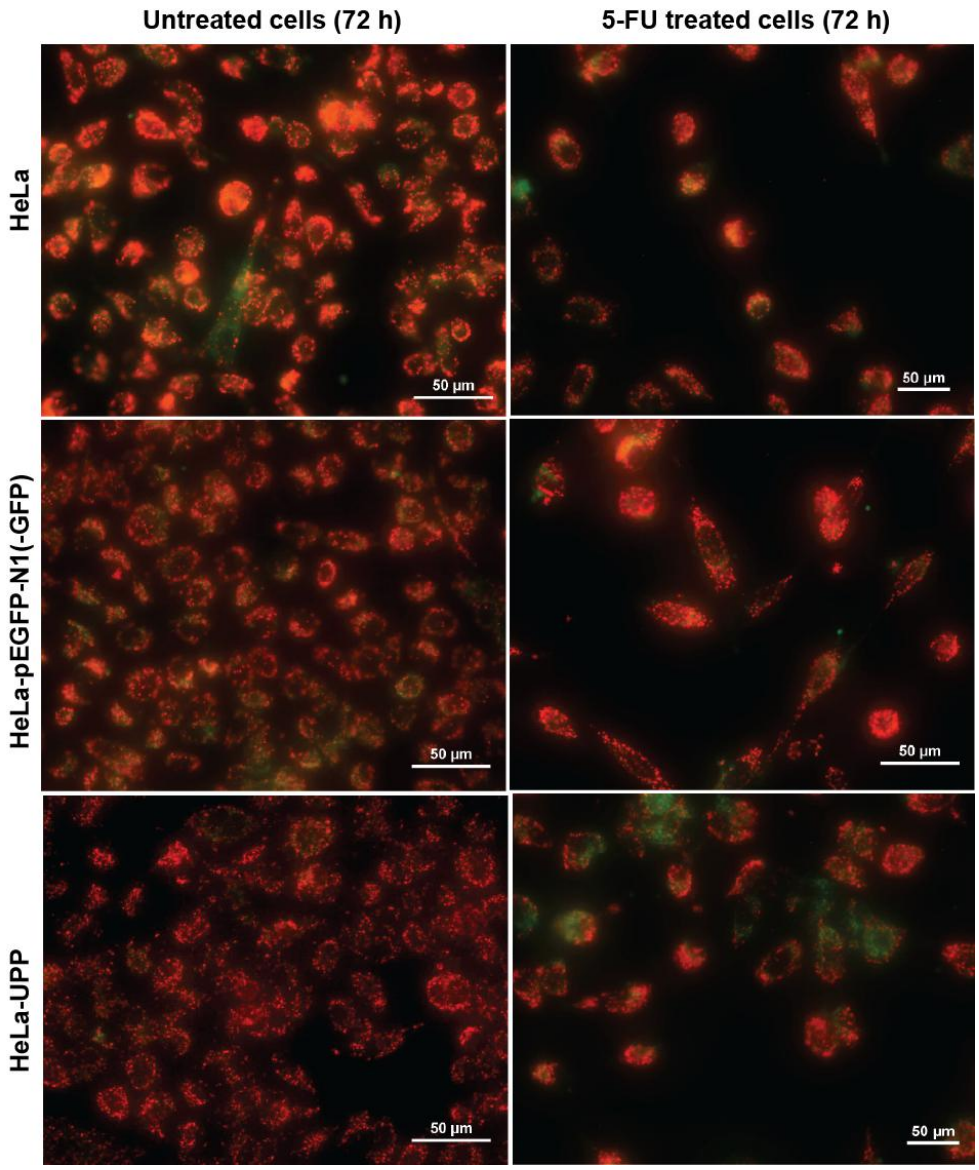

Figure 2.15: Fluorescence microscopic images of JC-1 stained HeLa, HeLa-pEGFP-N1(-GFP) and HeLa-UPP cells demonstrated the damage in mitochondrial membrane potential in HeLa-UPP cells following 5-FU treatment.

2.4.10 Cell cycle analysis using PI staining

5-FU acts during S phase in cell cycle by interrupting DNA synthesis through the inhibition of thymidylate synthetase [112]. The cell cycle analysis in the present study revealed that 5-FU treatment induced G1 and S phase arrest in Hela-pEGFP-N1(-GFP) cells. Interestingly, 5-FU treated HeLa-UPP cells were observed to be predominantly arrested at S phase without significant G1 arrest (Figure 2.16). The differential response of HeLa-UPP and HeLa-pEGFPN1(-GFP) to 5-FU treatment could be due to the AtUPRTase activity, in addition to the inherent mammalian 5-FU metabolizing mechanism [16] in Hela-UPP. The presence of AtUPRT is expected to contribute to higher rate of conversion of 5-FU into 5-FdUMP which in turn, inhibits more of thymidylate synthetase, and there by arresting the HeLa-UPP cells at S phase more efficiently.

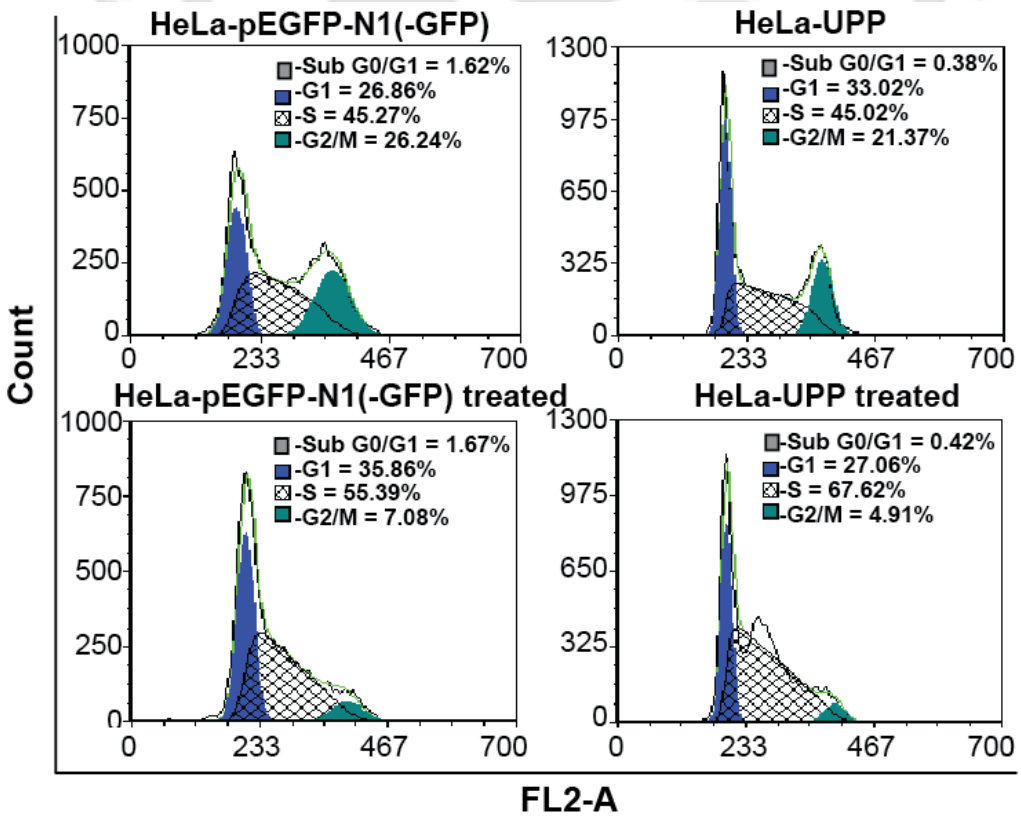

Figure 2.16: Cell cycle analysis showing the G1/S phase arrest of HeLa-pEGFP-N1(-GFP) cells and complete S phase arrest of HeLa-UPP cells upon 5-FU treatment.

2.4.11 RT PCR analysis

In order to gain further insight on the 5-FU mediated cell cycle arrest in HeLa-UPP cells, quantitative real time PCR analyses were carried out for examining the expression of cyclin D1 and p21, two key genes involved in regulation of cell cycle. Although upregulation of cyclin D1 in response to 5-FU treatment is reported [113], our results show the upregulation of p21 also, along with cyclin D1 in 5-FU treated HeLa-UPP cells (Figure 2.17). Though p21 is known to block the cell cycle at G1 phase, its inhibiting role is highly dependent on its relative expression level with respect to CDK4/cyclin D1. At low p21: CDK4/cyclin D1 ratio, p21 promotes the kinase activity of the CDK4/cyclin D1 complex inducing cells to enter into S phase [114]. However, p21 can inhibit the same kinase activity of the complex blocking the cell cycle at G1 phase at high p21: CDK4/cyclin D1 ratio. The lower p21:cyclin D1 expression ratio observed in HeLa-UPP cells, as compared to the HeLa-pEGFP-N1(-GFP), could be responsible for the noted increase in the S phase arrest in the AtUPRT expressing HeLa cells. However, the complete elucidation of the mechanism involved in 5-FU mediated alteration of cell cycle in HeLa-UPP cells requires further investigation in future.

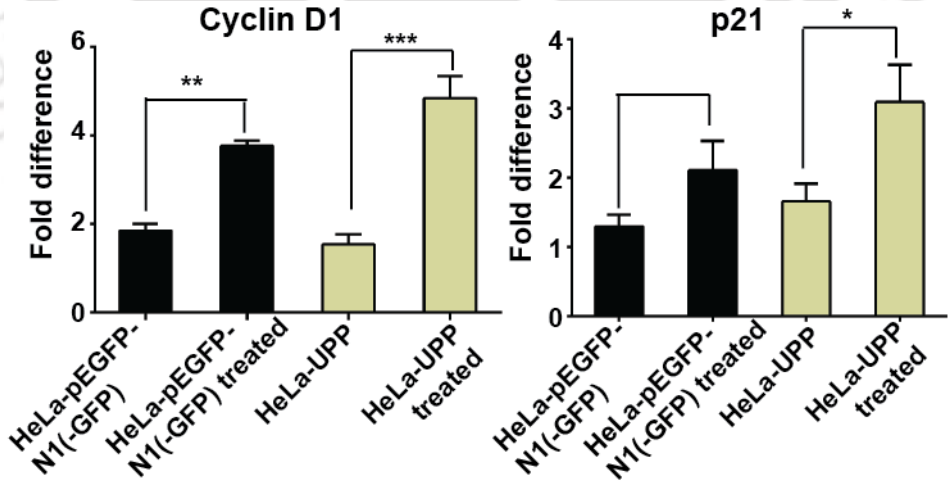

Figure 2.17: Quantitative real-time PCR analysis of cyclin D1 and p21 in 5-FU treated HeLa-UPP and HeLa-pEGFP-N1(-GFP) cells. The statistical significance was estimated by ANOVA using GraphPad Prism 6 software, where *$p < 0.05$, **$p < 0.01$ and ***$p < 0.001$.

2.4.12 Clonogenic assay

By performing the clonogenic assay, the survival fraction of HeLa-UPP cells, following the treatment with 4 µM 5-FU, was calculated to be 0.227 which was 0.53 and 0.62 times of HeLa and HeLa-pEGFP-N1(-GFP), respectively (Figure 2.18).

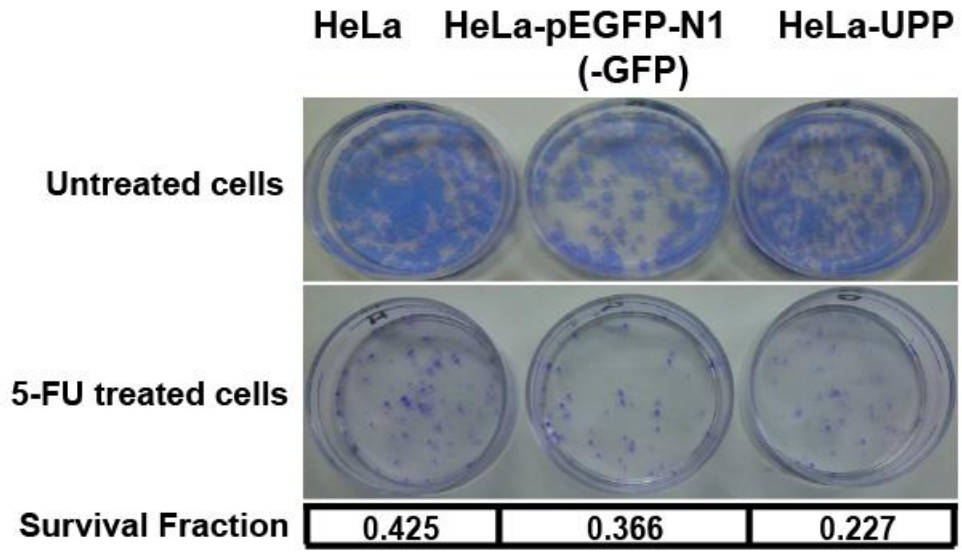

Figure 2.18: Clonogenic assay revealing the survival efficiencies of HeLa, HeLa-pEGFP-N1(-GFP) and HeLa-UPP cells after 5-FU treatment.

2.5 Conclusion

AtUPRT was cloned into mammalian expression vector and expressed in HeLa cells establishing stable HeLa-UPP cells. The HeLa-UPP cells were efficiently sensitized towards chemotherapeutic agent 5-FU with IC50 value of 5.2 µM. Induction of apoptosis and associated damage in mitochondrial membrane was demonstrated in 5-FU treated HeLa-UPP cells. 5-FU treatment was also shown to arrest HeLa-UPP cells in S-phase due to proposed tweaking in the relative expression level of cyclin D1 and p21 by the prodrug in presence of AtUPRT. Survival efficiency of 5-FU treated HeLa-UPP was found to be 0.53 and 0.62 fold lower than non- and vector-transfected HeLa cells implying the importance of AtUPRT in augmenting the treatment efficacy of 5-FU in vitro. The work presented in this chapter 2 is the first report of successful expression of a plant (*A. thaliana*) UPRT in human cancer cells with substantial sensitization toward prodrug 5-

FU. The current investigations could serve as a platform for future studies exploring potential of plant UPRTs in cancer gene therapy.

CHAPTER 3

Plant Phytaspase- Heterologous expression and functional characterization on its Caspase like behavior

[The major part of this chapter is published as- Sharmila Narayanan, Pallab Sanpui, Lingaraj Sahoo and Siddhartha Sankar Ghosh **(2016).** Heterologous Expression and Functional Characterization of Phytaspase, a Caspase-Like Plant Protease, ***International Journal of Biological Macromolecules***. 95, 288-293]

CHAPTER 3

Plant Phytaspase- Heterologous Expression and Functional Characterization on Its Caspase like Behavior

3.1 Introduction

A family of cysteine-dependent aspartate-specific proteases, widely known as caspases, is the central module responsible for the initiation and execution of 'apoptosis' – a well-studied form of PCD in animals [115]. Although characteristics hallmarks of PCD in plants – such as cell shrinkage, DNA fragmentation and release of cytochrome c from mitochondria – resembles to that of animals, surprisingly they lack structural homologs to animal caspases. However, recent studies have established the presence of several plant proteases that are structurally not similar to caspases but demonstrate 'caspase-like' aspartate-specific proteolytic activities during PCD in plants [103, 104]. One such functional analogue of caspases is phytaspase which is a member of the family of serine-dependent subtilisin-like proteases and capable of hydrolyzing synthetic peptide substrates of caspase 6, 8 and 9 [104, 105]. Studies on phytaspase from tobacco (*Nicotiana tabacum*) reveals that it is produced as inactive pre-proenzyme (pre-prophytaspase, 763 amino acids, 82 kDa), autocatalytically processed inside the cell into an active mature enzyme (mature phytaspase, 646 amino acids, 69.5 kDa) and finally secreted into the 'apoplast'[103, 104]. Although complete cellular mechanism remains to be explored, mature phytaspases are believed to enter the cytoplasm and prepare the cell for PCD under biotic/abiotic stress. Moreover, a strong correlation between phytaspase expression and plant PCD has been established [116].

A number of plant-based natural products and their derivatives, owing to their therapeutic potential, have made their ways into clinical trials for treating various diseases [1]. Additionally, potential of various plant genes such as, linamarase [117], thymidine kinase1[118], saporin [75, 76] and horseradish peroxidase (HRP) [119] in suicide gene

therapy have been demonstrated. Alternatively, cancer cells could be sensitized toward drug-induced apoptosis through overexpression of caspases [101]. In this regard, the idea of sensitizing cancer cells by caspase-like plant serine proteases such as, phytaspase seems interesting but remains unexplored.

In addition to the only known protein target VirD2, two human peptide hormones – gastrin and cholecystokinin (CCK) – have recently been identified as heterologous substrate of phytaspase [105]. Gastrin and CCK collectively influence the digestive function with latter having additional role in neuropsychiatric disorders. Inactivation of these hormones by phytaspase-mediated hydrolysis might lead to therapeutic implications. The limited knowledge on the structure-function relation of recombinant phytaspase, coupled with the fact that several therapeutically important plant proteins including *Arabidopsis* thaumatin-like protein [120] and *Solanum nigrum* osmotin-like protein [121] retained functional activities when expressed in *E. coli*, has motivated the present investigation on heterologous expression of phytaspase in bacterial as well as mammalian system.

Herein this chapter, heterologous cloning of pre-prophytaspase and mature phytaspase (catalytic domain of the protease) in mammalian expression vector and bacterial expression vectors were carried out. As the main objective was to analyze the effect of phytaspase by expressing it into the cancer cells (similar to AtUPRT gene in Chapter 2), several attempts were made in generating the stable cells lines without success. Herein, the effect of phytaspase was examined by bacterially expressed recombinant phytaspase when it was exogenously supplied to the cancer cells. After conducting multiple trials to express pre-prophytaspase and mature phytaspase as His tagged proteins and GST tagged proteins bacterially, the systematic studies were carried forward further on GST-mature phytaspase, which was obtained sufficiently in soluble fraction. The mature phytaspase (69.5 kDa) was expressed with an N-terminal glutathione S-transferases (GST) tag to facilitate protein purification through affinity chromatography. Following thrombin-mediated removal of GST, secondary structure of recombinant mature phytaspase was studied by circular dichroism (CD). The caspase-like activity of the recombinant phytaspase was assessed through *in silico* studies and results were verified by *in vitro*

enzymatic assay with synthetic caspase peptide substrates. Extending the study to evaluate the caspase like activity of recombinant phytaspase on cancer cells, phytaspase bound Mn doped ZnS QDs-Chitosan NPs (phytaspase-nanocomposites) was established for delivering phytaspase in to the cancer cells. Following the thorough characterization, anticancer property of phytaspase-nanocomposites was also determined in human cervical cancer (HeLa) cells in the presence of chemotherapeutic drug. Finally, the effect of phytaspase expression on the toxicity of chemotherapeutic drugs on cancer cells was explored in adenocarcinomic lung epithelial (A549) cells following their transient transfection with the plant phytaspase.

3.2 Outline of the work

1) Amplification of pre-prophytaspase gene from the full length cDNA synthesized mRNA isolated from *N. tabacum*.

2) Pre-prophytaspase gene was cloned into pGEM-T Easy vector and subsequently pre-prophytaspase and mature phytaspase genes were amplified.

3) The amplified genes were subcloned into mammalian expression vectors (pEGFP-N1) and bacterial expression vectors (pET-28a and pGEX-4T2).

4) Bacterial strain *E. coli* (BL21) was transformed with pET-28a-pre-prophytaspase, pET-28a-mature phytaspase, pGEX-4T2-pre-prophytaspase and pGEX-4T2-mature phytaspase.

5) Expressions of His-pre-prophytaspase, His-mature phytaspase, GST-pre-prophytaspase and GST-mature phytaspase were examined in transformed *E.coli* BL21 (DE3).

6) Purification of GST-pre-prophytaspase and GST-mature phytaspase was carried out.

7) Sequence identification and structural characterization of recombinant GST-mature phytaspase were determined.

8) *In silico* studies- homology modeling and molecular docking of recombinant GST cleaved recombinant mature phytaspase with caspase synthetic substrates were performed.

9) Caspase like activity and kinetic parameters of recombinant mature phytaspase with caspase 8 substrate were determined.

10) Cytotoxic effect of exogenous supply of phytaspase using nanocomposites into the HeLa cells was evaluated in the presence of cisplatin.

11) Effect of transient expression of phytaspase in A549 cells and their treatment with doxorubicin were evaluated.

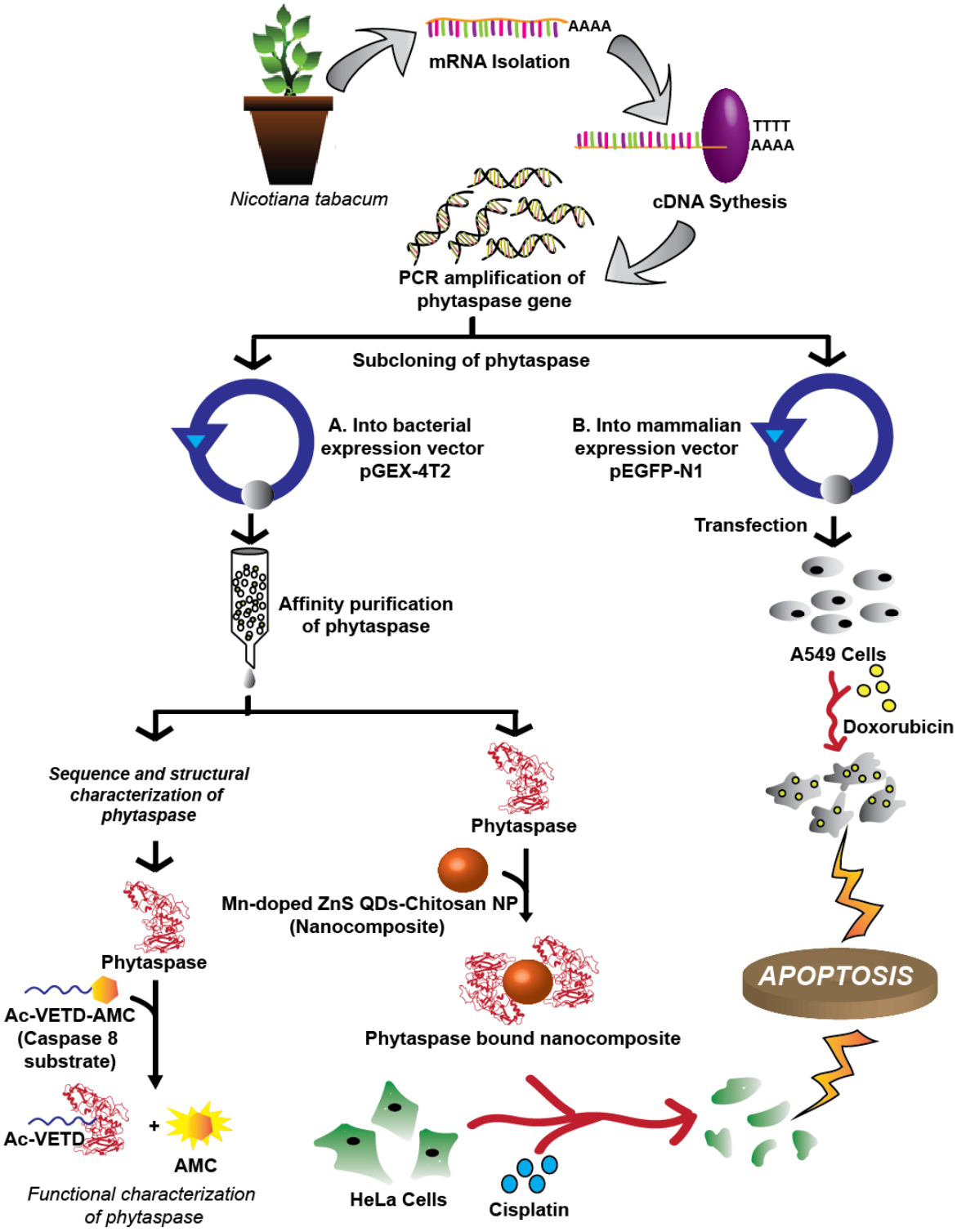

Figure 3.1: Scheme briefly representing overview of work carried out on characterization of recombinant *N. tabacum* phytaspase and its effect on cancer cells.

3.3 Experimental section

3.3.1 Materials

pGEM-T Easy vector (Promega), pET-28a vector (Novagen), pGEX-4T2 vector (Amersham), Restriction Enzymes (NEB), Isopropyl β-D-1-thiogalactopyranoside (IPTG) (Himedia), Luria-Bertani (LB) broth media (Sigma), glutathione-agarose beads (Sigma), polyvinylidene fluoride (PVDF) membrane (Pall), anti-GST antibody (produced in rat, Sigma), in-Gel trypsin digestion kit (Sigma), ZipTip C_{18} (Sigma), α-Cyano-4-hydroxycinnamic acid (CHCA) matrix (Sigma), RevertAid H-minus Reverse Transcriptase Kit (Fermentas), Soilrite (Keltech Energies Ltd.), anti-rat horseradish peroxidase (HRP)-conjugated secondary antibody (Sigma), chemiluminescent peroxidase substrate-1 (Sigma), Thrombin (GE Healthcare), caspase substrates (Sigma), Dulbecco's Modified Eagle's Medium (DMEM) (Sigma), Lipofectamine 3000 Transfection kit (Invitrogen), GenElute Mammalian Total RNA Miniprep Kit (Sigma) and Verso cDNA Kit (Thermo Scientific).

3.3.2 Instruments

MALDI-TOF/TOF mass spectrometer (4800 Pulse, Applied Biosystem), CD spectropolarimeter (Jasco J-815), Amicon Ultra-15 Centrifugal filter unit (Millipore), FluoroMax-4 (HORIBA) spectrofluorometer, Quartz cuvette (OPTIGLASS LIMITED U.K.), UV/visible spectrophotometer (Beckman Coulter, DU 730), Multimode plate-reader (Tecan Infinite® 200 PRO multimode reader), Gel Documentation System (Gel Doc™ XR+, Bio-Rad Life Sciences), Transmission electron microscopy (TEM, JEM 2100; Jeol, Peabody, MA, USA), UV−visible spectrophotometer (JASCO V-630), fluorescence spectrophotometer (LS55, PerkinElmer)

3.3.3 Bacterial strains

Cloning strain used were *E. coli* (DH5α) and expression strains used were *E.coli* BL21 (DE3) and BL21 (DE3)-pLysS.

3.3.4 Cell lines

Non-transformed human dermal fibroblasts (HDFs) cells obtained from Himedia, Cancer cell lines-A549, HeLa and MCF-7 obtained from National Centre for Cell Science (NCCS), Pune, were maintained in DMEM containing with 10% FBS and penicillin (50 U/ml)-streptomycin (50 mg/ml) at 37^0C in a humidified incubator supplied with 5% CO_2.

3.3.5 Primers used for the amplification of pre-prophytaspase and mature phytaspase genes

Sl.no	Primer Name	Type	Length	Sequence (5'-3')
1	Pre-prophytaspase	pGEM-T Easy-Forward	26	CTAGCTTATGTTCAAGAAATTATTATTCC
2	Pre-prophytaspase	pGEM-T Easy-Reverse	23	CTTATAATCAGTTCTGTCCTCAC
3	Pre-prophytaspase	pET-28a Forward	28	AGAAGCTTTGATGGCCAATTGTATTACC
4	Pre-prophytaspase	pET-28a Reverse	23	TGCTCGAGTCACAGAGGATCCAC
5	Mature phytaspase	pET-28a Forward	26	ACAAGCTTTGACGACACACACGTCTC
6	Mature phytaspase	pET-28a Reverse	23	TGCTCGAGTCACAGAGGATCCAC
7	Pre-prophytaspase	pGEX-4T2 Forward	26	ATGTCGACGATGGCCAATTGTATTAC
8	Pre-prophytaspase	pGEX-4T2 Reverse	23	TTCGGCCGTCACAGAGGATCCAC
9	Mature phytaspase	pGEX-4T2 Forward	23	CGGTCGACTACGACACACACGTC
10	Mature phytaspase	pGEX-4T2 Reverse	23	TTCGGCCGTCACAGAGGATCCAC
11	Pre-prophytaspase	pEGFP-N1-Forward	28	CTCTCGAGTTATGGCCAATTGTATTACC
12	Mature phytaspase	pEGFP-N1-Forward	25	ACTCGAGAATGACGACACACGTC
13	Pre-pro & Mature phytaspase	pEGFP-N1-Reverse	24	TTCAAGCTTTCACAGAGGATCCAC

Table 3.1: Primers used for amplification of pre-prophytaspase and mature phytaspase for cloning into pGEM-T Easy, pET-28a, pGEX-4T2 and pEGFP-N1 vectors.

3.3.6 PCR conditions used for amplification of pre-prophytaspase and mature phytaspase genes

Same as mentioned in the Chapter 2 section 2.3.6.

3.3.7 Isolation of total RNA and synthesis of cDNA

Tobacco plant (*Nicotiana tabacum*) was cultivated in Soilrite in green house under optimized conditions of 25± 2^0C temperature, 70-80% humidity and 16 h day-8 h night cycle. Total RNA was isolated from the leaves of well-grown tobacco plant by previously described procedure [107]**.** The full length cDNA was synthesized from isolated mRNA by RevertAid H-minus Reverse Transcriptase Kit using OligodT_{18} primers.

3.3.8 Cloning of pre-prophytaspase into pGEM-T Easy vector

The pre-prophytaspase gene was amplified by PCR from the cDNA templates using gene specific forward and reverse primers (Section 3.3.5). The amplified pre-prophytaspase gene was cloned into pGEM-T Easy vector and clones were confirmed by DNA sequencing (DNA sequencing facility, Delhi University South Campus & Xcelris, Ahmedabad).

3.3.9 Subcloning of pre-prophytaspase and mature phytaspase into bacterial (pET-28a and pGEX-4T2) expression vector

The genes encoding pre-prophytaspase and mature phytaspase (without signal peptide and pro-domain) were amplified for subcloning into bacterial expression vectors. PCR amplification of genes was carried out by using pre-prophytaspase gene containing pGEM-T Easy vector as template. The forward and reverse primers used for amplification for cloning into pET-28a were having overhangs for restriction enzymes *Hind*III and *Xho*I, respectively (Section 3.3.5). Likewise, the primers for cloning into pGEX-4T2 were having overhangs for restriction enzymes *Sal*I and *Eag*I, respectively (Section 3.3.5). The PCR amplified pre-prophytaspase and mature phytaspase genes were subsequently cloned into pET-28a and pGEX-4T2 vector for expression into bacterial system with N-terminal His tag and N-terminal GST tag, respectively.

3.3.10 Subcloning of pre-prophytaspase and mature phytaspase into mammalian (pEGFP-N1) expression vector

The pre-prophytaspase and mature phytaspase genes were also subcloned into pEGFP-N1 mammalian expression vector. The gene amplification was performed using forward primer and reverse primer with overhangs containing restriction enzyme sites for *Xho*I and *Hind*III, respectively (Section 3.3.5). The amplified genes were cloned into pEGFP-N1 with stop codon between genes and green fluorescent protein (GFP) gene sequences in the vector, so that GFP protein is not expressed.

3.3.11 Transfection of HeLa and MCF-7 cell lines with pEGFP-N1-pre-prophytaspase and pEGFP-N1- mature phytaspase constructs

As the primary objective was to study the effect of expression of phytaspase in cancer cells, transfection of HeLa and MCF-7 cells was carried out with pEGFP-N1-pre-prophytaspase and pEGFP-N1- mature phytaspase constructs using Lipofectamine 3000 Transfection kit as per manufacturer's protocol. The procedure for the selection of stable cell lines was followed as given in Chapter 2 (2.3.12). Failure in obtaining any phytaspase gene amplification in RT PCR using cDNA synthesized from total RNA of transfected HeLa and MCF-7 cells, shifted the entire focus from gene therapy to study the effect of exogenous supply of bacterially expressed recombinant phytaspase on the cancer cells.

3.3.12 Expression induction of bacterial recombinant His-pre-prophytaspase, His-mature phytaspase, GST-pre-prophytaspase and GST-mature phytaspase

The pET-28a-pre-prophytaspase, pET-28a-mature phytaspase, pGEX-4T2-pre-prophytaspase and pGEX-4T2-mature phytaspase constructs were transformed into *E. coli* BL21 (DE3) strain. The pET-28a-pre-prophytaspase and pET-28a-mature phytaspase transformed cells were grown in 500 ml LB broth media containing kanamycin (50µg/ml) at 37^0C, 180 rpm. Whereas, pGEX-4T2-pre-prophytaspase and pGEX-4T2-mature phytaspase transformed cells were grown in the same condition in LB broth media containing ampicillin (100 µg/ml). Once the optical density at 590 nm (OD_{590}) reached 0.6, the cultures were grown at 25^0C, 180 rpm for 8-10 h in the presence of IPTG (0.5

mM) for inducing phytaspase expression. Finally, the induced cells were pelleted down by centrifugation (6500 rpm, 5 min, 4^0C), re-suspended in lysis buffer (10 mM Tris-HCl pH 7.5 containing 100 mM NaCl) and lysed by sonication (at 33% amplitude for 35 cycles of 3 s pulse followed by 25 s gap). The cell lysates were centrifuged at 12100 rpm, 4^0C for 20 minutes. The supernatants and pellets were separately run in 12% sodium dodecyl sulfate-polyacrylamide gel electrophoresis (SDS-PAGE) gel for checking the expression.

3.3.13 Expression and purification of bacterial recombinant GST-pre-prophytaspase and GST-mature phytaspase

After several different trials to express His tagged proteins, there was no success in obtaining His-pre-prophytaspase even when transformed in BL21 (DE3)-pLysS, whereas GST tag facilitated the stable expression of both the proteins [122]. As it was important to describe the comparative analysis on the precursor as well as mature enzyme, the GST fusion system was chosen for the further investigation. Initially, it was necessary to optimize the conditions for induction as the recombinant proteins were expressed mostly as inclusion bodies (IBs). The optimized conditions for expressing the GST-pre-prophytaspase and GST-mature phytaspase in soluble form were 0.5 mM IPTG at 18^0C, (180 rpm) for 16 h. Finally, the induced cells were pelleted down by centrifugation (6500 rpm, 5 min, 4^0C), re-suspended in 10 ml lysis buffer (10 mM Tris-HCl pH 7.5 containing 100 mM NaCl) and lysed by sonication (at 33% amplitude for 35 cycles of 3 s pulse followed by 25 s gap). The cell lysate was spun at 12100 rpm for 20 min at 4^0C and the filtered supernatant was loaded onto affinity column containing glutathione-agarose beads. After 30 min incubation, the column was washed eight times with 80 ml of 10 mM Tris-HCl (pH 7.5). Finally, the GST-tagged proteins were eluted from the affinity column by adding 10 ml of 50 mM Tris-HCl (pH 9.0) containing 10 mM reduced glutathione. The purified recombinant proteins were analyzed by SDS-PAGE in 12% gel.

3.3.14 Western blot analysis

Western blot analysis of purified GST-pre-prophytaspase and GST-mature phytaspase was carried out using anti-GST antibody. Following SDS-PAGE (12% gel) of purified GST-pre-prophytaspase and GST-mature phytaspase, protein bands were transferred to polyvinylidene fluoride (PVDF) membrane at 25 V in fresh Towbin buffer for 4 h. The membrane was blocked by 5% BSA in PBST buffer (0.01 M PBS containing 0.1% Tween 20) for 2 h. The membrane was then incubated overnight in 7 ml PBST buffer containing anti-GST antibody at 1:3500 dilution and 4% BSA at 4^0C. After thorough washing with PBST buffer the membrane was incubated with 7 ml PBST buffer containing anti-rat horseradish peroxidase (HRP)-conjugated secondary antibody at 1:3500 dilution and 3% BSA for 2 h at room temperature. After washing with PBST, the protein bands were developed by adding chemiluminescent peroxidase substrate-1. The bands were analyzed under gel documentation system.

3.3.15 Matrix-assisted laser desorption/ionization-time of flight/time of flight (MALDI-TOF/TOF) mass spectrometry

The amount of GST-pre-prophytaspase obtained was very little even after harvesting larger volume of culture (1.2 L) which could be due to endogenous protease cleavage or degradation or autoprocessing into mature phytaspase while its purification. Because of this difficulty, only GST-mature phytaspase was persuaded for further investigation. The sequence of GST-mature phytaspase was investigated by MALDI-TOF/TOF mass spectrometry. The purified protein was digested by in-Gel trypsin digestion kit. The digested peptides were desalted by ZipTip C_{18} according to the manufacturer's protocol. The samples were then mixed with CHCA matrix and spotted on to the analyzer plate. The data acquired from the analysis was searched through Mascot Database (Matrix Science) [123].

3.3.16 Protease activity assay

Colorimetric protease activity assay of the GST-mature phytaspase was performed by universally adopted protocol using casein as substrate [124, 125]. Casein is a well-known protease substrate [126]. GST-mature phytaspase was initially dialyzed against 10 mM

Tris-HCl (pH 7.5) for 2 h, and then finally against 10 mM sodium acetate buffer (pH 7.5) containing 5 mM calcium acetate for 3 h. Casein (0.65%) was prepared in 50 mM potassium phosphate buffer (pH 7.5). About 5 ml of casein substrate in 5 different dram vials were pre-warmed at 37^0C for 5 min. The dialyzed GST-mature phytaspase (6 µg/ml) was added to the substrate in the four vials leaving one blank dram vial and incubated for 10 min exactly at 37^0C. The reaction was inhibited by adding 5 ml of 110 mM trichloroacetic acid (TCA) and then the volumes in all the tubes including blank were made equal by adding the GST-mature phytaspase and incubated for 30 min at 37^0C. Filtered 2 ml supernatant of the above mixture was added with 5 ml of 500 mM sodium carbonate and finally the colour was developed by adding 1ml of 0.2 N Folin's reagent. The colour development was correlated with the tyrosine liberated due to casein digestion by protease. The darker the blue colour, the more tyrosine liberated and the more is protease activity. The absorbance was measured at 660 nm. To obtain the enzyme activity, standard curve was generated by reacting known concentration of standard L-tyrosine in micromoles with 0.2 N Folin's reagent.

The enzyme activity was calculated based on the formula,

$$\text{Enzyme Activity (Units/ml)} = \frac{\text{Tyrosine equivalent released (µmoles)} \times \text{Total volume in assay (ml)}}{\text{Time of assay (min)} \times \text{Volume of enzyme (ml)} \times \text{Volume taken for absorbance (ml)}}$$

3.3.17 Thrombin-cleavage of GST tag from the recombinant mature phytaspase

Several methods are known to cleave the fusion tags from the protein [127]. Thrombin was employed for enzymatic cleavage of GST tag from mature phytaspase [128] due to the presence of cleavage site of thrombin in pGEX-4T2 vector while the same being absent in the phytaspase protein itself (checked through PeptideCutter (ExPASy)). The GST-mature phytaspase was first bound to the glutathione-agarose affinity column by passing the cell lysate through the column and then washed thoroughly (with 70–80 ml volume of 100 mM HEPES buffer pH 7.4 containing 200 mM NaCl) as described above. The column was then loaded with 10 ml thrombin cleavage buffer (20 mM HEPES pH 8.0, 100 mM NaCl and 0.5 U/ml thrombin protease) and incubated for 3 h at 25^0C with gentle shaking. Elute containing mature phytaspase protein without GST tag was

collected in different fractions. The column was once again washed with buffer and incubated with 10 ml elution buffer (20 mM HEPES pH 8.0 containing 10 mM reduced glutathione) for 20 min to elute the GST protein tags from the column. Elutes were collected separately in different fractions. All the fractions were checked by 12% SDS-PAGE for successful thrombin cleavage of GST tag from recombinant mature phytaspase.

3.3.18 Secondary structure analysis

Circular dichroism spectroscopy was performed to determine the secondary structural conformation [129]. CD spectrum of the pure protein GST-mature phytaspase, mature phytaspase and GST were obtained within far-UV range (240 nm-190 nm) wavelength by Jasco J-815 CD spectropolarimeter at 25^0C using 1 mm pathlength quartz cuvette. Protein concentration was kept constant at 0.1mg/ml in 10 mM Tris-HCl buffer (pH 7.5) for all the three samples. CD spectrum for buffer control (baseline) was also obtained separately. The data were taken in 4 accumulations.

3.3.19 Homology modeling

The homology modeling of the recombinant mature phytaspase was performed in EasyModeller 4.0 [130, 131] with Modeller 9.14 (https://salilab.org/modeller) and Python 2.7 (www.python.org) as supporting software. Phytaspase was modeled on the templates PDB:3AFG, PDB:3I6S and PDB:3VTA (http://www.rcsb.org/pdb), selected based on sequence homology through BLAST search with the query protein. The quality of generated protein models were verified by SAVES (http://nihserver.mbi.ucla.edu/SAVES/) server and the structures were studied in PyMOL (www.pymol.org).

3.3.20 Molecular docking with caspase 8 and 3 substrates

Based on the previous reports, synthetic caspase 8 and 3 substrates were chosen, as the authors have shown the wild type phytaspase is capable of cleaving caspase 8 substrate but not the caspase 3 substrate [104]. The PDB format structures of caspase 8 substrate N-Acetyl-Val-Glu-Thr-Asp-7-Amino-4-methylcoumarin (Ac-VETD-AMC) and caspase 3 substrate N-Acetyl-Asp-Met-Gln-Asp-p-Nitroaniline (Ac-DMQD-pNA) were

generated using ChemDraw (Cambridge Software). The molecular docking of Ac-VETD-AMC and Ac-DMQD-pNA with modeled recombinant mature phytaspase structure was carried out by AutoDock4.2 software (autodock.scripps.edu) [132]. The supporting softwares required for docking studies were Python 2.5 (www.python.org) and MGL Tools 1.5.4 (mgltools.scripps.edu). The interactions between phytaspase and the substrates were analyzed in PyMOL.

3.3.21 Assessment of caspase like functional activity of GST-mature phytaspase and mature phytaspase

Caspase like functional activity of recombinant mature phytaspase was assessed by following previous methods with some modifications [133-135]. Synthetic fluorogenic caspase 8 substrate, Ac-VETD-AMC and chromogenic caspase 3 substrate, Ac-DMQD-pNA were chosen as substrates for the assay [136]. GST-mature phytaspase and mature phytaspase were concentrated and buffer was exchanged with assay buffer (100 mM HEPES pH 6.5, 500 mM NaCl, 10% sucrose, 0.1% 3-((3-cholamidopropyl) dimethylammonio)-1-propanesulfonate (CHAPS) and 10 mM dithiothreitol (DTT)) using Amicon Ultra-15 Centrifugal filter unit (Millipore). Substrate solution (1 ml) of Ac-VETD-AMC (50 μM) and Ac-DMQD-pNA (2 mM) were prepared in assay buffer. Different concentrations of proteins (1-6 nM) were transferred to 1.5 ml microfuge tubes and 50 μl of substrate (for caspase 8 or caspase 3) solution was added to each tube. The final volume in each tube was made to 1 ml with assay buffer. Appropriate control samples namely buffer, proteins and substrates were also prepared. The tubes were then incubated at 30^0C for 1 h. After incubation, release of AMC from the fluorogenic caspase 8 substrate was measured by recording fluorescence emission at 460 nm with excitation at 380 nm in FluoroMax-4 spectrofluorometer using 10 mm quartz cuvette. Similarly, pNA released from caspase 3 substrate was quantified by measuring absorbance at 405 nm in a UV/visible spectrophotometer using 10 mm quartz cuvette. All the experiments were performed in triplicates and assessed for statistical significance by one-way ANOVA (GraphPad Prism 6). The percentage of hydrolysis of substrate was obtained from increase in fluorescence intensity with respect to substrate control.

3.3.22 Determination of kinetic parameters of recombinant mature phytaspase

For determining kinetic parameters, different concentrations (0.5-5.5 µM) of substrate Ac-VETD-AMC were added to the wells of a 96-well microtiter plate and the total volume was made to 190 µl in each well with assay buffer. Purified mature phytaspase (9.37 nM) in volume of 10 µl was added to each well and mixed properly. Simultaneously, wells for the substrate control and the phytaspase control were also prepared. The plate was incubated for 1 h at 30^0C in dark condition and then the fluorescence was recorded at 380 nm excitation and 460 nm emission in multimode plate-reader (Tecan Infinite® 200 PRO multimode reader). The fluorescence reading of the substrate control was subtracted from the sample readings. The corresponding amount of AMC release was calculated from the calibration curve (fluorescence vs AMC concentration). The values of K_M and specificity constant (k_{cat}/K_M) were calculated by the non-linear regression analysis using GraphPad Prism 6.

3.2.23 Synthesis of Mn doped ZnS QDs-chitosan NPs (nanocomposites)

Chitosan (0.5 mg/ml) solution of 1ml was added to 9 ml water containing 21 mg zinc acetate and 12 mg manganese acetate and was heated at 80^0C for 15 minutes with continuous stirring. The reaction mixture was cooled down to room temperature followed by addition of 1 ml of 16 mg/ml sodium sulfide drop wise with continuous stirring. Synthesized Mn doped ZnS QDs (1ml) was centrifuged at 8000 rpm three times for washing thoroughly and finally resuspended in 1 ml of miliQ water. Acetic acid was added to it until it dissolved the precipitates completely and then sodium tripolyphosphate (TPP) (4 mg/ml) was added under stirring until the solution turns to milky white in appearance. The formed nanocomposites were diluted by adding 5 ml of MiliQ water. Finally, the formed nanocomposites solution was centrifuged at 8000 rpm and the pellet was resuspended in 6 ml MiliQ water. The absorbance profile of the synthesized sample was recorded in the UV−visible region on an UV−visible spectrophotometer. Fluorescence spectrophotometer was used for measuring the luminescence as well as for the calculating quantum yield (QY). The QY was measured by employing standard protocol using reference quinine sulfate (in 0.1 M sulfuric acid).

The equation used for calculating QY,

$$QY = QY_r \frac{m}{m_r} \frac{n^2}{n_r^2}$$

Where,

n = refractive index,

m = slope of integrated luminescence intensity vs absorbance plot,

r = reference quinine sulfate solution

The quantum yield of standard (QY_r) is 0.54 and 1.33 is the refractive index of solvent water.

3.2.24 Dynamic light scattering (DLS) and Zeta potential study on nanocomposites

Hydrodynamic diameter and net surface charge characterization of nanocomposites was carried out before and after binding to phytaspase by DLS and zeta potential measurement using Malvern Zetasizer Nano ZS.

3.2.25 Transmission electron microscopy (TEM) and field emission scanning microscopy (FESEM) analysis of nanocomposites

For the purpose of imaging synthesized nanocomposites, high resolution TEM was done at a maximum accelerating voltage of 200 KeV. The samples were prepared by drop-casting the 8 µl of nanocomposites on carbon coated grid and dried overnight at room temperature. For FESEM analysis, around 10 µl sample was casted on the glass slide covered with aluminium foil and allowed to dry.

3.2.26 Binding of phytaspase with nanocomposites

The binding efficiency of negatively charged phytaspase to the positively charged nanocomposites was calculated by detecting the intrinsic tryptophan fluorescence of phytaspase at the emission wavelength of 340 nm. Purified phytaspase was concentrated and dialyzed. Phytaspase (10 µg/ml) was added to different concentration of

nanocomposites (41-124 µg/ml) in 1X phosphate buffered saline (PBS), pH 7.4 and incubated at 37^0C for 1 h. At the end of the incubation, the samples were centrifuged at 10,000 rpm for 10 min at 4^0C. The supernatants were carefully collected without disturbing the pellet and finally the fluorescence was probed for calculating the binding efficiency. The formula employed to calculate binding efficiency,

$$\text{Binding Efficiency (\%)} = (\text{Phytaspase}_{\text{Initial}} - \text{Phytaspase}_{\text{Final}}/\text{Phytaspase}_{\text{Initial}}) \times 100$$

3.2.27 Intracellular uptake of nanocomposites and phytaspase-nanocomposites by confocal microscopy

For confocal microscopic imaging, HeLa and A549 cells around 1×10^6 cells were seeded on coverslip placed in 35 mm culture plate and incubated for 24 h at 37^0C in 5% CO_2 incubator for cell adherence. Later, the cells were treated with nanocomposites and phytaspase-nanocomposites for 3 h. Controls were also set simultaneously. The cells were washed thoroughly with ice cold 1X PBS and fixed using 0.1% formaldehyde and 70% ethanol. Carefully the coverslip was mounted onto a clean glass slide and sealed. The cellular uptake of nanocomposites and phytaspase-nanocomposites by HeLa cells was detected by consecutive imaging using confocal microscope (Zeiss LSM 880 microscope) by exciting the cells at 405 nm and recording in 500-700 nm emission range.

3.2.28 Effect of recombinant phytaspase on HeLa cells

In 96 well plate, HeLa cells (3000 cells/well) were seeded and incubated for 24 h in same conditions as mentioned earlier for attachment of cells. Post incubation, the cells were treated with different concentration of phytaspase, nanocomposites and phytaspase-nanocomposites complex in the presence and absence of cisplatin (0.44 µg/ml) for 48 h. Finally, the effect of phytaspase was evaluated using MTT cell viability assay. The cell viability (%) was calculate by the equation,

$$\text{Cell Viability (\%)} = \frac{(\text{Abs}_{570} - \text{Abs}_{690})\ \text{of treated cells}}{(\text{Abs}_{570} - \text{Abs}_{690})\ \text{of control cells}} \times 100$$

3.3.29 Transient expression of phytaspase in A549 cells and their treatment with doxorubicin

For the reverse transcriptase PCR analysis of transient expression of phytaspase gene in the cells, A549 cells (17×10^4 cells/well) were seeded in 6-well plate and kept overnight for adherence. Then, A549 cells were transiently transfected with pEGFP-N1-mature phytaspase construct and pEGFP-N1(-GFP) vector (designed by eliminating the GFP from pEGFP-N1 mammalian expression vector, mentioned in Chapter 2 Section 2.4.3) using Lipofectamine 3000 Transfection kit as per the manufacturer's protocol, separately for 6 h followed by fresh media replacement. After 24 h post transfection, the total RNA was isolated from pEGFP-N1-mature phytaspase, pEGFP-N1(-GFP) transfected and untransfected A549 cells by using GenElute Mammalian Total RNA Miniprep Kit. Complete cDNA was synthesized with mRNA template using Verso cDNA Kit. The mature phytaspase gene was amplified by PCR amplification on the template cDNA.

For evaluating the effect of mature phytaspase transient expression, 7×10^3 A549 cells were seeded per well in 96 well plates and grown for 24 h. After 24 h incubation, the cells were transfected with pEGFP-N1-mature phytaspase construct (100 ng). After 6 h of transfection, the transfection media was replaced with fresh DMEM containing 10% FBS and the cells were incubated for another 24 h. Subsequently, the media in each well were replaced with fresh media containing doxorubicin (8 nM to 35 nM) in triplicates. Following doxorubicin treatment for 48 h, cell viability was assessed by MTT assay. Appropriate control experiment was also carried with A549 cells transfected with pEGFP-N1(-GFP). The percentage (%) of cell viability was calculated using the formula mentioned in the above section.

3.3.30 Effect of transient expression of mature phytaspase in non-transformed human dermal fibroblasts (HDFs) cells

Transfection of HDFs cells with pEGFP-N1-phytaspase and pEGFP-N1(-GFP) was carried out similarly as mentioned above in the case of A549 cells. After 48 h of transfection, the cells were evaluated for viability by MTT assay.

3.4 Results and Discussion

3.4.1 PCR amplification and cloning of pre-prophytaspase gene in pGEM-T Easy vector

Pre-prophytaspase gene was PCR amplified from cDNA templates using gene specific primers (Figure. 3.2a) and subsequently cloned into pGEM-T Easy vector. The clones were confirmed by *Not*I restriction enzyme digestion (Figure. 3.2b).

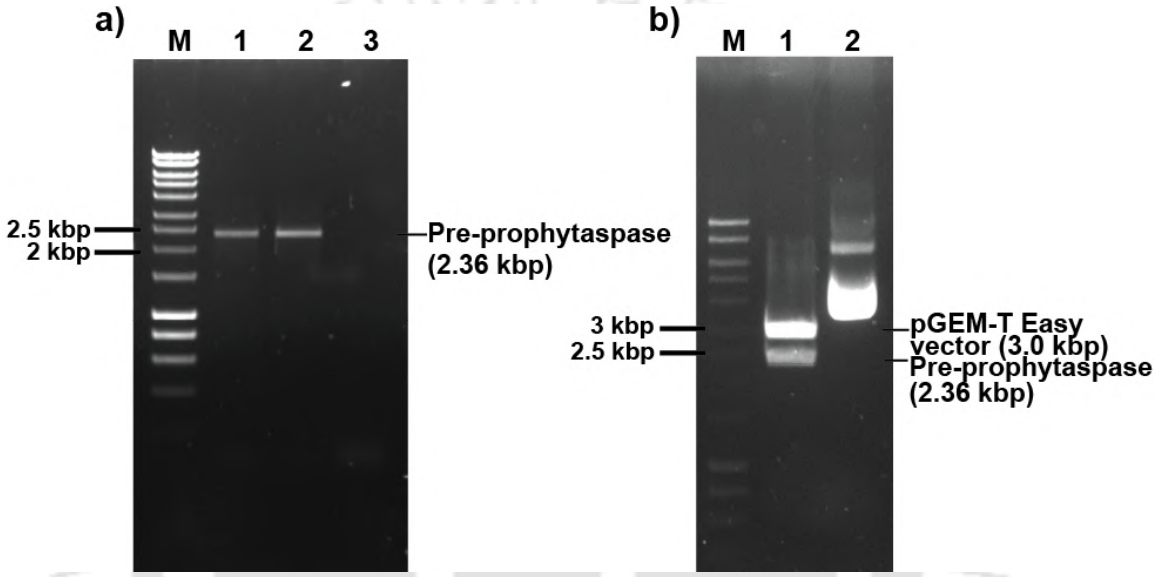

Figure 3.2: **a)** PCR amplification of pre-prophytaspase gene from cDNA of *Nicotiana tabacum* leaves. *Lane* M- DNA marker (10 kbp-200 bp), *lanes* 1 & 2- PCR amplified pre-prophytaspase gene (2.363 kbp) at 54^0C annealing temperature and *lane* 3- Negative control. **b)** Cloning of pre-prophytaspase into pGEM-T Easy vector. *Lane* M- DNA marker (10 kbp-200 bp), *lane* 1- Digested pGEM-T Easy vector (3 kbp) and pre-prophytaspase insert (2.363 kbp) by *Not*I restriction enzyme and *lane* 2- Undigested pGEM-T Easy-pre-prophytaspase construct.

3.4.2 DNA sequence analysis

DNA sequencing of cloned pre-prophytaspase gene confirmed the cloning of gene of interest (Figure. 3.3a, b & c).

a)

```
Query  1    ATGGCCAATTGTATTACCTTATATTTCTTGTTCCTTGCTATCTTACTTACTCTAAATCCA  60
            ||||||||||||||||||||||||||||||||||||||||||||||||||||||||||||
Sbjct  121  ATGGCCAATTGTATTACCTTATATTTCTTGTTCCTTGCTATCTTACTTACTCTAAATCCA  180

Query  61   TTTATTATGGCTCAGTCAGAAACTTATATCATCCATATGGACTTGTCAGCCATGCCAACA  120
            |||||||||||||||||||||||||| ||||||||||||||||||||||||||||||||||
Sbjct  181  TTTATTATGGCTCAGTCAGAAACTTATGTCATCCATATGGACTTGTCAGCCATGCCAACA  240

Query  121  GCTTTCTCTAGCCATCAAAATTGGTACTTGACCACTCTTGCTTCTGTATCAGATAGCTCA  180
            |||||||||||||||||||||||||||||||||||||||||||||||||||||||||| |||
Sbjct  241  GCTTTCTCTAGCCATCAAAATTGGTACTTGACCACTCTTGCTTCTGTATCAGATAGTTCA  300

Query  181  AGTCTTGGAACTGCAAGTAATAGAAATTCCCTTTCCTCATCAAAAATAGTTTATGCTTAC  240
            ||||||||||||||||||||||||||||||||||||||||||||||||||||||||||||
Sbjct  301  AGTCTTGGAACTGCAAGTAATAGAAATTCCCTTTCCTCATCAAAAATAGTTTATGCTTAC  360

Query  241  ACTAATGCCATTCATGGTTTTAGTGCAAGTCTTTCTTCTTCTGAGCTAGAAGTTATCAAA  300
            ||||||||||||||||||||||||||||||||||||||||||||||||||||||||||||
Sbjct  361  ACTAATGCCATTCATGGTTTTAGTGCAAGTCTTTCTTCTTCTGAGCTAGAAGTTATCAAA  420

Query  301  AATTCTCCAGGCTATCTTTCTTCAACTAAGGACATGACAGTTAAAAGTGACACGACACAC  360
            ||||||||||||||||||||||||||||||||||||||||||||||||||||||||||||
Sbjct  421  AATTCTCCAGGCTATCTTTCTTCAACTAAGGACATGACAGTTAAAAGTGACACGACACAC  480

Query  361  ACGTCTCAATTCCTTGGCCTAAATTCCAATTCTGGTGTATGGCCAAAGTCAGACTATGGC  420
            ||||||||||||||||||||||||||||||||||||||||||||||||||||||||||||
Sbjct  481  ACGTCTCAATTCCTTGGCCTAAATTCCAATTCTGGTGTATGGCCAAAGTCAGACTATGGC  540

Query  421  AAAGATGTTATAGTTGGATTAGTTGACACAGGGATTTGGCCAGAGAGTAAAAGCTATACT  480
            ||||||||||||||||||||||||||||||||||||||||||||||||||||||||||||
Sbjct  541  AAAGATGTTATAGTTGGATTAGTTGACACAGGGATTTGGCCAGAGAGTAAAAGCTATACT  600

Query  481  GATAATGGGATGACTGAAGTTCCATCAAGGTGGAAAGGAGAATGCGAAAGTGGCACTCAA  540
            |||||||||||||||||||||||||| ||||||||||||||||||||||||||||||||||
Sbjct  601  GATAATGGGATGACTGAAGTTCCATCAAGATGGAAAGGAGAATGCGAAAGTGGCACTCAA  660

Query  541  TTTAATTCCTCTTTATGCAACAAGAAACTCATTGGTGCGCGTTACTTCAACAAAGGCCTA  600
            ||||||||||||||||||||||||||||||||||||||||||||||||||||||||||||
Sbjct  661  TTTAATTCCTCTTTATGCAACAAGAAACTCATTGGTGCGCGTTACTTCAACAAAGGCCTA  720

Query  601  ATTGCTACCAATCCGAATATTACCATCTTGATGAATTCAGCTCGTGACACAGACGGGCAT  660
            ||||||||||||||||||||||||||||||||||||||||||||||||||||||||||||
Sbjct  721  ATTGCTACCAATCCGAATATTACCATCTTGATGAATTCAGCTCGTGACACAGACGGGCAT  780

Query  661  GGAACTCACACATCTTCTACAGCTGCAGGAAGTCATGTAGAATCTGTATCTTATTTTGGT  720
            |||||||||||||| ||||||||||||||||||||||||||||||||||||||||||||||
Sbjct  781  GGAACTCACACATCCTCTACAGCTGCAGGAAGTCATGTAGAATCTGTATCTTATTTTGGT  840

Query  721  TATGCCCCTGGTGCTGCTACAGGGATGGCACCAAAGGCTCATGTGGCAATGTACAAGGCT  780
            ||||||||||||||||||||||||||||||||||||||||||||||||||||||||||||
Sbjct  841  TATGCCCCTGGTGCTGCTACAGGGATGGCACCAAAGGCTCATGTGGCAATGTACAAGGCT  900
```

b)

```
Query  781   TTATGGGATGAGGGTACAATGTTATCTGACATTCTGGCTGCAATTGATCAGGCAATTGAG  840
              ||  ||||||||||||||||||||||||||||||||||||||||||||||||||||||||
Sbjct  901   TTGTGGGATGAGGGTACAATGTTATCTGACATTCTGGCTGCAATTGATCAGGCAATTGAG  960

Query  841   GATGGAGTGGATATATTATCCTTGTCATTAGGCATAGATGGTCGTGCGCTATATGATGAT  900
              ||||||||||||||||||||||||||||||||||||||||||||||||||||||||||||
Sbjct  961   GATGGAGTGGATATATTATCCTTGTCATTAGGCATAGATGGTCGTGCGCTATATGATGAT  1020

Query  901   CCGGTAGCTATTGCCACATTTGCAGCAATGGAGAAAGGTATATTTGTTTCCACTTCAGCA  960
              ||||||||||||||||||||||||||||||||||||||||||||||||||||||||||||
Sbjct  1021  CCGGTAGCTATTGCCACATTTGCAGCAATGGAGAAAGGTATATTTGTTTCCACTTCAGCA  1080

Query  961   GGAAATGAAGGGCCTGACGGTCAGACTTTGCACAACGGAACACCTTGGGTTCTCACTGTT  1020
              ||||||||||||||||||||||||||||||||||||||||||||||||||||||||||||
Sbjct  1081  GGAAATGAAGGGCCTGACGGTCAGACTTTGCACAACGGAACACCTTGGGTTCTCACTGTT  1140

Query  1021  GCTGCTGGCACAGTTGATCGCGAATTTATCGGGACACTAACTCTAGGTAATGGAGTTTCA  1080
              ||||||||||||||||||||||||||||||||||||||||||||||||||||||||||||
Sbjct  1141  GCTGCTGGCACAGTTGATCGCGAATTTATCGGGACACTAACTCTAGGTAATGGAGTTTCA  1200

Query  1081  GTCACTGGTTTATCTCTCTACCCCGGGAATTCAAGTTCAAGCGAAAGTTCCATCGTTTTT  1140
              ||||||||||||||||||||||||||||||||||||||||||||||||||||||||||||
Sbjct  1201  GTCACTGGTTTATCTCTCTACCCCGGGAATTCAAGTTCAAGCGAAAGTTCCATCGTTTTT  1260

Query  1141  CTCAAGACATGCCTAGAGGAGAAGGAACTGGAGAAAAATGCAAACAAAATCGCCATCTGC  1200
              ||||||||||||||||||||||||||||||||||||||||||||||||||||||||||||
Sbjct  1261  CTCAAGACATGCCTAGAGGAGAAGGAACTGGAGAAAAATGCAAACAAAATCGCCATCTGC  1320

Query  1201  TATGACACGAATGGATCAATAAGTGACCAACTGTACAATGTAAGAAACTCAAAAGTTGCT  1260
              ||||||||||||||||||||||||||||||||||||||||||||||||||||||||||||
Sbjct  1321  TATGACACGAATGGATCAATAAGTGACCAACTGTACAATGTAAGAAACTCAAAAGTTGCT  1380

Query  1261  GGTGGTGTCTTCATAACAAATTACACAGACTTGGAATTCTACCTCCAAAGCGAATTCCCA  1320
              ||||||||||||||||||||||||||||||||||||||||||||||||||||||||||||
Sbjct  1381  GGTGGTGTCTTCATAACAAATTACACAGACTTGGAATTCTACCTCCAAAGCGAATTCCCA  1440

Query  1321  GCTGTGTTTTTGAACTTTGAAGATGGTGATAAAGTTTTGGAGTACATCAAGAATAGTCAT  1380
              ||||||||||||||||||||||||||||||||||||||||||||||||||||||||||||
Sbjct  1441  GCTGTGTTTTTGAACTTTGAAGATGGTGATAAAGTTTTGGAGTACATCAAGAATAGTCAT  1500

Query  1381  TCACCTAAAGCAAGACTTGAATTTCAAGTGACACATCTTGGTACTAAACCAGCACCAAAA  1440
              ||||||||||||||||||||||||||||||||||||||||||||||||||||||||||||
Sbjct  1501  TCACCTAAAGCAAGACTTGAATTTCAAGTGACACATCTTGGTACTAAACCAGCACCAAAA  1560

Query  1441  GTTGCTAGCTATAGCTCAAGGGGACCATCACAAAGCTGCCCCTTTATCCTCAAGCCTGAC  1500
              ||||||||||||||||||||||||||||||||||||||||||||||||||||||||||||
Sbjct  1561  GTTGCTAGCTATAGCTCAAGGGGACCATCACAAAGCTGCCCCTTTATCCTCAAGCCTGAC  1620

Query  1501  CTGATGGCTCCTGGAGCCTTAATATTAGCTTCATGGCCTCAAAAATCACCCGCAACTAAA  1560
              ||||||||||||||||||||||||||||||||||||||||||||||||||||||||||||
Sbjct  1621  CTGATGGCTCCTGGAGCCTTAATATTAGCTTCATGGCCTCAAAAATCACCCGCAACTAAA  1680
```

c)

```
Query  1561  ATTAACTCGGGAGAGCTTTTCAGTAACTTCAACATCATATCCGGTACGTCAATGTCATGC  1620
              ||||||||||||||||||||||||||||||||||||||||||||||||||||||||||||
Sbjct  1681  ATTAACTCGGGAGAGCTTTTCAGTAACTTCAACATCATATCCGGTACGTCAATGTCATGC  1740

Query  1621  CCTCATGCTGCTGGTGTAGCTTCACTTTTGAAAGGAGCACACCCCAAATGGAGCCCTGCT  1680
              ||||||||||||||||||||||||||||||||||||||||||||||||||||||||||||
Sbjct  1741  CCTCATGCTGCTGGTGTAGCTTCACTTTTGAAAGGAGCACACCCCAAATGGAGCCCTGCT  1800

Query  1681  GCCATCCGGTCGGCCATGATGACCACAGCCGACGCATTGGACAACACGCAAAGGCCCATC  1740
              ||||||||||||||||||||||||||||||||||||||||||||||||||||||||||||
Sbjct  1801  GCCATCCGGTCGGCCATGATGACCACAGCCGACGCATTGGACAACACGCAAAGGCCCATC  1860

Query  1741  CGAGACATCGGTCGCAACAATAATGCTGCCAGTCCCCTAGCCATGGGAGCTGGCCATATC  1800
              ||||||||||||||||||||||||||||||||||||||||||||||||||||||||||||
Sbjct  1861  CGAGACATCGGTCGCAACAATAATGCTGCCAGTCCCCTAGCCATGGGAGCTGGCCATATC  1920

Query  1801  AATCCAAATAAGGCACTAGACCCTGGACTTATCTATGACATTACATCACAGGACTATATC  1860
              ||||||||||||||||||||||||||||||||||||||||||||||||||||||||||||
Sbjct  1921  AATCCAAATAAGGCACTAGACCCTGGACTTATCTATGACATTACATCACAGGACTATATC  1980

Query  1861  AATCTCCTCTGTGCTCTAGATTTTACATCTCAACAGATAAAAGCCATTACAAGGTCCTCT  1920
              ||||||||||||||||||||||||||||||||||||||||||||||||||||||||||||
Sbjct  1981  AATCTCCTCTGTGCTCTAGATTTTACATCTCAACAGATAAAAGCCATTACAAGGTCCTCT  2040

Query  1921  GCTTATTCTTGTTCCAACCCATCATTGGACTTAAACTATCCATCATTCATAGGCTATTTC  1980
              ||||||||||||||||||||||||||||||||||||||||||||||||||||||||||||
Sbjct  2041  GCTTATTCTTGTTCCAACCCATCATTGGACTTAAACTATCCATCATTCATAGGCTATTTC  2100

Query  1981  AATTATAACAGCAGTAAGTCAGATCCTAAAAGGATACAAGAATTCCAGAGGACAGTGACT  2040
              ||||||||||||||||||||||||||||||||||||||||||||||||||||||||||||
Sbjct  2101  AATTATAACAGCAGTAAGTCAGATCCTAAAAGGATACAAGAATTCCAGAGGACAGTGACT  2160

Query  2041  AATGTAGGAGATGGTATGTCTGTTTATACAGCCAAATTGACCTCAATGGATGAATATAAA  2100
              ||||||||||||||||||||||||||||||||||||||||||||||||||||||||||||
Sbjct  2161  AATGTAGGAGATGGTATGTCTGTTTATACAGCCAAATTGACCTCAATGGATGAATATAAA  2220

Query  2101  GTTAGTGTTGCACCTGACAAGTTGGTTTTCAAAGAGAAGTATGAAAAGCAAAGCTACAAG  2160
              ||||||||||||||||||||||||||||||||||||||||||||||||||||||||||||
Sbjct  2221  GTTAGTGTTGCACCTGACAAGTTGGTTTTCAAAGAGAAGTATGAAAAGCAAAGCTACAAG  2280

Query  2161  CTAAGGGTAGAAGGTCCATTGCTAGTAGATAATTATCTTGTTTATGGTTCTTTGAGCTGG  2220
              |||||| ||||||||||||||||||||||||||||||||||||||||||||||||||||||
Sbjct  2281  CTAAGGATAGAAGGTCCATTGCTAGTAGATAATTATCTTGTTTATGGTTCTTTGAGCTGG  2340

Query  2221  GTGGAAACTAGCGGTAAATATGTAGTAAAAAGTCCCATTGTCGCCACTACCATAGGAGTG  2280
              ||||||||||||||||||||||||||||||||||||||||||||||||||||||||||||
Sbjct  2341  GTGGAAACTAGCGGTAAATATGTAGTAAAAAGTCCCATTGTCGCCACTACCATAGGAGTG  2400

Query  2281  GATCCTCTGTGAGGACAGAACTGATTATAAGTC  2313
              |||||||||||||||||||||||||||||||
Sbjct  2401  GATCCTCTGTGAGGACAGAACTGATTATAAGTC  2433
```

Figure 3.3:a, b & c DNA sequencing result of pre-prophytaspase gene sequence. Query- Cloned pre-prophytaspase gene sequence and Subject- Pre-prophytaspase gene sequence from NCBI database (GQ249168.1)

3.4.3 Subcloning of pre-prophytaspase and mature phytaspase into bacterial (pET-28a and pGEX-4T2) expression vector

The gene (2.36 kbp), encoding pre-prophytaspase and the gene (1.94 kbp), encoding mature phytaspase without pro-domain and signal peptide, were PCR amplified from pGEM-T Easy-pre-prophytaspase construct and subcloned into bacterial expression vectors pET-28a with N-terminal His-tag and pGEX-4T2 with N-terminal GST-tag. Release of pre-prophytaspase (2.36 kbp) and mature phytaspase (1.94 kbp) fragments from the recombinant clones was confirmed by double digestion with *Hind*III and *Xho*I restriction enzymes for pET-28a cloning (figure. 3.4 a & b) and with *Sal*I and *Eag*I restriction enzymes for pGEX-4T2 cloning (figure 3.4 c & d).

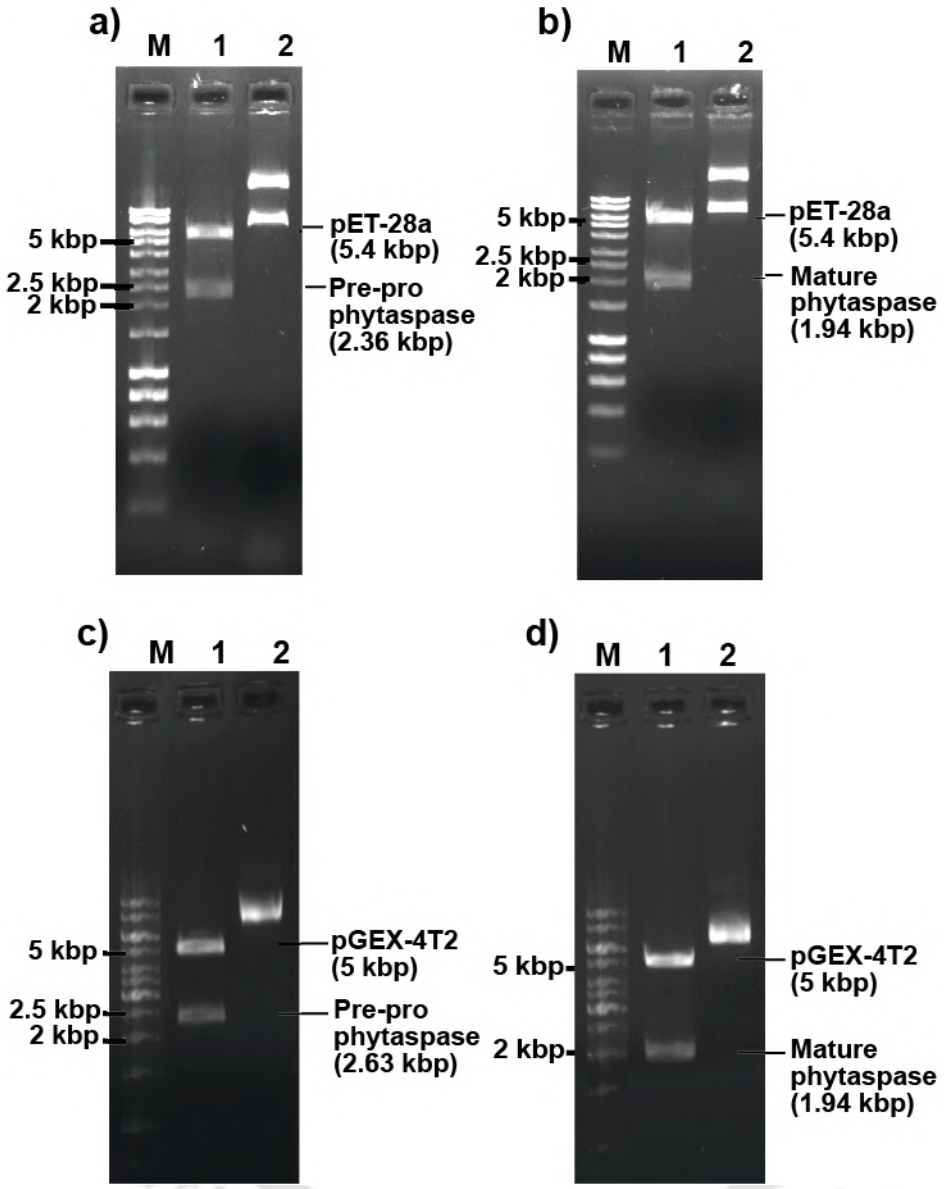

Figure 3.4:a. Subcloning of pre-prophytaspase into pET-28a vector. *Lane M*- DNA marker (10 kbp-200 bp), *lane 1*- Digested pET-28a-pre-prophytaspase construct and *lane 2*-Undigested pET-28a-pre-prophytaspase. **b.** Subcloning of mature phytaspase into pET-28a vector. *Lane M*- DNA marker (10 kbp-200 bp), *lane 1*- Digested pET-28a-mature phytaspase construct and *lane* 2- Undigested pET-28a-mature phytaspase. **c.** Subcloning of pre-prophytaspase into pGEX-4T2 expression vector. *Lane M*- DNA marker (10 kbp-200 bp), *Lane 1*- Digested pGEX-4T2-preprophytaspase construct and *lane 2*-Undigested pGEX-4T2-pre-prophytaspase. **d.** Subcloning of mature phytaspase into pGEX-4T2 vector. *Lane M*- DNA marker (10 kbp-200 bp), *lane 1*- Digested pGEX-4T2-

mature phytaspase construct and *lane 2*- Undigested pGEX-4T2-mature phytaspase construct.

3.4.4 Subcloning of pre-prophytaspase and mature phytaspase into mammalian (pEGFP-N1) expression vector

Phytaspase genes were also PCR amplified using primers with overhangs for *Xho*I and *Hind*III for subcloning into pEGFP-N1 (Clontech) mammalian expression vector with stop codon between phytaspase and GFP gene sequences (Figure 3.5).

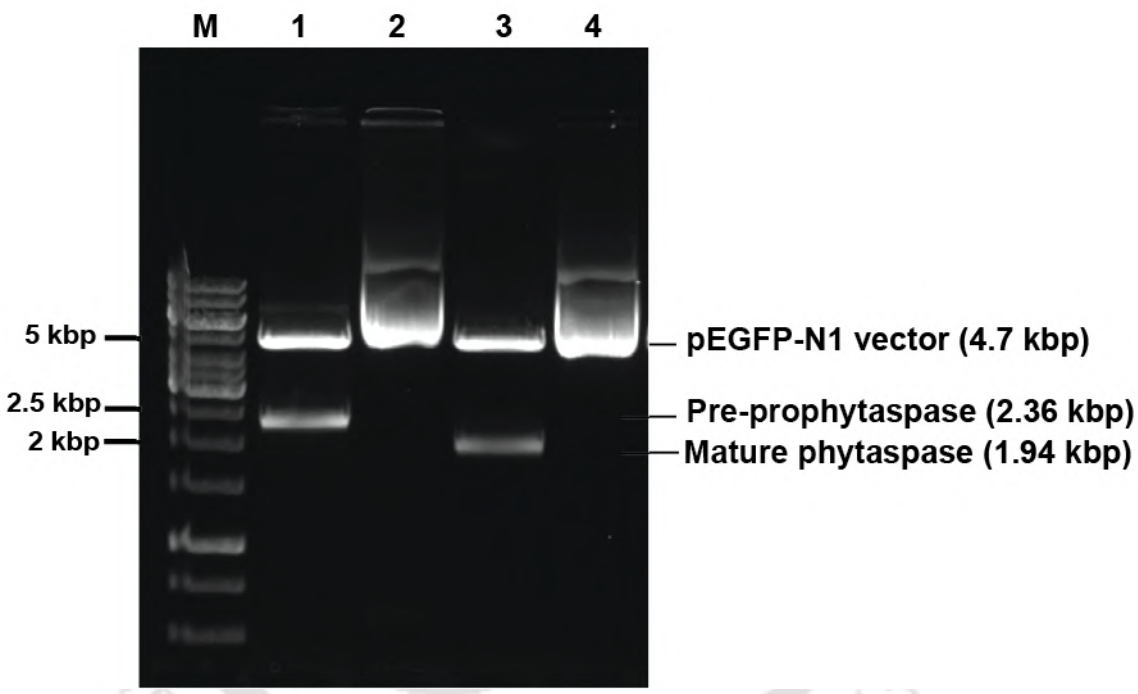

Figure 3.5: Subcloning of pre-prophytaspase and mature phytaspase into pEGFP-N1 mammalian expression vector. *Lane M*- DNA marker (10 kbp-200 bp), *lane 1*- Digested pEGFP-N1-pre-prophytaspase construct, *lane 2*- Uncut pEGFP-N1-pre-prophytaspase construct, *lane 3*- Digested pEGFP-N1-mature phytaspase construct and *lane 4*- Uncut pEGFP-N1-mature phytaspase construct.

3.4.5 Expression induction of bacterial recombinant His-pre-prophytaspase, His-mature phytaspase, GST-pre-prophytaspase and GST-mature phytaspase

In order to obtain, correctly folded active form of phytaspase by avoiding its expression as inclusion bodies (IBs), the comparative expression analysis was done on His-tag fusion system and GST-tag fusion system. The induced *E. coli* BL21 containing His tag fusion system, showed no traces of expression of pre-prophytaspase even after several attempt with varying parameters (Figure 3.6a). Additionally, transformation in the bacterial expression strain *E. coli* BL21 (DE3)-pLysS did not help in expression. The expression of His-mature phytaspase was completely observed in IBs (Figure 3.6b. lane 5). Whereas in the case of GST tagged phytaspases, there was expression in both the cases even though it was as IBs (Figure 3.7).

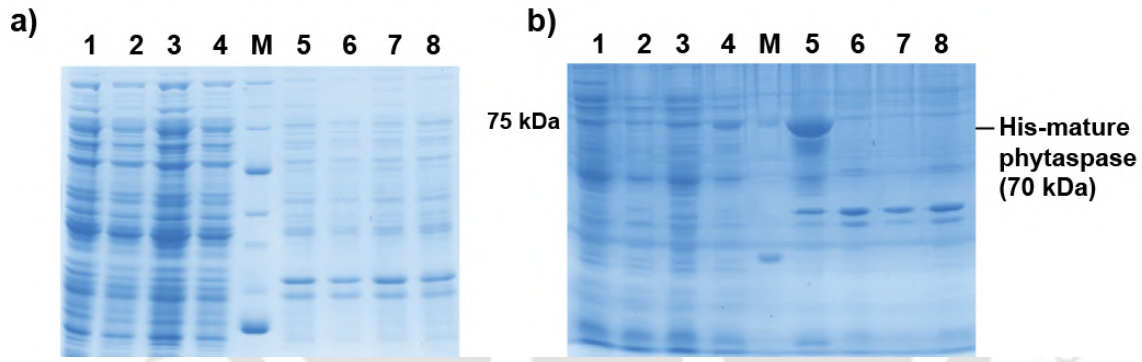

Figure 3.6: SDS PAGE (12%) confirming **a.** The absence of induced expression of His-pre-prophytaspase in *E.coli* BL21(DE3). *Lane 1 & 2*- Uninduced cells-pellet and supernatant of *E. coli* BL21 (DE3), *lane 3 & 4*- Uninduced cells-pellet and supernatant of *E. coli* BL21 (DE3) containing pET-28a-pre-prophytaspase, *lane M*- Protein marker (10-180 kDa), *lane 5 & 6*- IPTG induced cells-pellet and supernatant of *E. coli* BL21 (DE3) containing pET-28a-pre-prophytaspase and *lane 7 & 8*- IPTG induced cells-pellet and supernatant of *E. coli* BL21 (DE3). **b.** The presence of IPTG induced expression of His-mature phytaspase in *E.coli* BL21 (DE3). *Lane 1 & 2*- Uninduced cells-pellet and supernatant of *E. coli* BL21 (DE3), *lane* 3 & 4- Uninduced cells-pellet and supernatant of *E. coli* BL21 (DE3) containing pET-28a-mature phytaspase, *lane M*- Protein marker (10-180 kDa), *lane 5 & 6*- IPTG induced cells-pellet and supernatant of *E. coli* BL21 (DE3)

containing pET-28a-mature phytaspase showing the expression in pellet as IBs and *lane 7 & 8*- IPTG induced cells-pellet and supernatant of *E. coli* BL21 (DE3).

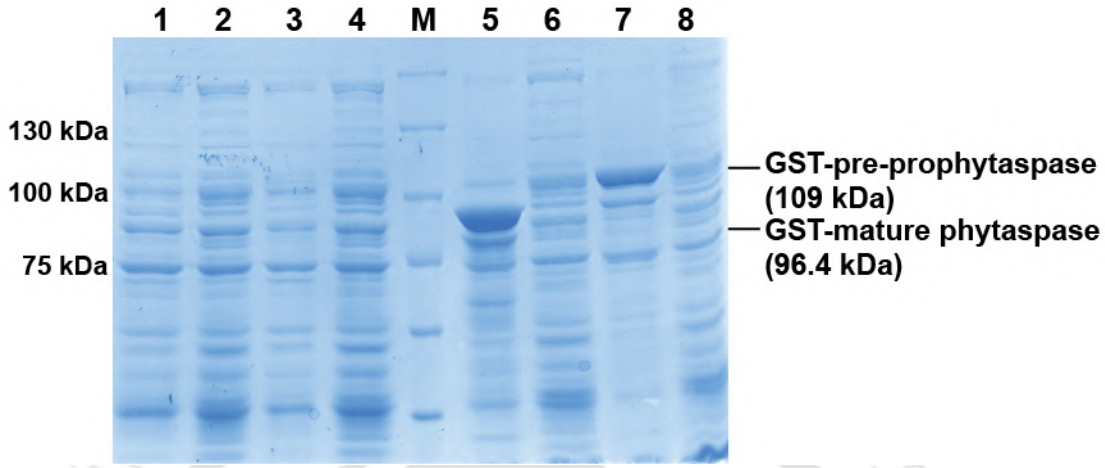

Figure 3.7: SDS-PAGE (12%) depicting induction of GST-pre-prophytaspase and GST-mature phytaspase expression in *E. coli* BL21 (DE3). *Lane 1 & 2*- Uninduced *E. coli* BL21 (DE3) containing pGEX-4T2- mature phytaspase cell lysate supernatant and pellet respectively, *lane 3 & 4*- Uninduced *E. coli* BL21 (DE3) containing pGEX-4T2-pre-prophytaspase cell lysate supernatant and pellet respectively, *lane M*- Protein marker (10-180 kDa), *lanes 5 & 6*- Pellet and supernatant fraction of cell lysate (following centrifugation) from IPTG induced *E. coli* BL21 cells containing pGEX-4T2- mature phytaspase and *lane 7 & 8*- Pellet and supernatant fraction of cell lysate from IPTG induced *E. coli* BL21 cells containing pGEX-4T2-pre prophytaspase.

3.4.6 Purification of bacterial recombinant GST-pre-prophytaspase and GST-mature phytaspase

Nonetheless, optimization of various induction parameters revealed that an induction with 0.5 mM IPTG at 18^0C and shaking speed of 180 rpm for 16 h resulted in successful expression of the recombinant GST-pre-prophytaspase and GST-mature phytaspase in soluble form. GST-mature phytaspase was purified by affinity chromatography and SDS-PAGE demonstrated prominent bands of GST-mature phytaspase (96.4 kDa) in purified protein samples (Figure 3.8b).The yield of protein was calculated to be 0.1 mg from 500 ml of bacterial culture (Bradford assay). Similar to GST-mature phytaspase, GST-pre-

prophytaspase was also obtained in soluble fraction successfully though in very little amount. To surprise, the protein band in the last wash fraction of washing was observed, which was corresponding to the size of mature phytaspase (69 kDa). This band was also visible in all the eluted fractions where there was appearance of mixture of three bands, one of which was GST-pre-prophytaspase (109 kDa) (Figure 3.8a). Unlike GST-mature phytaspase, the purification and quantification of GST-pre-prophytaspase was a really challenging due to the degradation/processing of the protein while its purification.

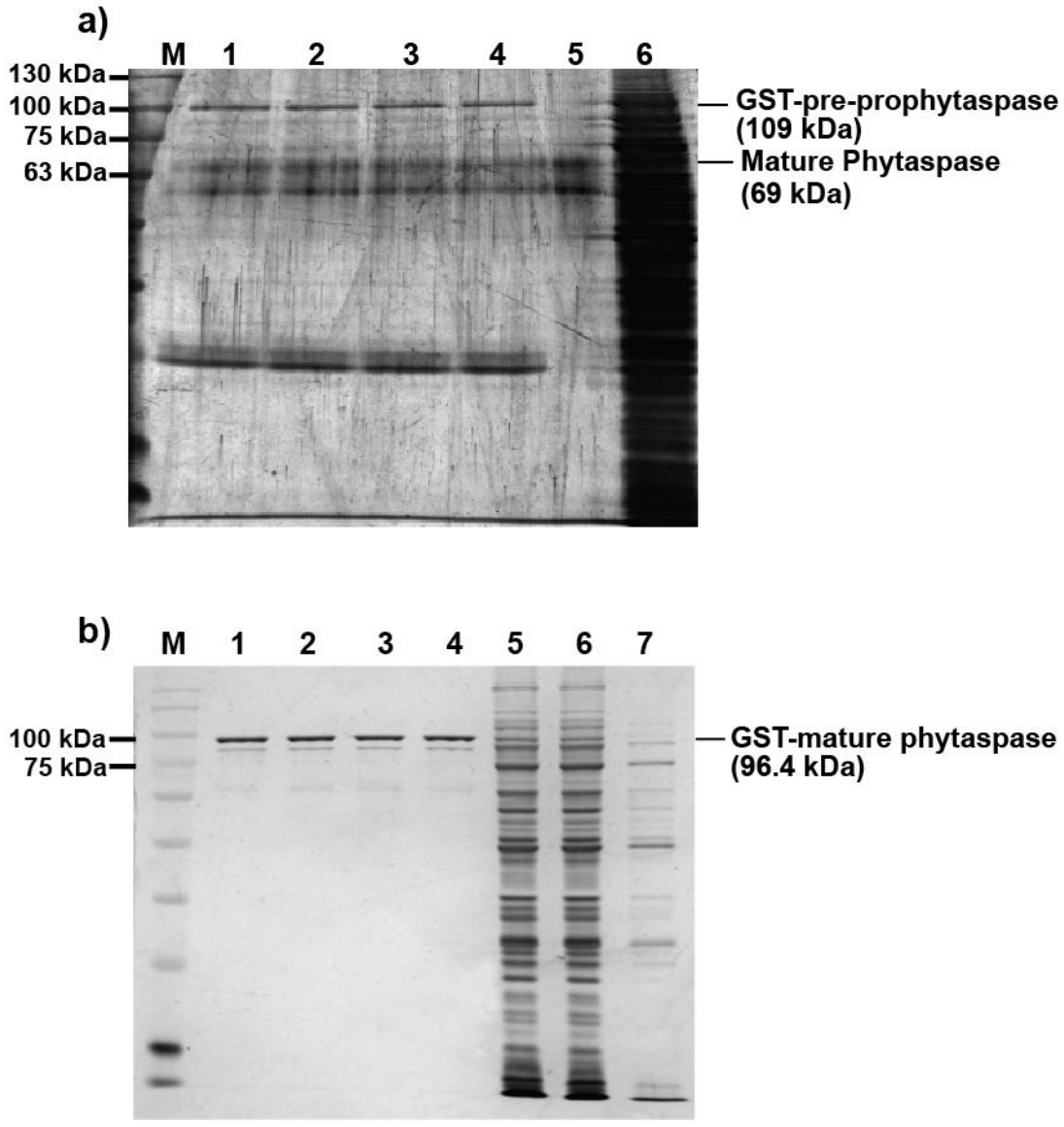

Figure 3.8a: Affinity chromatography purification of GST-pre-prophytaspase from glutathione-agarose beads. *Lane* M- Protein marker (10-180 kDa), *lane* 1-4- Eluted

fractions from the column, *lane* 5- Last wash after loading and *lane* 6- Flow through. **b.** Affinity chromatography of purified GST-mature phytaspase. *Lane M*- Protein marker (10-180 kDa), *lanes 1, 2, 3 & 4*- Different fractions of purified GST-mature phytaspase, *lanes 5 & 6*- Flow through and *lane 7*- First washing after loading.

3.4.7 Western blot analysis to detect the targeted purification of GST-pre-prophytaspase and GST-mature phytaspase

The appearance of band (Figure 3.9a) on the blot using anti-GST antibody confirms the purified GST-pre-prophytaspase, but the inability to detect any band in the lower part of GST-pre-prophytaspase led to an assumption that the protein may have undergone degradation at N-terminal by endoproteases while purification or may be self-processing of mature phytaspase from GST-pre prophytaspase have taken place. However, commenting on this requires further validation by amino acid sequencing or by expressing mutant pre-prophytaspase. The purified GST-mature phytaspase (96.4 kDa) band was also confirmed by western blotting using anti-GST antibody as demonstrated in figure 3.9b lane 2.

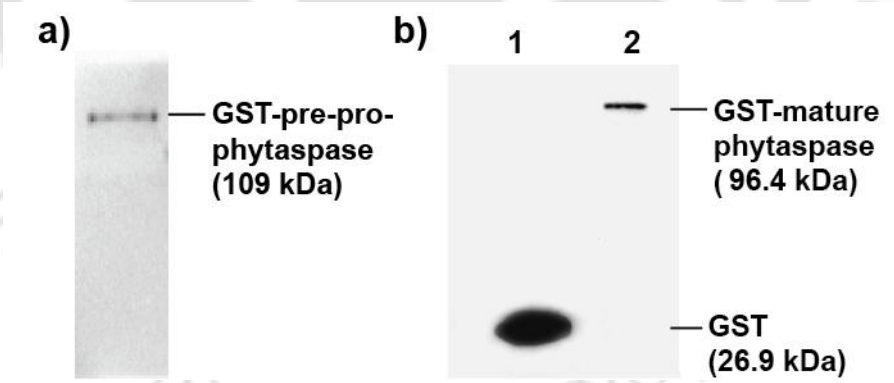

Figure 3.9: Western blot analysis ***a.*** Presence of band confirms the purification of GST-pre-prophytaspase (109 kDa), ***b.*** *Lane 1*- Lower molecular weight band corresponds to GST protein (26.9 kDa) and *lane 2*- Higher molecular weight band corresponds to GST-mature phytaspase protein (96.4 kDa)

3.4.8 Sequence identification of GST-mature phytaspase using MALDI-TOF/TOF mass spectrometry

Difficulties in obtaining sufficient amount of GST-pre-prophytaspase, unabled further characterization of the protein. However, thorough investigation on GST-mature phytaspase was carried forward. MALDI-TOF/TOF mass spectrum of purified GST-mature phytaspase (trypsin-digested) is shown in figure. 3.10. The peak values obtained were searched through the Mascot database and trypsin-digested peptides with masses (m/z) 1664.9250, 1824.8968, 1990.9564 and 3621.6067 corroborated with amino acid sequence of phytaspase in NCBI database (gi253740260) with a score of 123 establishing 11% coverage of protein sequence. The mass spectrometric analysis confirmed the presence of plant phytaspase in the purified protein samples.

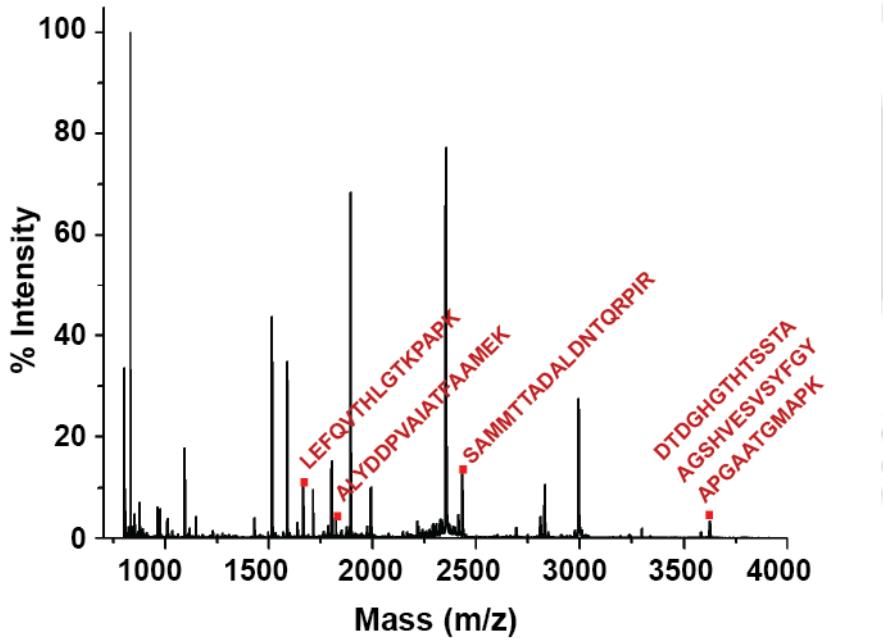

Figure 3.10: MALDI-TOF/TOF spectral analysis of GST-mature phytaspase. Peptides with masses (m/z 1664.9250, 1824.8968, 1990.9564 and 3621.6067) were found to match with phytaspase sequence.

3.4.9 Protease activity

A standard curve for known concentration of L-tyrosine amino acid was generated measuring absorbance at 660 nm. Addition of 1 ml of GST-mature phytaspase (6 µg/ml)

to the casein substrate released only 0.0044 µmol of free tyrosine (Figure. 3.11). The enzyme activity was calculated as 0.00484 Units/ml or 0.807 Units/mg. The results showed very poor digestion of casein by the GST-mature phytaspase.

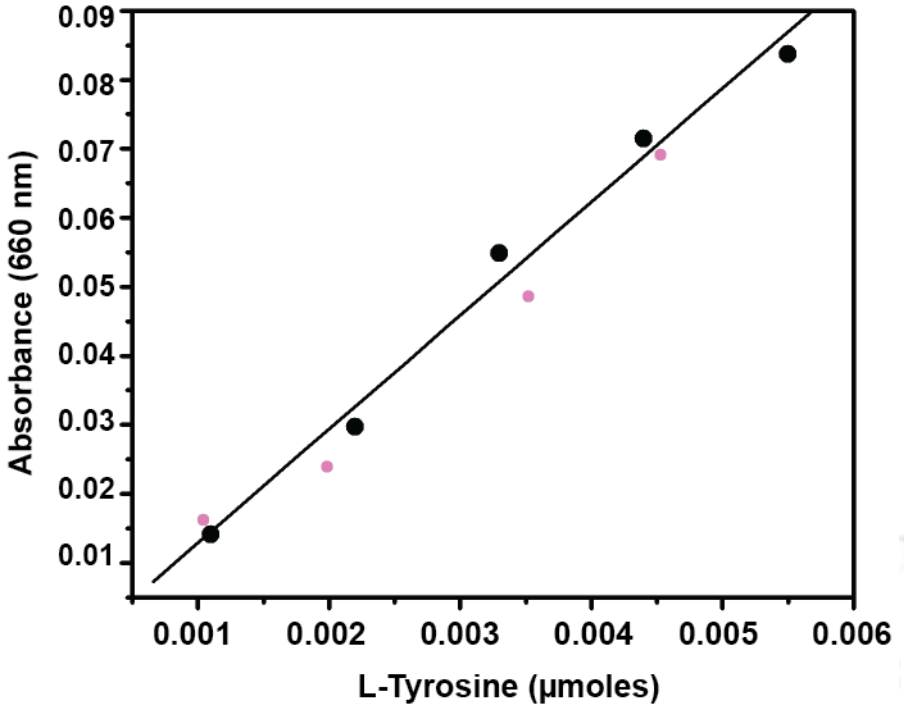

Figure 3.11: Graph for concentration of L-tyrosine (µmol) vs absorbance (660 nm). Black dots- Standard L-tyrosine amino acid and pink dots- Free tyrosine liberated measures enzymatic activity of GST-mature phytaspase on casein substrate.

Not to limit the determination of non-specific protease activity of GST-mature phytaspase with only casein, the protease activity was also performed with azocasein and azocoll substrates. The results showed no protease activity against these substrates.

3.4.10 Removal of GST tag from mature phytaspase by thrombin cleavage

Due to very low protease activity of GST-mature phytaspase for casein (Figure 3.11), and no protease activity towards azocasein and azocoll, there were two questions raised. Firstly, does the mature phytaspase have its protease activity towards specific substrate? or secondly, does the removal of the N-terminal GST tag necessary for the protease to perform its activity? To address both the questions, it was important to remove the GST

tag from purified protein by thrombin-mediated cleavage. Figure 3.12 showed gradual removal of GST tag with increasing incubation time of GST-mature phytaspase with thrombin. During thrombin cleavage, in addition to cleaved mature phytaspase (70.47 kDa), slight release of GST (26.01 kDa) was also observed which was finally removed by dialysis.

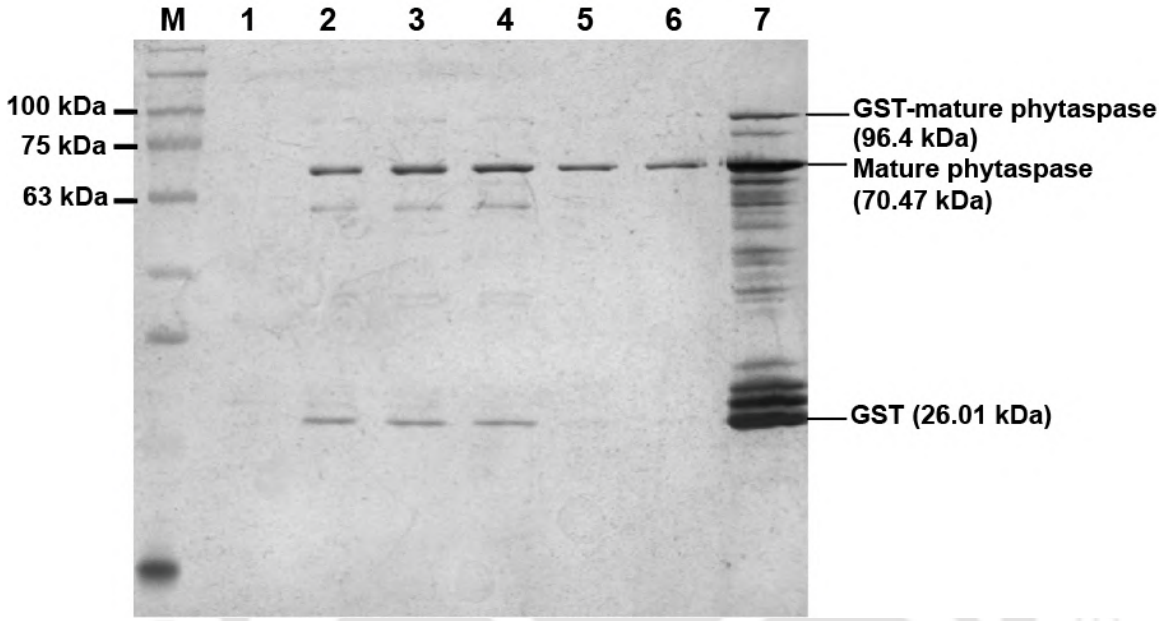

Figure 3.12: Enzymatic cleavage of GST tag from mature phytaspase by thrombin. *Lane M*- Protein marker (10-180 kDa), *lanes 1, 2, 3 & 4*- Thrombin cleavage of GST tag at 0 h, 1 h, 2 h, and 3 h respectively showing high molecular weight mature phytaspase (70.47 kDa) and low molecular weight GST (26.01 kDa) bands, *lanes 5 & 6*- Dialyzed mature phytaspase and *lane 7*- Elute containing mixture of GST-mature phytaspase (96.4 kDa), mature phytaspase (70.47 kDa) and GST (26.01 kDa).

3.4.11 Secondary structure analysis of recombinant mature phytaspase

Secondary structure of the recombinant mature phytaspase was analyzed by CD spectroscopy (Figure. 3.13). Spectral similarity with other plant serine proteases (hirtin, latex glycoprotein (LGP)) [137, 138] indicated that phytaspase belonged to α+β class of proteins. Estimation of secondary structure (Yang's reference) revealed that phytaspase consisted of 24.9% α-helix, 36.6% β-sheet, 13.3% turns and 25.2% random coil. Since this was, to the best of knowledge, the first reported CD spectra of any plant phytaspase,

further analyses were performed with GST and GST-mature phytaspase. The presence of GST in GST-mature phytaspase resulted in variation of secondary structure with 31.1% α-helix, 42.3% β-sheet, 0.7% turns and 25.9% random coils. The spectral similarity with other plant serine proteases indicated that bacterially expressed recombinant mature phytaspase might retain its functional activity justifying further functional analyses of the same.

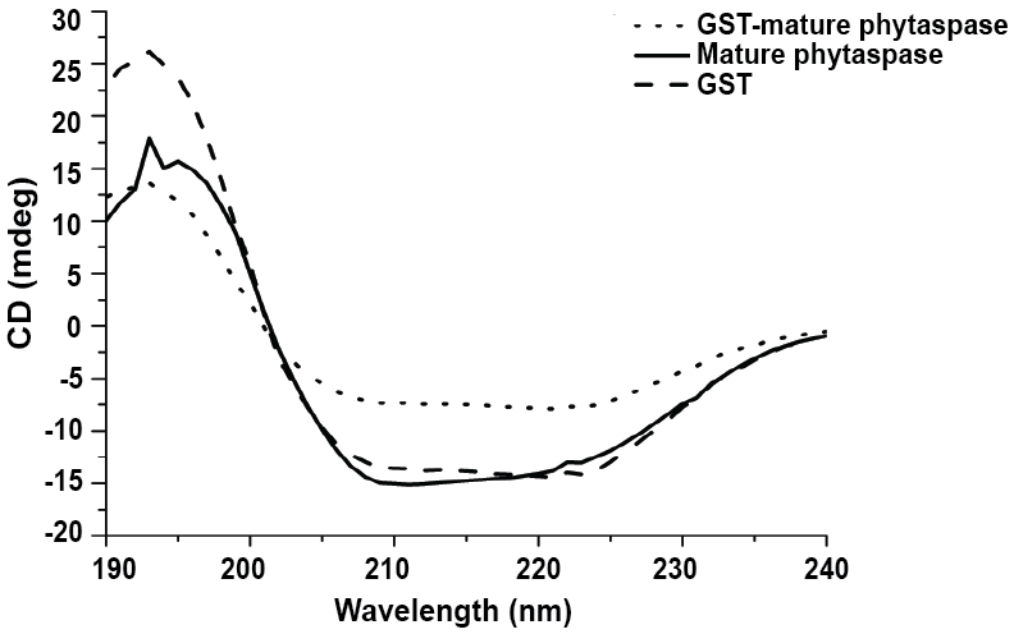

Figure 3.13: CD spectra of GST-mature phytaspase, mature phytaspase and GST in far-UV region (240 nm-190 nm).

3.4.12 Homology modeling of recombinant mature phytaspase

Templates of three subtilisin-like serine proteases namely cucumisin (PDB:3VTA), tomato subtilase 3 (SBT3, PDB:3I6S) and Tk-SP from *Thermococcus kodakaraensis* (PDB:3AFG) were selected on the basis of amino acids sequence homology with phytaspase. Three dimensional (3D) structures of recombinant mature phytaspase was constructed through homology modeling, based on crystal structures of the closest homologs, using EasyModeller 4.0. Careful visualization of modeled structures in PyMOL revealed that the additional 9 amino acid residues at the N-terminus of the mature phytaspase (resulting from thrombin-cleavage) did not affect the relative spatial

arrangement of catalytic site of the protein. Alignment of 3D structure of mature phytaspase with that of SBT3 demonstrated similarity in spatial positioning of catalytic triad D^{41}-H^{112}-S^{429} of recombinant mature phytaspase with SBT3 catalytic triad (D^{144}-H^{215}-S^{538}) residues [139] in the subtilisin domain (Figure. 3.14a), possibly due to 53.35% sequence similarity between phytaspase and SBT3. Moreover, this structural conservation indicated that phytaspase might also feature protease-associated domain and fibronectin (Fn) III-like domain in addition to the predicted subtilisin-like domain (Figure. 3.14b).

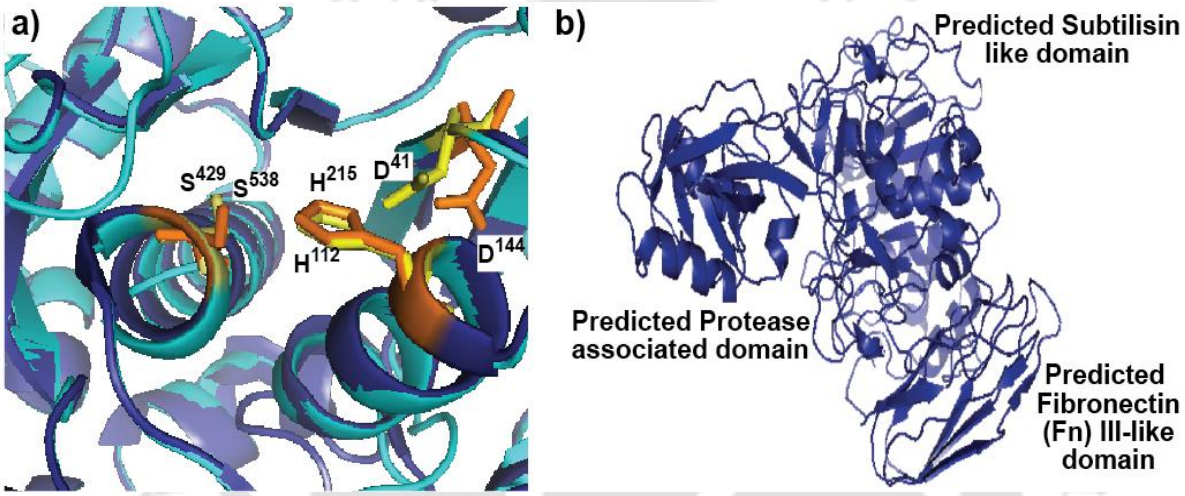

Figure 3.14: a. Alignment of secondary structures of recombinant mature phytaspase and *S. lycopersicum* SBT3 (generated through EasyModeller 4.0) highlighting the positions of catalytic triad residues (catalytic triads of phytaspase and SBT3 in yellow and orange; respectively), **b.** Modeled 3D structure of recombinant mature phytaspase.

3.4.13 Molecular docking of recombinant mature phytaspase with caspase substrates

In light of existing evidence on canonical catalytic triad of phytaspase, molecular docking of recombinant mature phytaspase with substrates for caspase 8 and caspase 3 was performed. When docked to recombinant mature phytaspase (depicted in cyan), Ac-VETD-AMC (caspase 8 substrate, depicted in black) lay in close contact with predicted active site residues (D^{41}-H^{112}-S^{429}) and oxyanion hole residues (N^{214} and H^{223}) fixing the P1 aspartic acid side chain of substrate (Figure 3.15a). These observations corroborated well with the results obtained in previous docking study with synthetic phytaspase

inhibitor, Ac-VAD-CHO [104]. The binding energy of recombinant phytaspase for caspase 8 substrate was estimated to be -3.4 kcal/mol. However, the same was found to be -0.34 kcal/mol for caspase 3 substrate (Ac-DMQD-pNA) (Figure 3.15b), much higher than that of Ac-VETD-AMC. With the prediction of favourable binding of Ac-VETD-AMC to the reactive pocket of phytaspase, *in silico* studies indicated the potential of Ac-VETD-AMC in assessing functional activity of recombinant phytaspase.

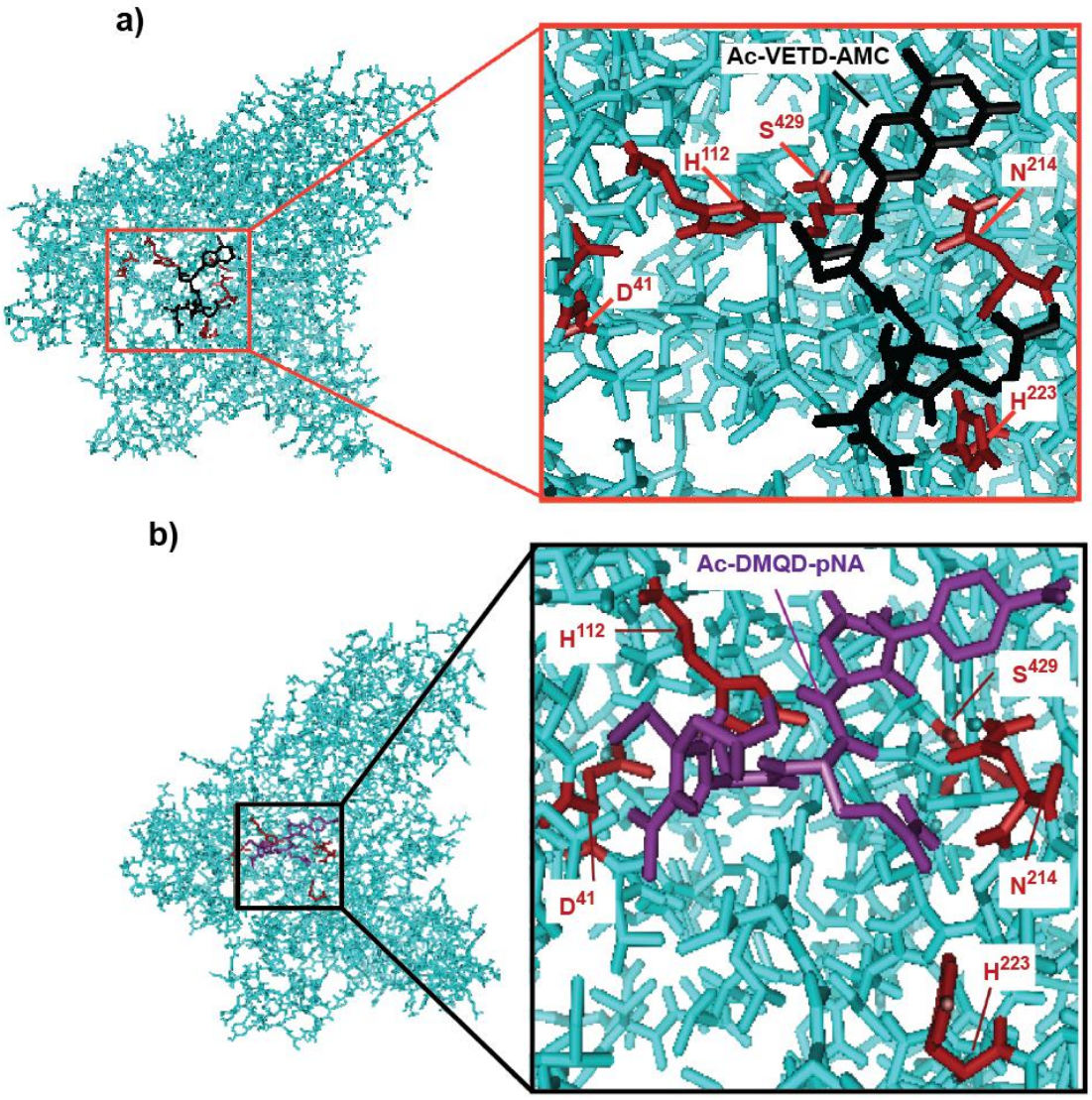

Figure 3.15: Molecular docking of recombinant mature phytaspase with caspase 8 (Ac-VETD-AMC) and 3 substrate (Ac-DMQD-pNA). **a.** Molecular docking of phytaspase

(cyan) with Ac-VETD-AMC (black) demonstrating that the ligand Ac-VETD-AMC lies in close proximity to the predicted catalytic triad residues (red). **b.** Molecular docking of phytaspase with Ac-DMQD-pNA.

3.4.14 Assessment of caspase-like functional activity

Caspase-like functional activity of the GST-mature phytaspase and mature phytaspase was assessed by measuring their capability of hydrolyzing synthetic caspase 8 substrate, Ac-VETD-AMC. Recombinant mature phytaspase – after removal of the GST tag – showed significant hydrolyzing capability for Ac-VETD-AMC as probed by the fluorescence of liberated AMC (Figure. 3.16). The results showed that hydrolysis of Ac-VETD-AMC gradually increased with increasing mature phytaspase concentration. The kinetic parameters, Michaelis constant (K_M) and specificity constant (k_{cat}/K_M) of mature phytaspase for substrate Ac-VETD-AMC were also calculated to be 1.587 µM and 4.67 × 10^3 $M^{-1}min^{-1}$, respectively. However, caspase 3 substrate (Ac-DMQD-pNA) was not hydrolyzed by recombinant phytaspase confirming previously reported observation that phytaspase is incapable of cleaving caspase 3 synthetic substrates [136]. The results demonstrated that the removal of N-terminal GST tag was essential to render bacterially expressed recombinant mature phytaspase with caspase 8-like activity similar to native plant mature phytaspase.

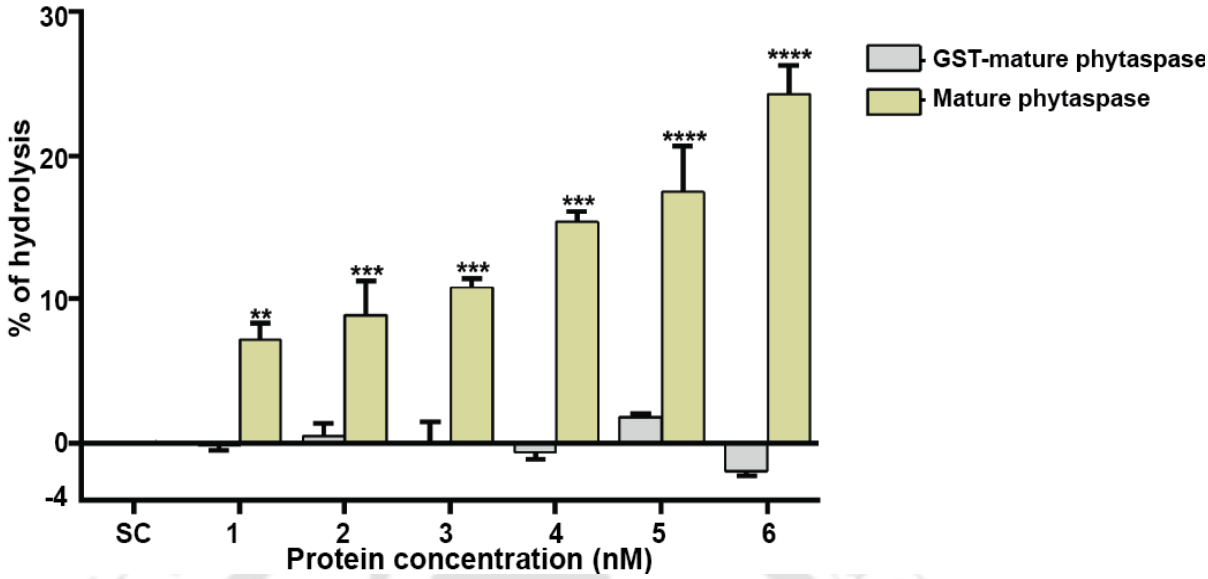

Figure 3.16: Measuring caspase 8-like activity of GST-mature phytaspase and mature phytaspase. Hydrolysis (%) of caspase 8 substrate (Ac-VETD-AMC) is plotted at different concentrations (nM) of GST-mature phytaspase and mature phytaspase. SC-Substrate control. Statistical significance was assessed by one-way ANOVA: **p<0.01, ***p<0.001, ****p<0.0001.

3.4.15 Synthesis of Mn doped ZnS QD-Chitosan NPs (nanocomposites)

UV-absorption spectrum showing blue shift in absorption spectra from 340 nm of bulk ZnS to 304 nm suggested formation of ZnS QDs [140]. There was an increase in the absorption spectra at 280 nm when the recombinant mature phytaspase was bound to nanocomposites (Figure 3.17a). Synthesized nanocomposites at 590 nm revealed characteristic emission peak of the Mn doped ZnS QDs by exciting at 300 nm UV light [140] as depicted in figure 3.17b. The quantum yield of nanocomposites was found to be 2.1% with respect to the reference quinine sulfate dye.

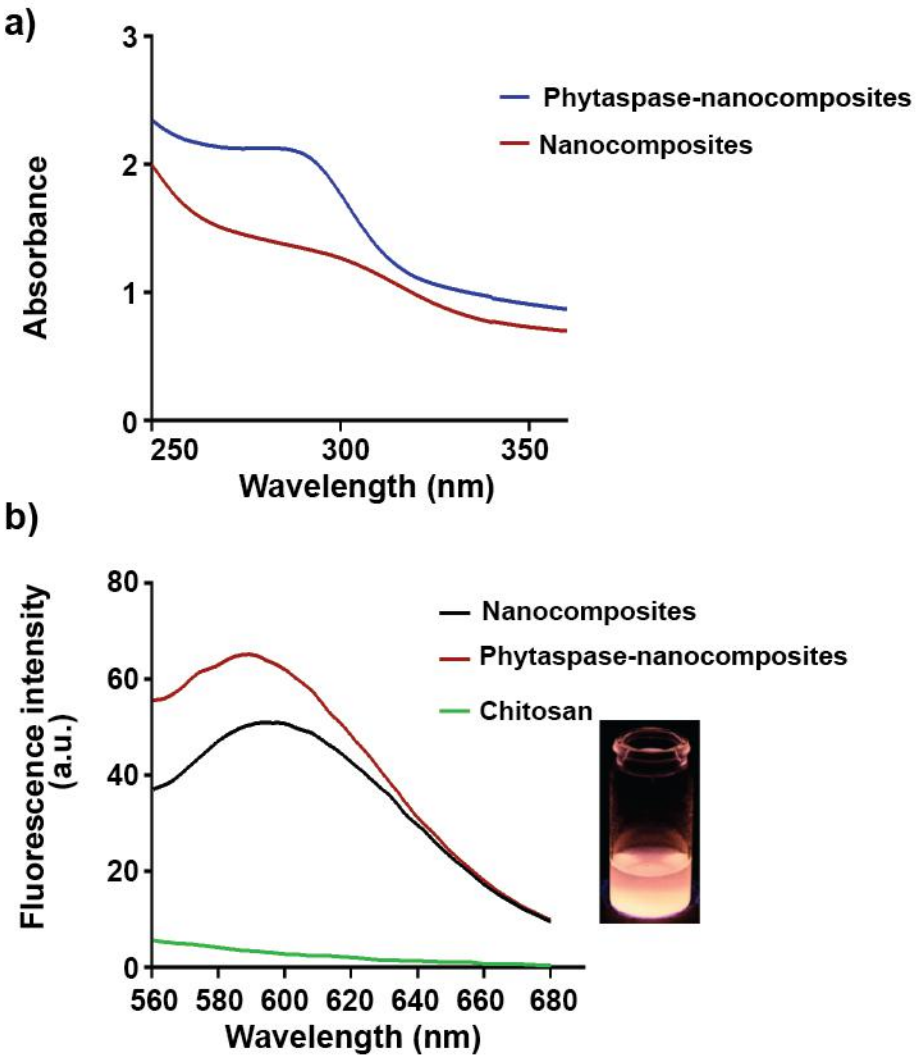

Figure 3.17: a. UV-visible absorption spectrum of nanocomposites and phytaspase-nanocomposites and **b.** Emission spectrum of nanocomposites displaying bright luminescence when excited with 300 nm wavelength of light.

3.4.16 Dynamic light scattering (DLS) and zeta potential study

Hydrodynamic diameter of phytaspase-nanocomposites was 217 ± 2.15 nm, which was slightly increased than only nanocomposites (203 ± 2 nm) (Figure 3.18).

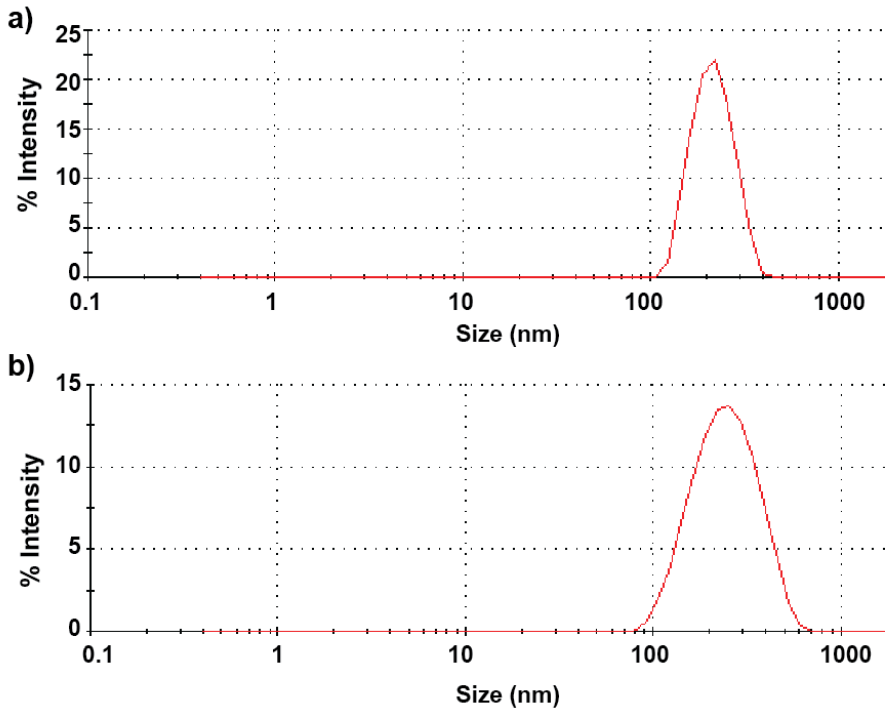

Figure 3.18: Hydrodynamic study using DLS. **a**) Nanocomposites (average diameter 203 ± 2 nm and **b**) Phytaspase-nanocomposites (average diameter 217 ± 2.15nm).

Zeta potential studies determined that the overall net charge of nanocomposites was reduced to + 9.84 ± 0.23 mV from + 22.75 ± 1.2 mV when conjugated with phytaspase (Figure 3.19). In other way, the positive zeta potential value after binding of phytaspase to nanocomposites will facilitate its delivery into the cancer cells.

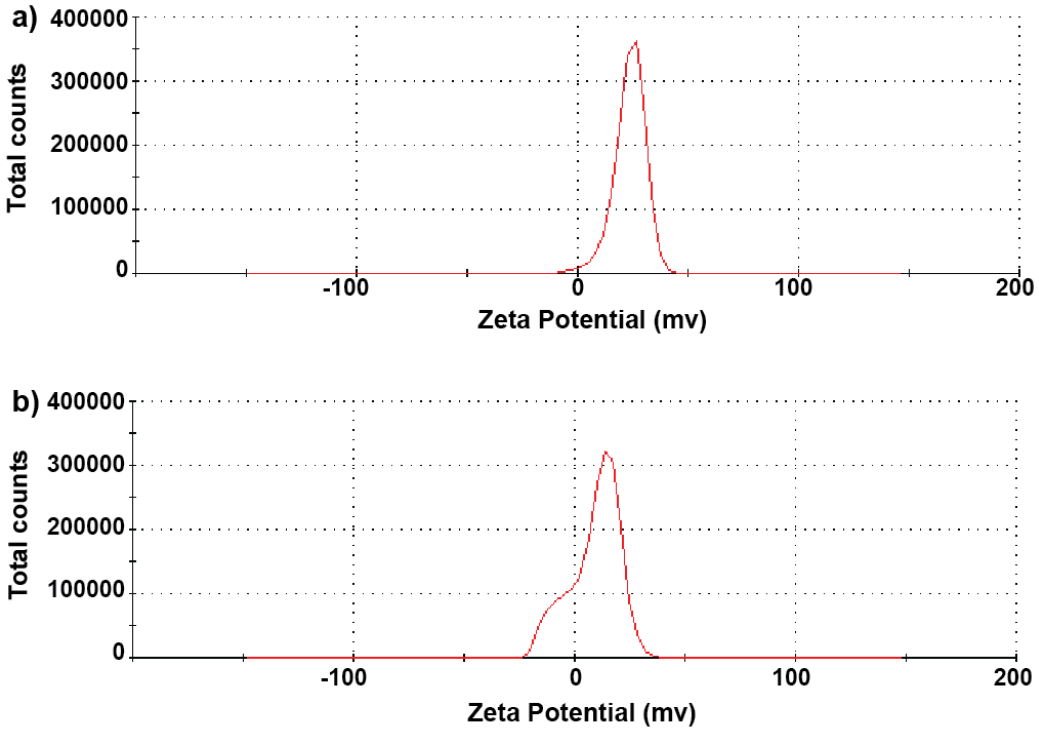

Figure 3.19: Zeta potential studies showed that net surface charge of **a.** Nanocomposites was + 22.75 ± 1.2 mV, **b.** Phytaspase-nanocomposites was + 9.84 ± 0.23 mV.

3.4.17 TEM and FESEM analysis

TEM images showed formation of the nanocomposites with a particle size of around ≤100nm (Figure 3.20). The FESEM image showing nanocomposites with average particle size of 102 ± 16 nm determined using ImageJ further corroborates the TEM analysis (Figure 3.21). In both the cases, particle size is suitable for intracellular delivery [141, 142]. It is important to mention here that the particle size measurement obtained using TEM and FESEM was smaller than the DLS measurement. The apparent higher particle size obtained in DLS measurement is due to the formation of hydration layer.

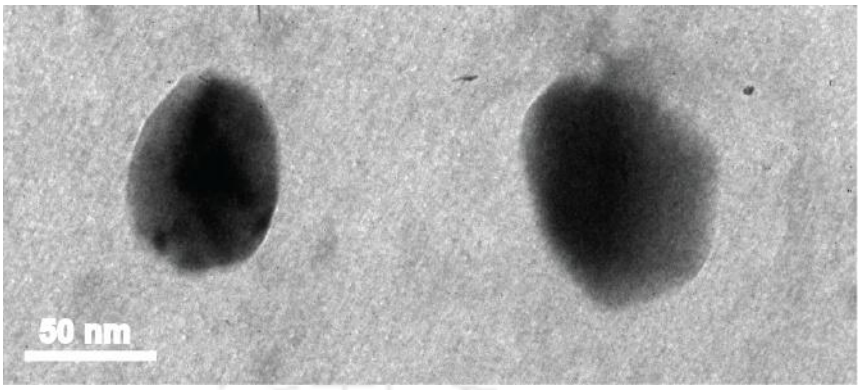

Figure 3.20: TEM image of synthesized nanocomposites with particle size around ≤100 nm.

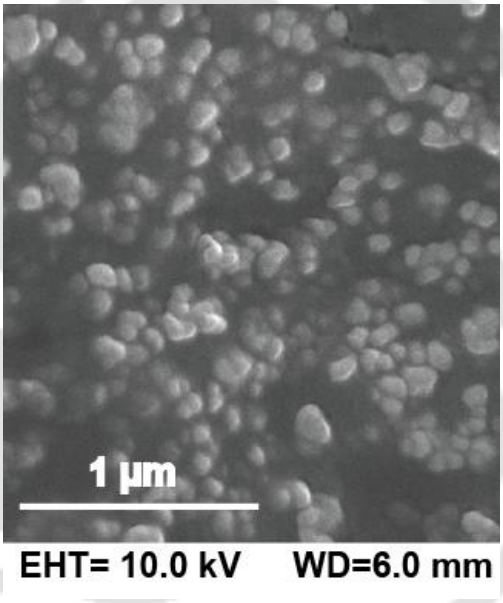

Figure 3.21: FESEM imaging (at scale bar 1µm) showing formation of nanocomposites with the average particle size 102 ± 16 nm.

3.4.18 Binding efficiency of phytaspase to nanocomposites

Binding efficiency of recombinant mature phytaspase to nanocomposites was calculated by probing the decrease in fluorescence of supernatant with the increase in amount of nanocomposites (Figure 3.22). The maximum binding efficiency of phytaspase (10 µg/ml) was found to be 65.5% with the highest concentration of nanocomposites (124 µg/ml) in PBS buffer, pH 7.4.

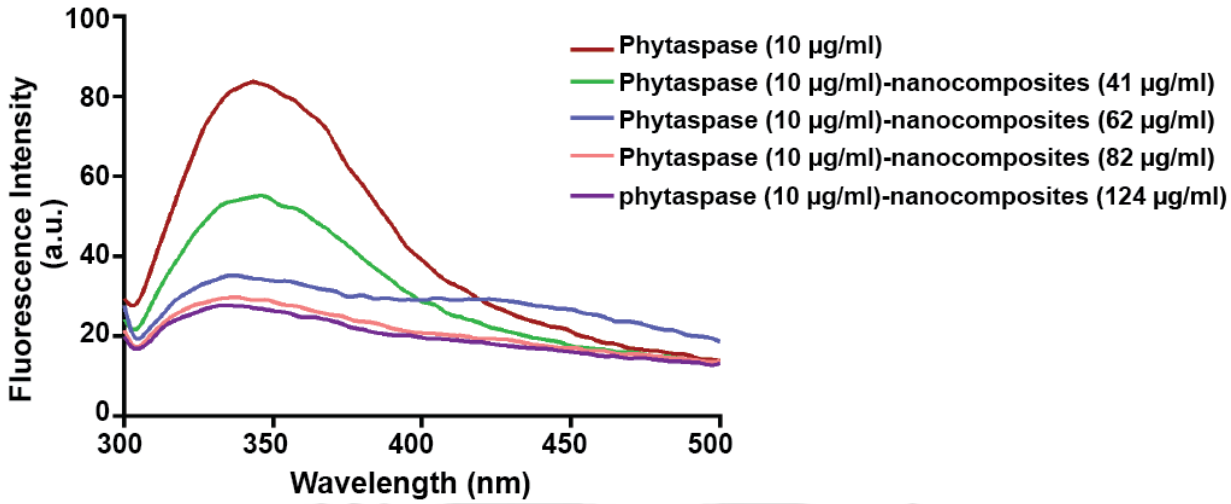

Figure 3.22: Binding of constant amount of phytaspase (10 µg/ml) to increasing amount of nanocomposites (41-124 µg/ml).

3.4.19 Confocal microscopic imaging

The image acquired illustrated the uptake of nanocomposites into HeLa, but not A549 cells (Figure 3.23a & b). Based on the results, HeLa cells were chosen to study the effect of phytaspase delivery using nanocomposites. Figure 3.23c, showed the entry of phytaspase-nanocomposites into the HeLa cells. Z-stacking of the image substantiated the uptaking of phytaspase-nanocomposites complex by the HeLa cells (Figure 3.23d).

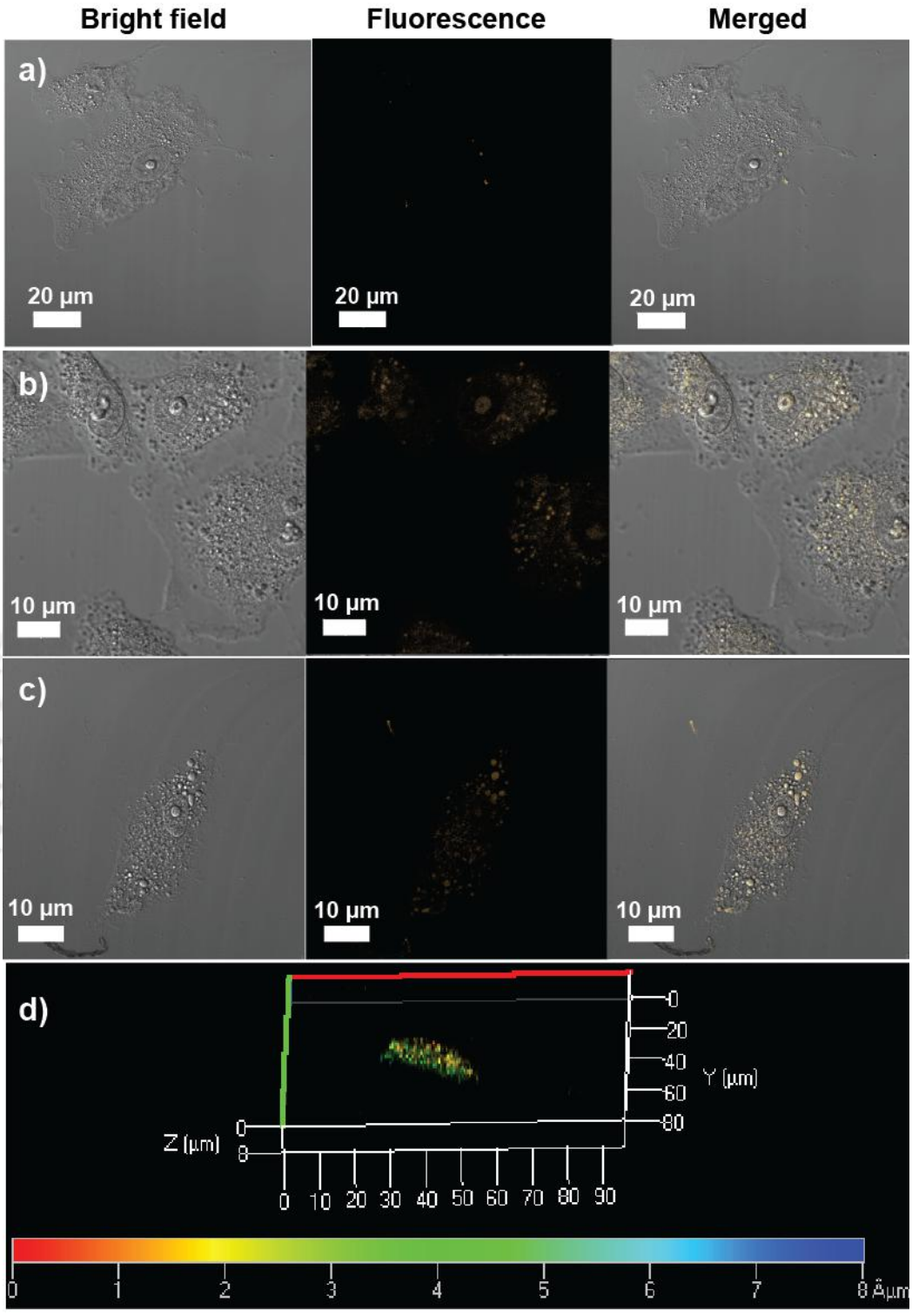

Figure 3.23: Confocal microscopic images of intracellular uptake of **a & b.** Nanocomposites into A549 cells and HeLa cells respectively, **c.** Phytaspase-

nanocomposites into HeLa cells and **d.** Z-stacking of image taken clearly reveals the successful uptake of phytaspase-nanocomposites by HeLa cells.

3.4.20 Effect of phytaspase-nanocomposites on HeLa cells

Cell viability assay result revealed that even though initially phytaspase-nanocomposites complex did not exert any effect but at high concentration there was a significant cell death (Figure 3.24).

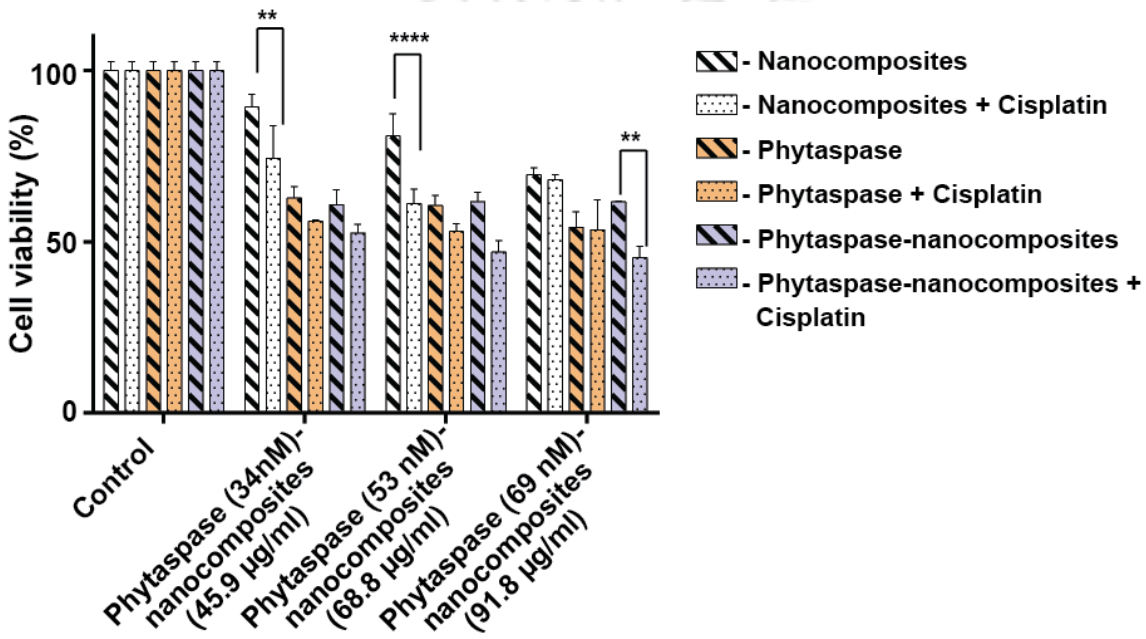

Figure 3.24: Cell viability assessment to evaluate the effect of phytaspase, nanocomposites and phytaspase-nanocomposites on HeLa cells in the presence and absence of cisplatin (0.44 µg/ml) after 48 h. Satistical significance was evaluated using two way ANOVA using GraphPad Prism 6.0, where **p<0.01 and ****p<0.0001.

3.4.21 Transient expression of mature phytaspase in A549 cells

Phytaspase gene was amplified from cDNA synthesized from total RNA isolated from pEGFP-N1-mature phytaspase transfected A-549 cells using gene specific primers. RT-PCR analysis on A549 cells transfected with pEGFP-N1-phytaspase revealed the presence of legitimate band of 1.94 kbp establishing the expression of mature phytaspase at mRNA level (Figure 3.25). The 1.94 kbp PCR amplified product was seen

corresponding to the phytaspase gene (positive control). However, the expression of phytaspase at protein level could not be verified due to unavailability of commercial antibodies for phytaspase.

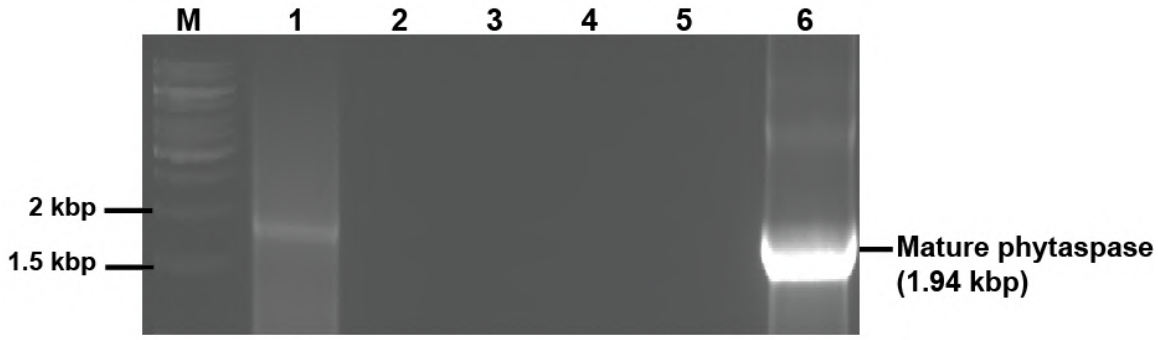

Figure 3.25: Confirmation of mature phytaspase expression by agarose gel electrophoresis. *Lane M*- DNA marker (10 kbp-250 bp), *lane 1*- PCR amplified mature phytaspase gene (1.94 kbp) from cDNA synthesized from pEGFP-N1-mature phytaspase transfected A549 cells, *lane 2*- pEGFP-N1(-GFP) vector transfected A549 cells, *lane 3*- Untransfected A549 cells, *lanes 4 & 5*- Negative control and *lane 6*- Positive control.

3.4.22 Effect of transient expression of mature phytaspase in A549 cells on doxorubicin treatment

MTT assay confirmed that expression of mature phytaspase itself did not affect the viability of either A549 cells or non-transformed human dermal fibroblast (HDFs) cells significantly (Figure 3.26a & b). However, when cells were treated with anticancer drug doxorubicin, mature phytaspase expressing A549 cells became more sensitized towards doxorubicin as compared to control (pEGFP-N1(-GFP)-transfected) A549 cells. Transient expression of mature phytaspase essentially led to IC_{50} value of 37.6 nM of doxorubicin as compared to 45.2 nM in pEGFP-N1(-GFP)-transfected A549 cell (Figure 3.27). This was an interesting finding where a plant mature phytaspase could sensitize A549 cancer cells to undergo apoptosis at low concentration of chemotherapeutic drug.

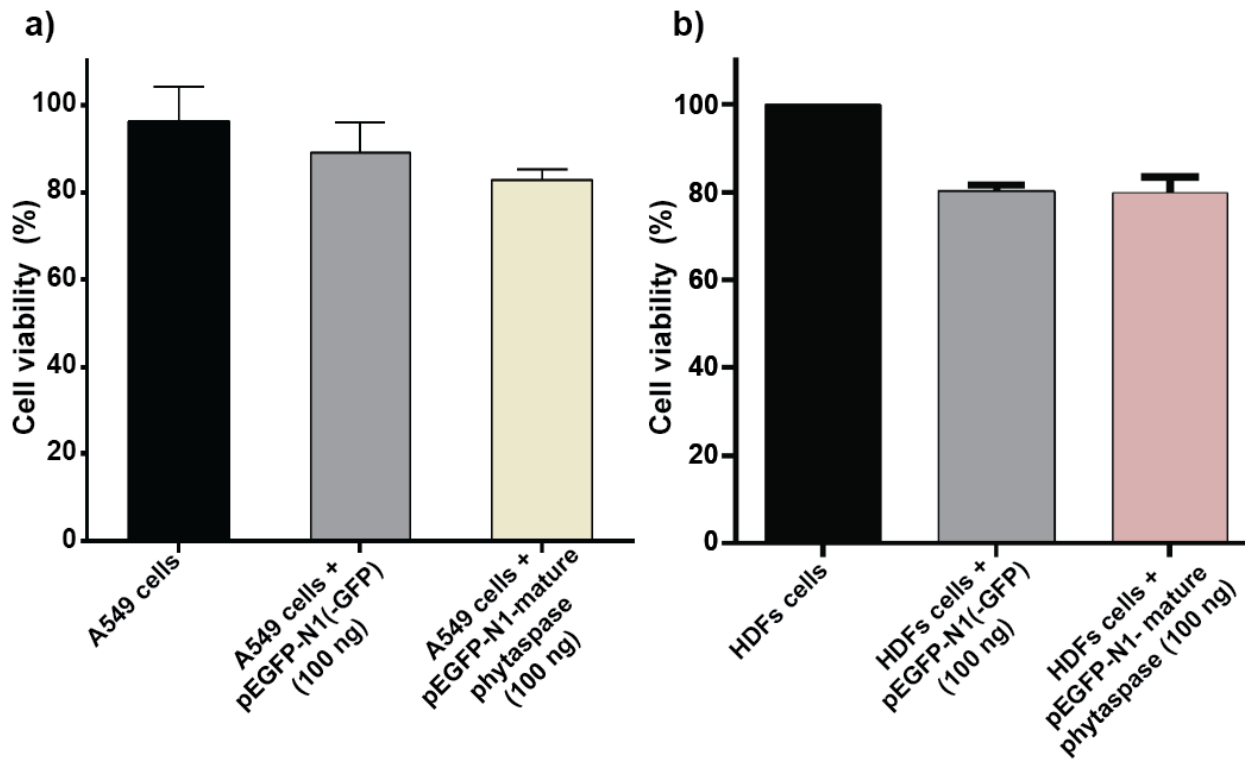

Figure 3.26: a. Cell viability assessment of nontransfected, pEGFP-N1(-GFP) and pEGFP-N1-mature phytaspase transfected A549 cells and **b.** Cell viability of nontransfected, pEGFP-N1(-GFP) and pEGFP-N1-mature phytaspase transfected HDFs cells.

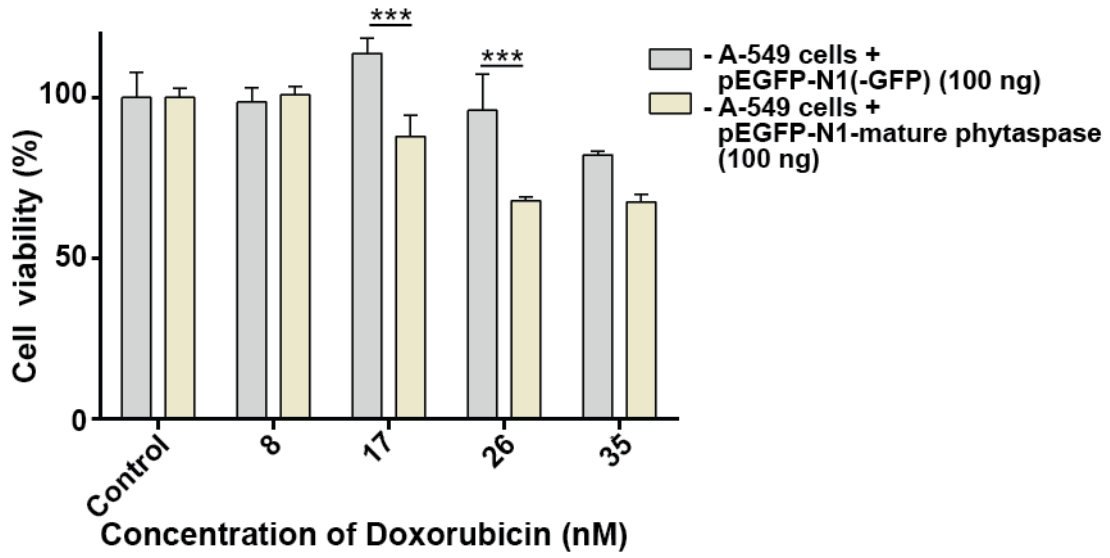

Figure 3.27: Cell viability of mature phytaspase-expressing and vector (pEGFP-N1(-GFP))-transfected A549 cells following treatment with varying concentrations of doxorubicin for 48 h. Statistical significance was evaluated by one-way ANOVA, where ***$p<0.001$.

3.5 Conclusion

In conclusion, successful cloning of tobacco phytaspase in *E. coli* BL21 (DE3) have been demonstrated. However, trials made to obtain the pre-prophytaspase in larger amount were not successful. Therefore, only purified recombinant mature phytaspase was subjected to further functional characterization. The caspase-8 like activity of the recombinant phytaspase was not only investigated *in silico*, but also validated with enzymatic assay with peptide substrate, Ac-VETD-AMC. This further denoted the importance of removal of GST tag from mature phytaspase to be active. The nanocomposites based delivery of phytaspase to the HeLa cells, not only facilitated the delivery of phytaspase but also was helpful in imaging cellular uptake due to the bright luminescence of QDs. Fascinatingly at higher concentration, bacterially expressed phytaspase showed to intracellularly exert significant cell death in the presence of cisplatin. In addition, transient expression of phytaspase in A549 cells led to sensitization of the cancer cells toward doxorubicin-mediated PCD. There is no report so far, on expression of phytaspase in heterologous system. The insight gained in present study may

not only help in understanding the structure-function correlation of recombinant phytaspase, but also serve as a platform for future studies for obtaining functionally active phytaspase using bacterial system avoiding otherwise cumbersome procedure and/or pertaining the implication of caspases-like phytaspase in future gene therapy.

CHAPTER 4

Conclusions and Future Prospects

CHAPTER 4

Conclusions and Future Prospects

This part outlines the conclusions and emphasizes on the future prospects of work done in the current thesis. Based on the fact “plants being never surpassed remain valued medicines”, this whole thesis is a primary complement to the concept of using plant based genes/proteins, despite the use of general cancer therapeutic strategies-surgery, chemotherapy and radiotherapy.

Review of scientific literature fairly provides the factual information, which broadly covers the aspects of cancer therapy. More specifically, the significance of well studied therapeutically important plant genes and proteins are detailed and the important need of studying AtUPRT-counterpart of bacterial UPRT and phytaspase-counterpart of mammalian caspase has been explained here.

It is germane to mention here, AtUPRT and phytaspase genes were for the first time cloned into the mammalian expression vectors and in addition phytaspase was also cloned into bacterial expression vectors. Both the genes cloned were verified by restriction digestion and thorough sequence analysis. Stable expression of AtUPRT in HeLa cells was validated by reverse transcriptase PCR. AtUPRT expressed into HeLa cells increasingly sensitized the cells towards prodrug 5-FU. Apoptosis including mitochondrial apoptosis analysis by flow cytometric analysis, JC-1 staining, methylene blue staining illustrated the higher rate of apoptosis in cells expressing AtUPRT. S-phase cell cycle arrest in HeLa cells expressing AtUPRT denoted accelerated rate of conversion of 5-FU into 5-FUMP which in turn inhibits thymidylate synthetase thereby halting the cells in S-phase. Survival efficiency analysis revealed that survival fraction of HeLa-UPP cells was considerably lesser than survival fraction of HeLa and HeLa-pEGFP-N1 which evidenced that AtUPRT augments the long term effect of 5-FU on HeLa cells even after the removal of 5-FU.

The extensive study on phytaspase started with the expression of pre-prophytaspase and mature phytaspase with His-tag and GST-tag. His-tagged expression was disappointing as we could not obtain His-pre-prophytaspase. Hence, the focus was shifted to GST tagged phytaspase expression for the comparative study between pre-prophytaspase and mature phytaspase as GST is reported to stabilize recombinant protein expression. With initial efforts of optimizing various parameters, GST-pre-prophytaspase and GST-mature phytaspase was successfully purified which was validated through western blot analysis. Further intended studies on GST-pre-prophytaspase was discontinued as obtaining the large amount of purified GST tagged protein was difficult, which was assumed to be due to endoproteases degradation activity or auto-processing of GST-pre-prophytaspase into mature phytaspase. Unable to detect any caspase 8-like activity of GST-mature phytaspase was overcome by thrombin cleavage of GST-tag from mature phytaspase. This observation highlights the importance of removal of GST tag from phytaspase for it to retain its functionality. Intracellular delivery of functionally active phytaspase conjugated with remarkably luminescent QDs based nanocomposites exerted significant reduction in cell viability upon cisplatin treatment reflecting the caspase like activity of phytaspase augmenting the rate of chemotherapeutic drug induced cell apoptosis. With enormous difficulties in establishing stable expression of phytaspase in various cancer cells, the attempt of transient expression of phytaspase was fairly successful in A549 cells. Similar to the bacterially expressed phytaspase, mature phytaspase expression in A549 cells imparted cell death in the presence of doxorubicin.

This work on *A. thaliana* UPRT and *N. tabacum* phytaspase provides groundwork in plant suicide gene/protein therapy by broadening the traditional boundaries of suicide gene therapy and protein therapy. Due to limited information, it remains difficult to elaborate the underlying cellular mechanisms which are influenced by these plant enzymes. However, in future, one could always look for descriptive approach to unveil the molecular aspects responsible for the cell cycle arrest and apoptosis in cells expressing AtUPRT and phytaspase. Additionally, aiming to extend the study with other plant UPRTs and phytaspases will also definitely reinforce this approach which is promising in the future cancer therapeutics.

REFERENCES

[1] A. Saklani, S.K. Kutty, Plant-derived compounds in clinical trials, Drug discovery today 13(3-4) (2008) 161-71.

[2] A.R. David, M.R. Zimmerman, Cancer: an old disease, a new disease or something in between?, Nature reviews. Cancer 10(10) (2010) 728-33.

[3] A. Sudhakar, History of Cancer, Ancient and Modern Treatment Methods, Journal of cancer science & therapy 1(2) (2009) 1-4.

[4] L. Naldini, Gene therapy returns to centre stage, Nature 526(7573) (2015) 351-60.

[5] D. Cross, J.K. Burmester, Gene Therapy for Cancer Treatment: Past, Present and Future, Clinical Medicine and Research 4(3) (2006) 218-27.

[6] P. Zarogoulidis, K. Darwiche, A. Sakkas, L. Yarmus, H. Huang, Q. Li, L. Freitag, K. Zarogoulidis, M. Malecki, Suicide Gene Therapy for Cancer – Current Strategies, Journal of genetic syndrome & gene therapy 4 (2013).

[7] S.Q. Lv, K.B. Zhang, E.E. Zhang, F.Y. Gao, C.L. Yin, C.J. Huang, J.Q. He, H. Yang, Antitumor efficiency of the cytosine deaminase/5-fluorocytosine suicide gene therapy system on malignant gliomas: an in vivo study, Medical science monitor : international medical journal of experimental and clinical research 15(1) (2009) BR13-20.

[8] C.R. Miller, C.R. Williams, D.J. Buchsbaum, G.Y. Gillespie, Intratumoral 5-fluorouracil produced by cytosine deaminase/5-fluorocytosine gene therapy is effective for experimental human glioblastomas, Cancer research 62(3) (2002) 773-80.

[9] K. Kawamura, R. Bahar, H. Namba, M. Seimiya, K. Takenaga, H. Hamada, S. Sakiyama, M. Tagawa, Bystander effect in uracil phosphoribosyltransferase/5-fluorouracil-mediated suicide gene therapy is correlated with the level of intercellular communication, International journal of oncology 18(1) (2001) 117-20.

[10] K. Kawamura, K. Tasaki, H. Hamada, K. Takenaga, S. Sakiyama, M. Tagawa, Expression of Escherichia coli uracil phosphoribosyltransferase gene in murine colon carcinoma cells augments the antitumoral effect of 5-fluorouracil and induces protective immunity, Cancer gene therapy 7(4) (2000) 637-43.

[11] F. Koyama, H. Sawada, H. Fuji, H. Hamada, T. Hirao, M. Ueno, H. Nakano, Adenoviral-mediated transfer of Escherichia coli uracil phosphoribosyltransferase (UPRT) gene to modulate the sensitivity of the human colon cancer cells to 5-

fluorouracil, European journal of cancer (Oxford, England : 1990) 36(18) (2000) 2403-10.

[12] J. Wang, X.X. Lu, D.Z. Chen, S.F. Li, L.S. Zhang, Herpes simplex virus thymidine kinase and ganciclovir suicide gene therapy for human pancreatic cancer, World journal of gastroenterology 10(3) (2004) 400-3.

[13] C. Fillat, M. Carrio, A. Cascante, B. Sangro, Suicide gene therapy mediated by the Herpes Simplex virus thymidine kinase gene/Ganciclovir system: fifteen years of application, Current gene therapy 3(1) (2003) 13-26.

[14] M. Bentires-Alj, A.C. Hellin, C. Lechanteur, F. Princen, M. Lopez, G. Fillet, J. Gielen, M.P. Merville, V. Bours, Cytosine deaminase suicide gene therapy for peritoneal carcinomatosis, Cancer gene therapy 7(1) (2000) 20-6.

[15] J. Li, S. Huang, J. Chen, Z. Yang, X. Fei, M. Zheng, C. Ji, Y. Xie, Y. Mao, Identification and characterization of human uracil phosphoribosyltransferase (UPRTase), Journal of human genetics 52(5) (2007) 415-22.

[16] D.B. Longley, D.P. Harkin, P.G. Johnston, 5-fluorouracil: mechanisms of action and clinical strategies, Nature reviews. Cancer 3(5) (2003) 330-8.

[17] M. Tiraby, C. Cazaux, M. Baron, D. Drocourt, J.P. Reynes, G. Tiraby, Concomitant expression of E. coli cytosine deaminase and uracil phosphoribosyltransferase improves the cytotoxicity of 5-fluorocytosine, FEMS microbiology letters 167(1) (1998) 41-9.

[18] T.A. O'Brien, D.T. Tuong, L.M. Basso, R.S. McIvor, P.J. Orchard, Coexpression of the uracil phosphoribosyltransferase gene with a chimeric human nerve growth factor receptor/cytosine deaminase fusion gene, using a single retroviral vector, augments cytotoxicity of transduced human T cells exposed to 5-fluorocytosine, Human gene therapy 17(5) (2006) 518-30.

[19] P. Gopinath, S.S. Ghosh, Understanding apoptotic signaling pathways in cytosine deaminase-uracil phosphoribosyl transferase-mediated suicide gene therapy in vitro, Molecular and cellular biochemistry 324(1-2) (2009) 21-9.

[20] P. Gopinath, S.S. Ghosh, Implication of functional activity for determining therapeutic efficacy of suicide genes in vitro, Biotechnology letters 30(11) (2008) 1913-21.

[21] T.W. Nicholas, S.B. Read, F.J. Burrows, C.A. Kruse, Suicide gene therapy with Herpes simplex virus thymidine kinase and ganciclovir is enhanced with connexins to improve gap junctions and bystander effects, Histology and histopathology 18(2) (2003) 495-507.

[22] V. Marin, E. Cribioli, B. Philip, S. Tettamanti, I. Pizzitola, A. Biondi, E. Biagi, M. Pule, Comparison of different suicide-gene strategies for the safety improvement of genetically manipulated T cells, Human gene therapy methods 23(6) (2012) 376-86.

[23] S.R. Riddell, M. Elliott, D.A. Lewinsohn, M.J. Gilbert, L. Wilson, S.A. Manley, S.D. Lupton, R.W. Overell, T.C. Reynolds, L. Corey, P.D. Greenberg, T-cell mediated rejection of gene-modified HIV-specific cytotoxic T lymphocytes in HIV-infected patients, Nature medicine 2(2) (1996) 216-23.

[24] C. Berger, M.E. Flowers, E.H. Warren, S.R. Riddell, Analysis of transgene-specific immune responses that limit the in vivo persistence of adoptively transferred HSV-TK-modified donor T cells after allogeneic hematopoietic cell transplantation, Blood 107(6) (2006) 2294-302.

[25] R.S.Y. Wong, Apoptosis in cancer: from pathogenesis to treatment, Journal of Experimental & Clinical Cancer Research : CR 30(1) (2011) 87.

[26] L.T. Jia, S.Y. Chen, A.G. Yang, Cancer gene therapy targeting cellular apoptosis machinery, Cancer treatment reviews 38(7) (2012) 868-76.

[27] A.C. Bellail, L. Qi, P. Mulligan, V. Chhabra, C. Hao, TRAIL agonists on clinical trials for cancer therapy: the promises and the challenges, Reviews on recent clinical trials 4(1) (2009) 34-41.

[28] J.Y. Lang, J.L. Hsu, F. Meric-Bernstam, C.J. Chang, Q. Wang, Y. Bao, H. Yamaguchi, X. Xie, W.A. Woodward, D. Yu, G.N. Hortobagyi, M.C. Hung, BikDD Eliminates Breast Cancer Initiating Cells and Synergizes with Lapatinib for Breast Cancer Treatment, Cancer cell 20(3) (2011) 341-56.

[29] A. Di Stasi, S.K. Tey, G. Dotti, Y. Fujita, A. Kennedy-Nasser, C. Martinez, K. Straathof, E. Liu, A.G. Durett, B. Grilley, H. Liu, C.R. Cruz, B. Savoldo, A.P. Gee, J. Schindler, R.A. Krance, H.E. Heslop, D.M. Spencer, C.M. Rooney, M.K. Brenner, Inducible apoptosis as a safety switch for adoptive cell therapy, The New England journal of medicine 365(18) (2011) 1673-83.

[30] R.S. MacGill, T.A. Davis, J. Macko, H.J. Mauceri, R.R. Weichselbaum, C.R. King, Local gene delivery of tumor necrosis factor alpha can impact primary tumor growth and metastases through a host-mediated response, Clinical & experimental metastasis 24(7) (2007) 521-31.

[31] K.Y. Choi, M. Swierczewska, S. Lee, X. Chen, Protease-Activated Drug Development, Theranostics 2(2) (2012) 156-78.

[32] T. Gargett, M.P. Brown, The inducible caspase-9 suicide gene system as a “safety switch” to limit on-target, off-tumor toxicities of chimeric antigen receptor T cells, Frontiers in Pharmacology 5 (2014).

[33] M. Druskovic, D. Suput, I. Milisav, Overexpression of caspase-9 triggers its activation and apoptosis in vitro, Croatian medical journal 47(6) (2006) 832-40.

[34] P. Hensley, M. Mishra, N. Kyprianou, Targeting caspases in cancer therapeutics, Biological chemistry 394(7) (2013) 831-43.

[35] L. Yang, Application of Apoptosis to cancer treatment, Springer2005.

[36] S. Nitta, K. Numata, Biopolymer-Based Nanoparticles for Drug/Gene Delivery and Tissue Engineering, International Journal of Molecular Sciences 14(1) (2013) 1629.

[37] A.R. Sharma, S.K. Kundu, J.-S. Nam, G. Sharma, C.G. Priya Doss, S.-S. Lee, C. Chakraborty, Next Generation Delivery System for Proteins and Genes of Therapeutic Purpose: Why and How?, BioMed Research International 2014 (2014) 11.

[38] E.R. Lorden, H.M. Levinson, K.W. Leong, Integration of drug, protein, and gene delivery systems with regenerative medicine, Drug Delivery and Translational Research 5(2) (2015) 168-186.

[39] N. Nayerossadat, T. Maedeh, P.A. Ali, Viral and nonviral delivery systems for gene delivery, Advanced Biomedical Research 1 (2012).

[40] S. Mali, Delivery systems for gene therapy, Indian Journal of Human Genetics 19(1) (2013) 3-8.

[41] M. Ramamoorth, A. Narvekar, Non Viral Vectors in Gene Therapy- An Overview, Journal of Clinical and Diagnostic Research : JCDR 9(1) (2015) GE01-6.

[42] Y. Seow, M.J. Wood, Biological Gene Delivery Vehicles: Beyond Viral Vectors, Molecular Therapy: the Journal of the American Society of Gene Therapy 17(5) (2009) 767-77.

[43] M.S. Al-Dosari, X. Gao, Nonviral Gene Delivery: Principle, Limitations, and Recent Progress, The AAPS Journal 11(4) (2009).

[44] B. Leader, Q.J. Baca, D.E. Golan, Protein therapeutics: a summary and pharmacological classification, Nature reviews. Drug discovery 7(1) (2008) 21-39.

[45] T. Dingermann, Recombinant therapeutic proteins: production platforms and challenges, Biotechnology journal 3(1) (2008) 90-7.

[46] F.M. Wurm, Production of recombinant protein therapeutics in cultivated mammalian cells, Nature biotechnology 22(11) (2004) 1393-8.

[47] C.O. Weill, S. Biri, A. Adib, P. Erbacher, A practical approach for intracellular protein delivery, Cytotechnology 56(1) (2008) 41-8.

[48] I. Zidi, S. Mestiri, A. Bartegi, N.B. Amor, TNF-alpha and its inhibitors in cancer, Medical oncology (Northwood, London, England) 27(2) (2010) 185-98.

[49] R.S. Herbst, S.G. Eckhardt, R. Kurzrock, S. Ebbinghaus, P.J. O'Dwyer, M.S. Gordon, W. Novotny, M.A. Goldwasser, T.M. Tohnya, B.L. Lum, A. Ashkenazi, A.M. Jubb, D.S. Mendelson, Phase I dose-escalation study of recombinant human Apo2L/TRAIL, a dual proapoptotic receptor agonist, in patients with advanced cancer, Journal of clinical oncology : official journal of the American Society of Clinical Oncology 28(17) (2010) 2839-46.

[50] R. Tang, C.S. Kim, D.J. Solfiell, S. Rana, R. Mout, E.M. Velázquez-Delgado, A. Chompoosor, Y. Jeong, B. Yan, Z.-J. Zhu, C. Kim, J.A. Hardy, V.M. Rotello, Direct Delivery of Functional Proteins and Enzymes to the Cytosol Using Nanoparticle-Stabilized Nanocapsules, ACS Nano 7(8) (2013) 6667-6673.

[51] Z. Siprashvili, J.A. Reuter, P.A. Khavari, Intracellular Delivery of Functional Proteins via Decoration with Transporter Peptides, Molecular Therapy: the Journal of the American Society of Gene Therapy 9(5) (2004) 721-728.

[52] O. Zelphati, Y. Wang, S. Kitada, J.C. Reed, P.L. Felgner, J. Corbeil, Intracellular delivery of proteins with a new lipid-mediated delivery system, The Journal of biological chemistry 276(37) (2001) 35103-10.

[53] L. Zhang, J. Ren, H. Zhang, G. Cheng, Y. Xu, S. Yang, C. Dong, D. Fang, J. Zhang, A. Yang, HER2-targeted recombinant protein immuno-caspase-6 effectively induces apoptosis in HER2-overexpressing GBM cells in vitro and in vivo, Oncology reports 36(5) (2016) 2689-2696.

[54] R. Solaro, F. Chiellini, A. Battisti, Targeted Delivery of Protein Drugs by Nanocarriers, Materials 3(3) (2010) 1928.

[55] D.S. Pisal, M.P. Kosloski, S.V. Balu-Iyer, Delivery of therapeutic proteins, Journal of pharmaceutical sciences 99(6) (2010) 2557-75.

[56] A. Jain, A. Jain, A. Gulbake, S. Shilpi, P. Hurkat, S.K. Jain, Peptide and protein delivery using new drug delivery systems, Critical reviews in therapeutic drug carrier systems 30(4) (2013) 293-329.

[57] E. Simone, T. Dziubla, V. Shuvaev, V.R. Muzykantov, Synthesis and characterization of polymer nanocarriers for the targeted delivery of therapeutic enzymes, Methods in molecular biology (Clifton, N.J.) 610 (2010) 145-64.

[58] Y.E. Koshman, S.B. Waters, L.A. Walker, T. Los, P. de Tombe, P.H. Goldspink, B. Russell, Delivery and visualization of proteins conjugated to quantum dots in cardiac myocytes, Journal of molecular and cellular cardiology 45(6) (2008) 853-6.

[59] A. Dinca, W.M. Chien, M.T. Chin, Intracellular Delivery of Proteins with Cell-Penetrating Peptides for Therapeutic Uses in Human Disease, Int J Mol Sci 17(2) (2016).

[60] V. Biju, T. Itoh, M. Ishikawa, Delivering quantum dots to cells: bioconjugated quantum dots for targeted and nonspecific extracellular and intracellular imaging, Chemical Society reviews 39(8) (2010) 3031-56.

[61] R. Solaro, Targeted delivery of proteins by nanosized carriers, Journal of Polymer Science Part A: Polymer Chemistry 46(1) (2008) 1-11.

[62] J. Duan, Y. Zhang, W. Chen, C. Shen, M. Liao, Y. Pan, J. Wang, X. Deng, J. Zhao, Cationic polybutyl cyanoacrylate nanoparticles for DNA delivery, Journal of biomedicine & biotechnology 2009 (2009) 149254.

[63] K.S. Soppimath, T.M. Aminabhavi, A.R. Kulkarni, W.E. Rudzinski, Biodegradable polymeric nanoparticles as drug delivery devices, Journal of controlled release : official journal of the Controlled Release Society 70(1-2) (2001) 1-20.

[64] E. Rytting, J. Nguyen, X. Wang, T. Kissel, Biodegradable polymeric nanocarriers for pulmonary drug delivery, Expert opinion on drug delivery 5(6) (2008) 629-39.

[65] L. Chen, L.R. Wright, C.H. Chen, S.F. Oliver, P.A. Wender, D. Mochly-Rosen, Molecular transporters for peptides: delivery of a cardioprotective epsilonPKC agonist peptide into cells and intact ischemic heart using a transport system, R(7), Chemistry & biology 8(12) (2001) 1123-9.

[66] S. Toita, U. Hasegawa, H. Koga, I. Sekiya, T. Muneta, K. Akiyoshi, Protein-conjugated quantum dots effectively delivered into living cells by a cationic nanogel, Journal of nanoscience and nanotechnology 8(5) (2008) 2279-85.

[67] Y. Xu, B.R. Liu, H.-J. Lee, K.B. Shannon, J.G. Winiarz, T.-C. Wang, H.-J. Chiang, Y.-w. Huang, Nona-Arginine Facilitates Delivery of Quantum Dots into Cells via Multiple Pathways, Journal of Biomedicine and Biotechnology 2010 (2010) 11.

[68] K.T. Yong, Y. Wang, I. Roy, H. Rui, M.T. Swihart, W.C. Law, S.K. Kwak, L. Ye, J. Liu, S.D. Mahajan, J.L. Reynolds, Preparation of quantum dot/drug nanoparticle formulations for traceable targeted delivery and therapy, Theranostics 2(7) (2012) 681-94.

[69] V. Bagalkot, L. Zhang, E. Levy-Nissenbaum, S. Jon, P.W. Kantoff, R. Langer, O.C. Farokhzad, Quantum dot-aptamer conjugates for synchronous cancer imaging, therapy, and sensing of drug delivery based on bi-fluorescence resonance energy transfer, Nano letters 7(10) (2007) 3065-70.

[70] J. Shi, A.R. Votruba, O.C. Farokhzad, R. Langer, Nanotechnology in Drug Delivery and Tissue Engineering: From Discovery to Applications, Nano letters 10(9) (2010) 3223-3230.

[71] Y. Lu, S.X. Hou, T. Chen, [Advances in the study of vincristine: an anticancer ingredient from Catharanthus roseus], Zhongguo Zhong yao za zhi = Zhongguo zhongyao zazhi = China journal of Chinese materia medica 28(11) (2003) 1006-9.

[72] R. Silvestri, New prospects for vinblastine analogues as anticancer agents, Journal of medicinal chemistry 56(3) (2013) 625-7.

[73] M.L. Cortes, V. Garcia-Escudero, M. Hughes, M. Izquierdo, Cyanide bystander effect of the linamarase/linamarin killer-suicide gene therapy system, The journal of gene medicine 4(4) (2002) 407-14.

[74] M.L. Cortes, P. de Felipe, V. Martin, M.A. Hughes, M. Izquierdo, Successful use of a plant gene in the treatment of cancer in vivo, Gene therapy 5(11) (1998) 1499-507.

[75] N. Zarovni, R. Vago, M.S. Fabbrini, Saporin suicide gene therapy, Methods in molecular biology (Clifton, N.J.) 542 (2009) 261-83.

[76] N. Zarovni, R. Vago, T. Solda, L. Monaco, M.S. Fabbrini, Saporin as a novel suicide gene in anticancer gene therapy, Cancer gene therapy 14(2) (2007) 165-73.

[77] H. Stedt, H. Samaranayake, J. Kurkipuro, G. Wirth, L.S. Christiansen, T. Vuorio, A.M. Maatta, J. Piskur, S. Yla-Herttuala, Tomato thymidine kinase-based suicide gene therapy for malignant glioma--an alternative for Herpes Simplex virus-1 thymidine kinase, Cancer gene therapy 22(3) (2015) 130-7.

[78] L. Slot Christiansen, L. Egeblad, B. Munch-Petersen, J. Piškur, W. Knecht, New Variants of Tomato Thymidine Kinase 1 Selected for Increased Sensitivity of E. coli KY895 towards Azidothymidine, Cancers 7(2) (2015) 966-80.

[79] Y. Xu, J. Hou, Z. Liu, H. Yu, W. Sun, J. Xiong, Z. Liao, F. Zhou, C. Xie, Y. Zhou, Gene therapy with tumor-specific promoter mediated suicide gene plus IL-12 gene enhanced tumor inhibition and prolonged host survival in a murine model of Lewis lung carcinoma, Journal of translational medicine 9 (2011) 39.

[80] W.J. Sun, J. Xiong, W.F. Wang, Z.K. Liao, F.X. Zhou, Y.F. Zhou, [Anti-tumor effect of suicide gene therapy using chimeric promoter plus radiotherapy on cancer cell lines], Zhonghua zhong liu za zhi [Chinese journal of oncology] 33(4) (2011) 245-50.

[81] H. Zhang, Z.K. Liao, W.J. Sun, C. Huang, J. Xiong, F.X. Zhou, C.H. Xie, Y.F. Zhou, Enhanced suicide gene therapy using a tumor-specific promoter in combination with cisplatin, Molecular medicine reports 2(6) (2009) 1017-22.

[82] G. Block, B. Patterson, A. Subar, Fruit, vegetables, and cancer prevention: a review of the epidemiological evidence, Nutrition and cancer 18(1) (1992) 1-29.

[83] C.S. Hew, B.Y. Khoo, L.H. Gam, The anti-cancer property of proteins extracted from *Gynura procumbens* (Lour.) Merr, PloS one 8(7) (2013) e68524.

[84] E.G. De Mejia, V.I. Prisecaru, Lectins as bioactive plant proteins: a potential in cancer treatment, Critical reviews in food science and nutrition 45(6) (2005) 425-45.

[85] N. Tyagi, M. Tyagi, M. Pachauri, P.C. Ghosh, Potential therapeutic applications of plant toxin-ricin in cancer: challenges and advances, Tumour biology : the journal of the International Society for Oncodevelopmental Biology and Medicine 36(11) (2015) 8239-46.

[86] J.Y. Lin, Y.C. Chang, L.Y. Huang, T.C. Tung, The cytotoxic effects of abrin and ricin on Ehrlich ascites tumor cells, Toxicon : official journal of the International Society on Toxinology 11(4) (1973) 379-81.

[87] Ø. Fodstad, S. Olsnes, Studies on the Accessability of Ribosomes to Inactivation by the Toxic Lectins Abrin and Ricin, European Journal of Biochemistry 74(2) (1977) 209-215.

[88] O. Fodstad, G. Kvalheim, A. Godal, J. Lotsberg, S. Aamdal, H. Host, A. Pihl, Phase I study of the plant protein ricin, Cancer research 44(2) (1984) 862-5.

[89] J. Audi, M. Belson, M. Patel, J. Schier, J. Osterloh, Ricin poisoning: a comprehensive review, Jama 294(18) (2005) 2342-51.

[90] D.M. Neville, Jr., R.J. Youle, Monoclonal antibody-ricin or ricin A chain hybrids: kinetic analysis of cell killing for tumor therapy, Immunological reviews 62 (1982) 75-91.

[91] E.J. Wawrzynczak, G.J. Watson, A.J. Cumber, R.V. Henry, G.D. Parnell, E.P. Rieber, P.E. Thorpe, Blocked and non-blocked ricin immunotoxins against the CD4 antigen exhibit higher cytotoxic potency than a ricin A chain immunotoxin potentiated with ricin B chain or with a ricin B chain immunotoxin, Cancer immunology, immunotherapy : CII 32(5) (1991) 289-95.

[92] M.-u.-H. Nishawar Jan, Khurshid I. Andrabi, Programmed cell death or apoptosis: Do animals and plants share anything in common, Biotechnology and Molecular Biology Reviews 3(5) (2008) 111-126.

[93] T.J. Reape, P.F. McCabe, Apoptotic-like programmed cell death in plants, New Phytologist 180(1) (2008) 13-26.

[94] S. Dong, Z. Zhang, X. Zheng, Y. Wang, Mammalian pro-apoptotic bax gene enhances tobacco resistance to pathogens, Plant cell reports 27(9) (2008) 1559-69.

[95] M.B. Dickman, Y.K. Park, T. Oltersdorf, W. Li, T. Clemente, R. French, Abrogation of disease development in plants expressing animal, Proceedings of the National Academy of Sciences of the United States of America 98(12) (2001) 6957-62.

[96] S. Shabala, T.A. Cuin, L. Prismall, L.G. Nemchinov, Expression of animal CED-9 anti-apoptotic gene in tobacco modifies plasma membrane ion fluxes in response to salinity and oxidative stress, Planta 227(1) (2007) 189-197.

[97] P. Xu, S.J. Rogers, M.J. Roossinck, Expression of antiapoptotic genes bcl-xL and ced-9 in tomato enhances tolerance to viral-induced necrosis and abiotic stress, Proceedings of the National Academy of Sciences of the United States of America 101(44) (2004) 15805-10.

[98] N.V. Chichkova, J. Shaw, R.A. Galiullina, G.E. Drury, A.I. Tuzhikov, S.H. Kim, M. Kalkum, T.B. Hong, E.N. Gorshkova, L. Torrance, A.B. Vartapetian, M. Taliansky, Phytaspase, a relocalisable cell death promoting plant protease with caspase specificity, The EMBO journal 29(6) (2010) 1149-61.

[99] M.R. Islam, H. Kim, S.W. Kang, J.S. Kim, Y.M. Jeong, H.J. Hwang, S.Y. Lee, J.C. Woo, S.G. Kim, Functional characterization of a gene encoding a dual domain for uridine kinase and uracil phosphoribosyltransferase in Arabidopsis thaliana, Plant molecular biology 63(4) (2007) 465-77.

[100] S.E. Mainguet, B. Gakiere, A. Majira, S. Pelletier, F. Bringel, F. Guerard, M. Caboche, R. Berthome, J.P. Renou, Uracil salvage is necessary for early Arabidopsis development, The Plant journal : for cell and molecular biology 60(2) (2009) 280-91.

[101] K. Friedrich, T. Wieder, C. Von Haefen, S. Radetzki, R. Janicke, K. Schulze-Osthoff, B. Dorken, P.T. Daniel, Overexpression of caspase-3 restores sensitivity for drug-induced apoptosis in breast cancer cell lines with acquired drug resistance, Oncogene 20(22) (2001) 2749-60.

[102] J.K. SI Sikdar, Expression of a natural fusion gene for uracil phosphoribosyltransferase and uridine kinase from rice shows growth retardation by 5-fluorouridine or 5-fluorouracil in *Escherichia coli*, African Journal of Biotechnology 9(9) (2010) 1295-1303.

[103] N.V. Chichkova, A.I. Tuzhikov, M. Taliansky, A.B. Vartapetian, Plant phytaspases and animal caspases: structurally unrelated death proteases with a common role and specificity, Physiologia plantarum 145(1) (2012) 77-84.

[104] A.B. Vartapetian, A.I. Tuzhikov, N.V. Chichkova, M. Taliansky, T.J. Wolpert, A plant alternative to animal caspases: subtilisin-like proteases, Cell death and differentiation 18(8) (2011) 1289-97.

[105] R.A. Galiullina, P. Kasperkiewicz, N.V. Chichkova, A. Szalek, M.V. Serebryakova, M. Poreba, M. Drag, A.B. Vartapetian, Substrate Specificity and Possible Heterologous Targets of Phytaspase, a Plant Cell Death Protease, The Journal of biological chemistry 290(41) (2015) 24806-15.

[106] S.D. Kramer, B. Testa, The biochemistry of drug metabolism--an introduction: part 6. Inter-individual factors affecting drug metabolism, Chemistry & biodiversity 5(12) (2008) 2465-578.

[107] D.D. Bilgin, E.H. DeLucia, S.J. Clough, A robust plant RNA isolation method suitable for Affymetrix GeneChip analysis and quantitative real-time RT-PCR, Nature protocols 4(3) (2009) 333-40.

[108] D.J. Webb, C.M. Brown, Epi-fluorescence microscopy, Methods in molecular biology (Clifton, N.J.) 931 (2013) 29-59.

[109] C. Riccardi, I. Nicoletti, Analysis of apoptosis by propidium iodide staining and flow cytometry, Nature protocols 1(3) (2006) 1458-61.

[110] N.A. Franken, H.M. Rodermond, J. Stap, J. Haveman, C. van Bree, Clonogenic assay of cells in vitro, Nature protocols 1(5) (2006) 2315-9.

[111] K. Buch, T. Peters, T. Nawroth, M. Sanger, H. Schmidberger, P. Langguth, Determination of cell survival after irradiation via clonogenic assay versus multiple MTT Assay--a comparative study, Radiation oncology (London, England) 7 (2012) 1.

[112] J. Li, N. Hou, A. Faried, S. Tsutsumi, T. Takeuchi, H. Kuwano, Inhibition of autophagy by 3-MA enhances the effect of 5-FU-induced apoptosis in colon cancer cells, Annals of surgical oncology 16(3) (2009) 761-71.

[113] L. Deng, Z. Ren, Q. Jia, W. Wu, H. Shen, Y. Wang, Schedule-dependent antitumor effects of 5-fluorouracil combined with sorafenib in hepatocellular carcinoma, BMC cancer 13 (2013) 363.

[114] J. LaBaer, M.D. Garrett, L.F. Stevenson, J.M. Slingerland, C. Sandhu, H.S. Chou, A. Fattaey, E. Harlow, New functional activities for the p21 family of CDK inhibitors, Genes & development 11(7) (1997) 847-62.

[115] D.R. McIlwain, T. Berger, T.W. Mak, Caspase functions in cell death and disease, Cold Spring Harbor perspectives in biology 5(4) (2013) a008656.

[116] B.B.V.A. Alexander I. Tuzhikov, B. Vartapetian, Nina V. Chichkova, Abiotic Stress-Induced Programmed Cell Death in Plants: A Phytaspase Connection, in: P.A. Shanker (Ed.) Abiotic Stress Response in Plants - Physiological, Biochemical and Genetic Perspectives, InTech, 2011.

[117] V. Garcia-Escudero, R. Gargini, M. Izquierdo, Glioma regression in vitro and in vivo by a suicide combined treatment, Molecular cancer research : MCR 6(3) (2008) 407-17.

[118] Z. Khan, W. Knecht, M. Willer, E. Rozpedowska, P. Kristoffersen, A.R. Clausen, B. Munch-Petersen, P.M. Almqvist, Z. Gojkovic, J. Piskur, T.J. Ekstrom, Plant thymidine kinase 1: a novel efficient suicide gene for malignant glioma therapy, Neuro-oncology 12(6) (2010) 549-58.

[119] O. Greco, L.K. Folkes, P. Wardman, G.M. Tozer, G.U. Dachs, Development of a novel enzyme/prodrug combination for gene therapy of cancer: horseradish peroxidase/indole-3-acetic acid, Cancer gene therapy 7(11) (2000) 1414-20.

[120] X. Hu, A.S. Reddy, Cloning and expression of a PR5-like protein from Arabidopsis: inhibition of fungal growth by bacterially expressed protein, Plant molecular biology 34(6) (1997) 949-59.

[121] A. Campos Mde, M.S. Silva, C.P. Magalhaes, S.G. Ribeiro, R.P. Sarto, E.A. Vieira, M.F. Grossi de Sa, Expression in *Escherichia coli*, purification, refolding and antifungal activity of an osmotin from *Solanum nigrum*, Microbial cell factories 7 (2008) 7.

[122] H. Li, N. Liu, W.T. Wang, J.Y. Wang, W.Y. Gao, Cloning and characterization of GST fusion tag stabilized large subunit of *Escherichia coli* acetohydroxyacid synthase I, Journal of bioscience and bioengineering 121(1) (2016) 21-6.

[123] D.N. Perkins, D.J. Pappin, D.M. Creasy, J.S. Cottrell, Probability-based protein identification by searching sequence databases using mass spectrometry data, Electrophoresis 20(18) (1999) 3551-67.

[124] M.L. Anson, The estimation of pepsin, trypsin, papain, and cathepsin with hemoglobin, The Journal of General Physiology 22(1) (1938) 79-89.

[125] V.C. Otto Folin, On tyrosine and tryptophane determinations in proteins Journal of Biological Chemistry 73 (1927) 627-650.

[126] D.M. Leippe, D. Nguyen, M. Zhou, T. Good, T.A. Kirkland, M. Scurria, L. Bernad, T. Ugo, J. Vidugiriene, J.J. Cali, D.H. Klaubert, M.A. O'Brien, A bioluminescent assay for the sensitive detection of proteases, BioTechniques 51(2) (2011) 105-10.

[127] A. Charlton, M. Zachariou, Tag removal by site-specific cleavage of recombinant fusion proteins, Methods in molecular biology (Clifton, N.J.) 681 (2011) 349-67.

[128] S. Harper, D.W. Speicher, Purification of proteins fused to glutathione S-transferase, Methods in molecular biology (Clifton, N.J.) 681 (2011) 259-80.

[129] N.J. Greenfield, Using circular dichroism spectra to estimate protein secondary structure, Nature protocols 1(6) (2006) 2876-90.

[130] B.K. Kuntal, P. Aparoy, P. Reddanna, EasyModeller: A graphical interface to MODELLER, BMC Research Notes 3(1) (2010) 226.

[131] K.S. P. Rathi Suganya, Sukesh Kalva, Lilly M. Saleena, Homology modeling for human ADAM12 using PRIME, I-TASSER and EASYMODELLER, International Journal of Pharmacy and Pharmaceutical Sciences 6(2) (2014) 782-786.

[132] G.M. Morris, R. Huey, W. Lindstrom, M.F. Sanner, R.K. Belew, D.S. Goodsell, A.J. Olson, AutoDock4 and AutoDockTools4: Automated Docking with Selective Receptor Flexibility, J Comput Chem 30(16) (2009) 2785-91.

[133] A. Vaculova, B. Zhivotovsky, Caspases: determination of their activities in apoptotic cells, Methods Enzymol 442 (2008) 157-81.

[134] V. Kaushal, C. Herzog, R.S. Haun, G.P. Kaushal, Caspase Protocols in Mice, Methods in molecular biology (Clifton, N.J.) 1133 (2014) 141-54.

[135] D. Twiddy, D.G. Brown, C. Adrain, R. Jukes, S.J. Martin, G.M. Cohen, M. MacFarlane, K. Cain, Pro-apoptotic proteins released from the mitochondria regulate the protein composition and caspase-processing activity of the native Apaf-1/caspase-9 apoptosome complex, The Journal of biological chemistry 279(19) (2004) 19665-82.

[136] N.V. Chichkova, R.A. Galiullina, R.E. Beloshistov, A.V. Balakireva, A.B. Vartapetian, [Phytaspases: aspartate-specific proteases involved in plant cell death], Bioorganicheskaia khimiia 40(6) (2014) 658-64.

[137] G.K. Patel, A.A. Kawale, A.K. Sharma, Purification and physicochemical characterization of a serine protease with fibrinolytic activity from latex of a medicinal herb Euphorbia hirta, Plant physiology and biochemistry : PPB 52 (2012) 104-11.

[138] R. Rajesh, A. Nataraju, C.D. Gowda, B.M. Frey, F.J. Frey, B.S. Vishwanath, Purification and characterization of a 34-kDa, heat stable glycoprotein from Synadenium grantii latex: action on human fibrinogen and fibrin clot, Biochimie 88(10) (2006) 1313-22.

[139] C. Ottmann, R. Rose, F. Huttenlocher, A. Cedzich, P. Hauske, M. Kaiser, R. Huber, A. Schaller, Structural basis for Ca2+-independence and activation by homodimerization of tomato subtilase 3, Proceedings of the National Academy of Sciences of the United States of America 106(40) (2009) 17223-8.

[140] P. Sanpui, S.B. Pandey, A. Chattopadhyay, S.S. Ghosh, Incorporation of gene therapy vector in chitosan stabilized Mn2+-doped ZnS quantum dot, Materials Letters 64(22) (2010) 2534-2537.

[141] S.A. Kulkarni, S.S. Feng, Effects of particle size and surface modification on cellular uptake and biodistribution of polymeric nanoparticles for drug delivery, Pharmaceutical research 30(10) (2013) 2512-22.

[142] N. Oh, J.H. Park, Endocytosis and exocytosis of nanoparticles in mammalian cells, International journal of nanomedicine 9 Suppl 1 (2014) 51-63.

PUBLICATIONS

1. Sharmila Narayanan, Pallab Sanpui, Lingaraj Sahoo and Siddhartha Sankar Ghosh **(2016).** Unravelling the potential of a new uracil phosphoribosyltransferase (UPRT) from *Arabidopsis thaliana* in sensitizing HeLa cells towards 5-fluorouracil, ***International Journal of Biological Macromolecules.*** 91, 310-316.

2. Sharmila Narayanan, Pallab Sanpui, Lingaraj Sahoo and Siddhartha Sankar Ghosh **(2016).** Heterologous Expression and Functional Characterization of Phytaspase, a Caspase-Like Plant Protease, ***International Journal of Biological Macromolecules.*** 95, 288-293.

3. Sharmila Narayanan, Pallab Sanpui, Lingaraj Sahoo and Siddhartha Sankar Ghosh **(2016).** Tobacco Phytaspase: Our Journey toward Successful Expression of the Protein in Heterologous System. [Manuscript under review]

4. Sharmila Narayanan, Depanjalee Dutta, Pallab Sanpui, Lingaraj Sahoo and Siddhartha Sankar Ghosh **(2016).** Luminescent Mn doped ZnS QDs embedded chitosan NPs encapsulating Phytaspase caspase like protease for augmented chemotherapy of HeLa cells [Manuscript under preparation]

CONFERENCES

1. Poster presentation on “Phytaspase: Caspase like plant protease and its possible implication for cancer therapeutics” at International Conference on Plant Protease, University of Oxford, Oxford, **United kingdom** (2016)

2. Presented poster on “Emergence of Protein therapeutics in cancer medicine” in Research Conclave, Indian Institute of Technology Guwahati, **India** (2016)

3. Received **“Best Poster Award”** for poster presentation on “Recombinant Plant Phytaspase Ensemble Composite Nanoparticles for potentiating Caspase-like Activity in Cancer therapy at the 4th International Conference on Advanced Nanomaterials and Nanotechnology, IIT Guwahati, **India** (2015)

4. Poster presentation on “Unveilling the importance of caspase-like protease recombinant phytaspase in cancer therapeutics” at the International Conference on Cancer Research: New Horizons, Pune, **India** (2015)

5. Poster presentation on “Functional characterizations of bacterially expressed *Nicotiana tabacum* Phytaspase” at the International Conference on Stem Cells and Cancer, New Delhi, **India** (2014)

6. Participated in the National Conference on New Advances and Horizons in Nanoscience and Nanotechnology, Institute of Advanced Study in Science and Technology, Guwahati, **India** (2014)